Task 2.3

Task Title

Hydropower infrastructure adaptation to requirements of future operating conditions

Research Partners

Laboratory of Hydraulic Constructions (LCH) at EPFL, Laboratory of Hydraulics, Hydrology and Glaciology (VAW) at ETH Zurich, Lucerne University of Applied Sciences and Arts (HSLU)

Current Projects (presented on the following pages)

GPU-SPHEROS – A GPU-Accelerated Particle-Based Solver for Hydrodynamic Simulation of Hydraulic Turbines
S. Alimirzazadeh, E. Jahanbakhsh, A. Maertens, S. Leguizamon, F. Avellan

---

Characterisation of hydraulic behavior of surge tanks orifices
N.J. Adam, G. De Cesare, A. J. Schleiss, C. Münch-Alligné

Artificial sediment replenishment to restore the natural morphological conditions downstream of dams
E. Battisacco, M. J. Franca, A. J. Schleiss

The influence of Fluid-Structure Interaction (FSI) during hydraulic transients in pressurized pipes
D. Ferras, P. Manso, D.I.C. Covas, A.J. Schleiss

Design of steel-lined pressure tunnels and shafts: new and innovative probabilistic approaches for reliability assessment
G. Muller, A. Pachoud, P. Manso, A.J. Schleiss, A. Nussbaumer

---

Hydrograph variability applied to the gravel bed rivers
B. Plumb, C. Juez, M.J. Franca, A.J. Schleiss, W. K. Annable

Mitigation des impacts négatifs du changement climatique sur l'aménagement de Gebidem grâce à un nouveau potentiel de stockage à Oberaletsch
E. Calixte, F. Zeimetz, P. Manso, As. J. Schleiss

Potentiel hydroélectrique dans la vallée de Gorner suite au retrait du glacier
P. George-Molland, S. Stähly, P. Manso, A.J. Schleiss

Task Objectives

This task focus on

- investigating the infrastructural adaptation of existing hydropower systems to cope with more flexible operation and with increased erosion and sediment transport and to maintain the required level of safety under harsher operational conditions or under storage increase,
- identifying possible improvement margins through combined design of infrastructure, devices, and operation,
- and exploring the potential of lakes that can form following the retreat of glaciers.

Interaction Between the Partners – Synthesis

- The two main research institutes (ETHZ and EPFL) involved in this task jointly participate in the CTI research proposal FLEXSTOR (see details below).
- Research activities lead by the three partners jointly or independently are, almost inherently, multidisciplinary and in connection with other SCCER-SoE tasks given the specific content of this task 2.3 on infrastructure, which make use of given resources (task 2.1), in a given economical context (task 2.2), within environmental restrictions (task 2.4) for operation (task 2.5) with given equipment solutions (task 3.2).

Highlights 2016

- Hydropower potential in meshed water supply networks: a modelling framework for the optimal location of technical and economically feasible micro-hydropower plants has

been developed and tested in a few large-scale Swiss urban centres. The tested compact micro-hydropower plant was developed around a new turbine technology tested within the project.

- Seasonal storage. A comprehensive assessment of the hydropower infrastructure based on the hydropower georeferenced database HydroGIS has shown that in general there is a considerable amount of untapped storage potential that could be used to reduce electricity imports during the winter. Inversely few reservoirs risk not filling up in the future due to inflow reduction derived from climate change. Overall, the lack of a comprehensive database of water diversion structure is identified as a major obstacle to the assessment of the role of alpine reservoir for water and electricity supply resilience in future conditions with reduced glacial melt volumes and increased stochastic precipitation events. Several case studies show the advantage of robust design of new infrastructure for energy production coupled with mitigation of future climate change.
- Behaviour of hydraulic infrastructure under harsh operation conditions. A residual life estimator was developed based on steel lining fracture propagation by fatigue, which is also used to estimate the probability of failure of steel liner within a time horizon.
- Fluid-structure interaction: a numerical tool was developed and tested for modelling the interaction between fluid, pipe-wall and support structure of complex hydraulic pipelines, considering as well different fluid and material properties and boundary conditions.
- Hydro-abrasive erosion of Pelton turbines: a prediction model was enhanced by calibration with new, temporally highly-resolved data from a pilot plant study in Valais. Within this project, a one-day workshop was organized and held in the frame of the 28th IAHR Symposium on Hydraulic Machinery and Systems, Grenoble.
- Hydro-abrasion of hydraulic structures: A unique field test was performed in the sediment bypass tunnel (SBT) of the Solis reservoir. It consisted of flushing a defined volume of sediment of defined grain size distribution through the tunnel. The sediment had been dumped at the upstream SBT head just downstream of the intake gate. This test enables a more accurate calibration of the Swiss plate geophone measurement system installed at the downstream tunnel end to deduce sediment loads transported through the SBT during flushing events.
- Aeration and two-phase flow characteristics of bottom outlets: A large-scale hydraulic model was built and commissioned in the hydraulic laboratory at ETH Zurich. Preliminary results indicate that previous model studies presented in the literature largely underestimated the air demand down-stream of the intake gate, presumably due to scale effects or model restrictions.

SCCER SoE
SWISS COMPETENCE CENTER for ENERGY RESEARCH
SUPPLY of ELECTRICITY

SCCER-SoE Annual Conference 2016

In cooperation with the CTI
Energy
Swiss Competence Centers for Energy Research
Schweizerische Eidgenossenschaft
Confédération suisse
Confederazione Svizzera
Confederaziun svizra
Swiss Confederation
Commission for Technology and Innovation CTI

Untapped seasonal storage potential in Swiss hydropower schemes

Guittet M.(1), Akari S. (1), Capezzali M. (1), Vuille F. (1) and Manso P. (2)
(1)Energy Center, École polytechnique fédérale de Lausanne (EPFL); (2) Laboratoire de Constructions Hydrauliques, EPFL
Corresponding author: melanie.guittet@epfl.ch

LABORATOIRE DE CONSTRUCTIONS HYDRAULIQUES

ÉCOLE POLYTECHNIQUE FÉDÉRALE DE LAUSANNE | ENERGY CENTER

(1) Context and motivation

- CH's continued dependency on electricity imports, mainly in winter
- Growing need for additional capacity in seasonal energy storage
- Hydropower is expected to be the backbone of the energy transition
- Lack of common metrics to assess seasonal storage capacity

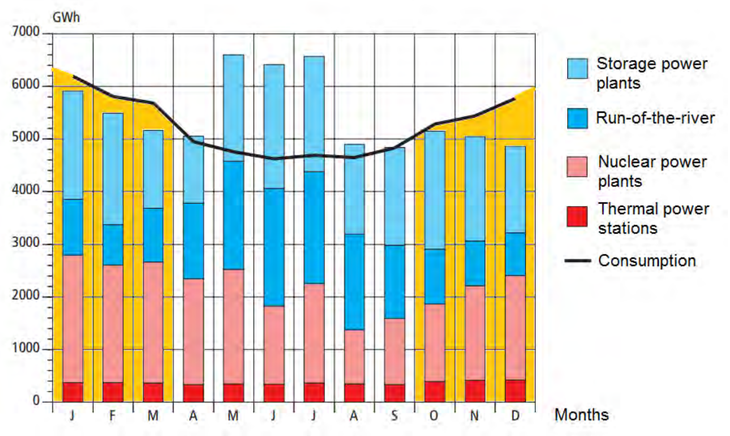

Since 2005, Switzerland has been importing electricity in winter, roughly from October to March, to compensate for the insufficient indigenous electricity production.

Fig. 1 Monthly electricity production and consumption (SFOE, 2015)

(2) Research questions

- What is the seasonal storage capacity in Swiss hydropower dams ?
- How could the untapped potential be captured?
- What is the impact on the Swiss energy transition ?

(3) Methodology to assess storage potential

Today's seasonal storage capacity (8.82 TWh) can be given by:

$$SSC = RLC * WEC$$

The untapped SS potential (SSP) is estimated with the help of the Water Turnover Ratio (WTR):

$$WTR = MAI / RLC$$

- **RLC** • reservoir live storage capacity [hm^3]
- **WEC** • water equivalent coefficient [kWh/m^3] or [GWh/hm^3]
- **MAI** • mean annual inflows [hm^3]
  It is the most robust hydrologic variable to estimate water resources in the context of Alpine watersheds where dam reservoirs are operated in intra-annual cycle.

For each given reservoir:

a) MAI is estimated based on all contributing catchment surfaces and cumulated inflows (SFOENV database of PREVAH modelled monthly flows) from the natural catchment and all diversions

b) WEC is estimated based on average annual WEC per powerhouse from the annual cumulated production and addition of all partial WECs to obtain a representative value for the entire cascade (the downstream limits coincide with the concession limits).

▶ **If WTR > 1 ⇔ RLC < MAI** the mean annual inflows are higher than the dam capacity → increasing the storage volume is an option (e.g. by dam heightening).
The seasonal storage potential is then **SSP = WEC*(WTR- 1)*MAI** [GWh] where MAI-RLC is the amount of water in excess of RLC

▶ **If WTR < 1 ⇔ RLC > MAI** the existing storage capacity is larger than natural inflows to the reservoir → more water can be diverted to this reservoir (e.g. by gravity or pumped diversion from neighboring catchments)
The seasonal storage potential is then **SSP = WEC*(RLC-MAI)** [GWh], where RLC-MAI is the unused reservoir volume.

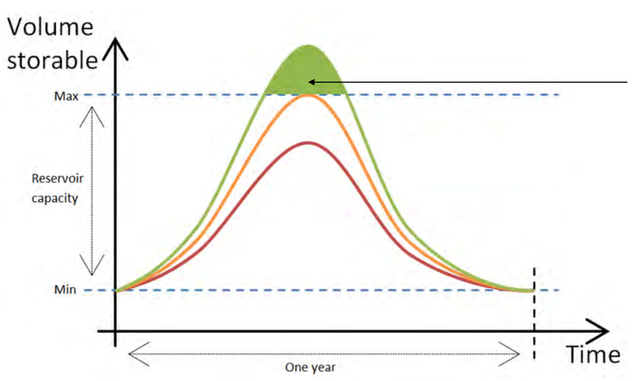

Fig.2 Typical curve of reservoir annual storage cycle (Akari 2016)

(4) Results

- We have analysed all Swiss hydropower reservoirs with a capacity above 1 million m^3 [3]:
  - 63 reservoirs > 1 hm^3
  - 40 reservoirs > 10 hm^3
  - 29 reservoirs > 30 hm^3
  - 36 reservoirs > 60 hm^3
- These 168 dams represent 8778 GWh of storage capacity, which is over 99% of the total Swiss hydropower storage capacity.
- The results show that a significant number of dams could increase storage in a significant way:
  - 48 dams could capture existing excess natural inflows if their current storage capacity were to be increased (green dots in Figure 3 below).
  - 7 dams are sub-optimally used, and could catch additional inflows using existing infrastructure (red bubbles in the figure below).

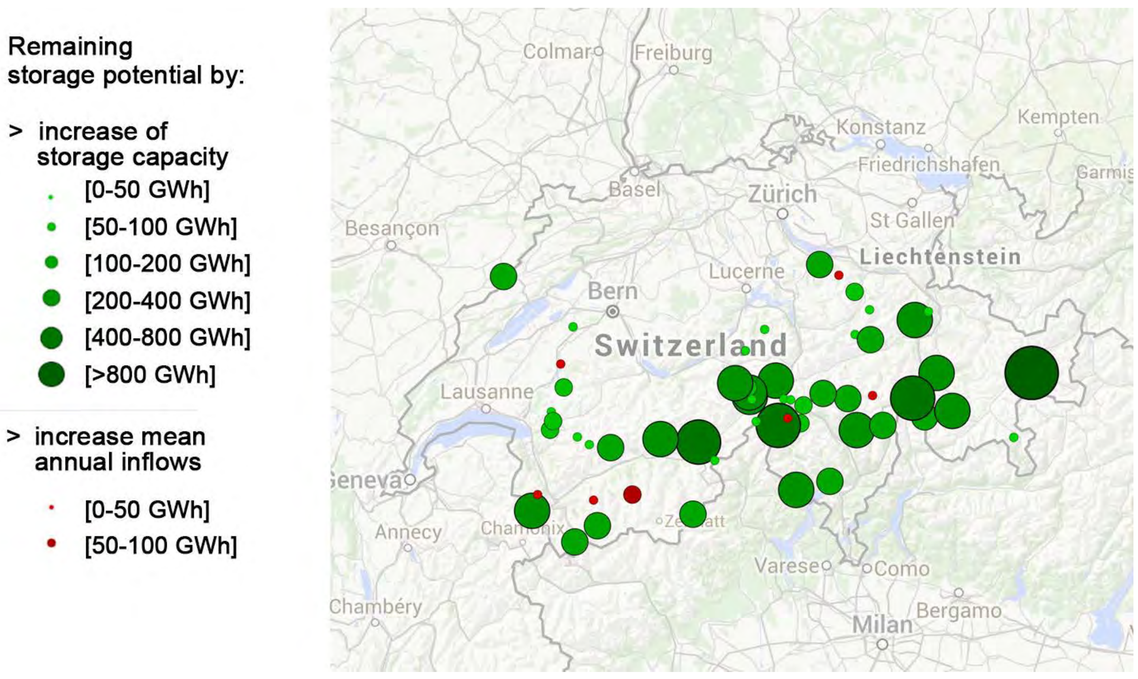

Fig. 3 Remaining hydropower storage potential per reservoir

(5) Conclusions

Based on our methodology and assumptions, 2 options exist to increase the seasonal storage capacity of Switzerland:

▶ **Increase storage capacity to capture excess natural inflows** (integrated river basin management by e.g. dam heightening, new dams, off-stream storage, reservoir interconnection) — **8000 GWh** (**98.5%** of potential)

▶ **Bring more water** (with additional inflows from pumping or gravity diversion from other basins) — **< 200 GWh** (**1.5%** of potential)

- The remaining storage potential of existing hydropower dams by catching additional inflows (through pumping or gravity diversions) into existing sub-optimal (oversized) reservoirs is less then **200 GWh**.
- Although relatively small, this contribution may increase in the future should the scenarios of glacier retreat and reduced annual inflows be confirmed as the result of climate changes in alpine catchments. This may help storing electricity from intermittent renewables (wind and solar).
- Based on the availability of excess natural inflows in several areas of Switzerland, the total remaining potential of hydropower storage is estimated to be about **8000 GWh**.
- Should this 8000 GWh potential be fully exploited, the seasonal storage capacity of hydropower in Switzerland would almost double. **Switzerland could then renew with electricity self-sufficiency, and thus avoid reliance on electricity imports in the winter season.**

References

1. Akari (2016), internship report, Energy Center, EPFL
2. SFOE, electricity statistics, 2015
3. SCD, Swiss Committee on Dams, Database of large Dams in Switzerland

SCCER SoE
SWISS COMPETENCE CENTER for ENERGY RESEARCH
SUPPLY of ELECTRICITY

SCCER-SoE Annual Conference 2016

In cooperation with the CTI
Energy
Swiss Competence Centers for Energy Research
Schweizerische Eidgenossenschaft
Confédération suisse
Confederazione Svizzera
Confederaziun svizra
Swiss Confederation
Commission for Technology and Innovation CTI

Design optimization of alpine desanding facilities

C. Paschmann, J.N. Fernandes, D.F. Vetsch, R.M. Boes – VAW, ETH Zurich

Short recapitulation of project objective

(*cf.* poster of SCCER-SoE Annual Conference 2015)

Hydro abrasive wear of turbines caused by sediments in the water has negative effects on the hydroelectric power generation. Desanding facilities are used as countermeasure, but they often do not operate satisfactorily. The design concepts shall be improved by means of a composite investigation, applying numerical simulations and field experiments at three desanding facilities. The latter comprised measurements of flow velocities and water turbidity, density and temperature.

Experimental setup and measurement routine

A ready-made system of trusses, a trolley and a motorized vertical linear unit have been employed. This setup was utilized as bearing structure for four acoustic Doppler velocimeters (ADV) and the point of water withdrawal in the basin (Fig. 1). It allowed moving the ADVs and the point of water withdrawal in the 3 directions of the basins.

By means of a mobile pump, a suction hose directed the water out of the basin and towards a Coriolis flow- and density meter and a turbidity sensor. At the end of that measuring line, water samples were collected for laboratory analyses.

At each facility, about 10 cross sections were monitored in terms of 3D flow velocities (80 points) and water turbidity, density and temperature (20 points). Additionally, turbidity measurements and water withdrawals were conducted in the inlet and outlet channels of the basins.

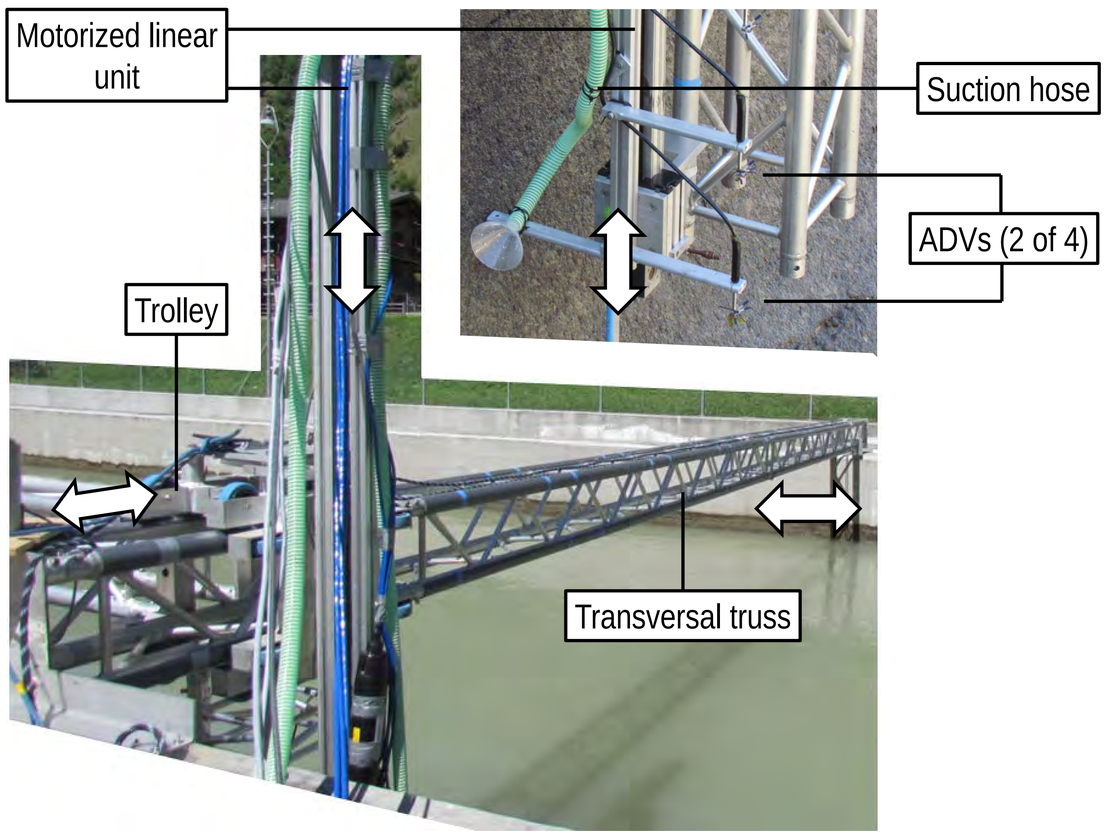

Figure 1 On-site modular bearing system including linear unit for the ADVs and the water sampling point (large picture); detail of ADV and water sampling point positioning (small picture); arrows indicate the direction of movement

Exemplary measurement results

The flow velocity data was averaged over time. The suspended sediment concentration (SSC) distribution was obtained by correlating the measured turbidities with the corresponding laboratory results of the taken water samples regarding SSC. Exemplarily, Fig. 2 shows contour plots of the normalized flow velocity distribution and distribution of the turbulent kinetic energy in three measurement cross sections of the facility *Saas Balen*. Fig. 3 shows the cross sectional SSC in comparison to the initial SSC in the diverted water at the same desanding facility.

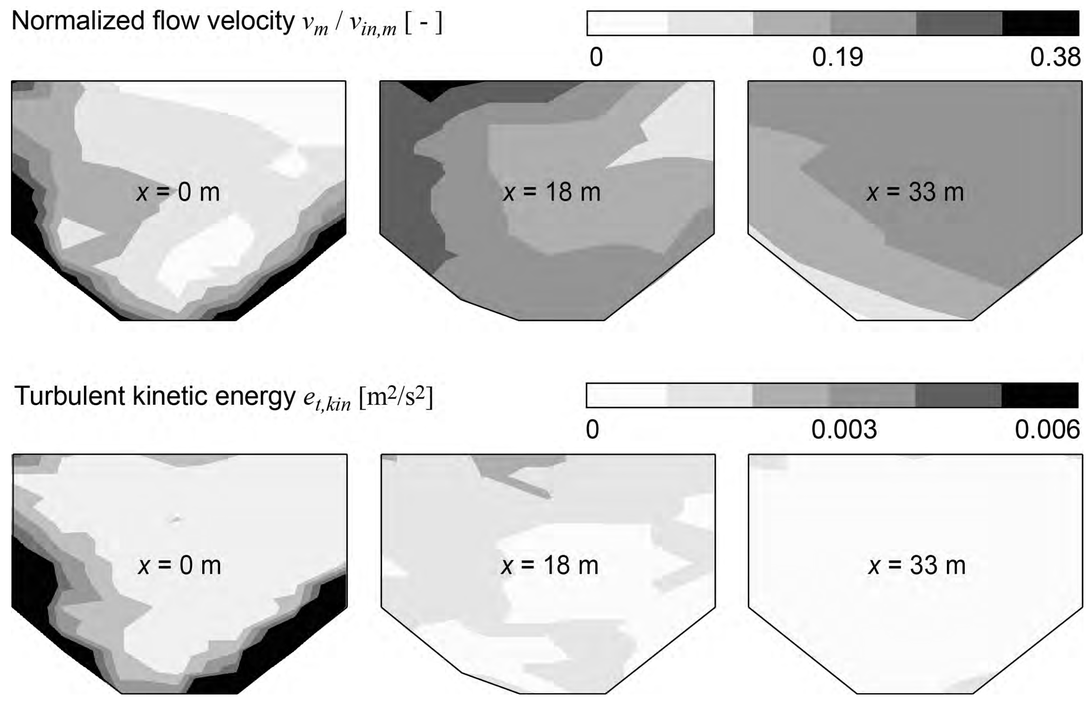

Figure 2 Contour plots of mean basin flow velocity magnitude v_m normalized with mean flow velocity in inlet channel upstream of basin $v_{in,m}$ (top) and turbulent kinetic energy $e_{t,kin}$ as a measure of turbulence (bottom) at the begin (x = 0 m), middle (x = 18 m) and end (x = 33 m) of the *Saas Balen* desanding facility.

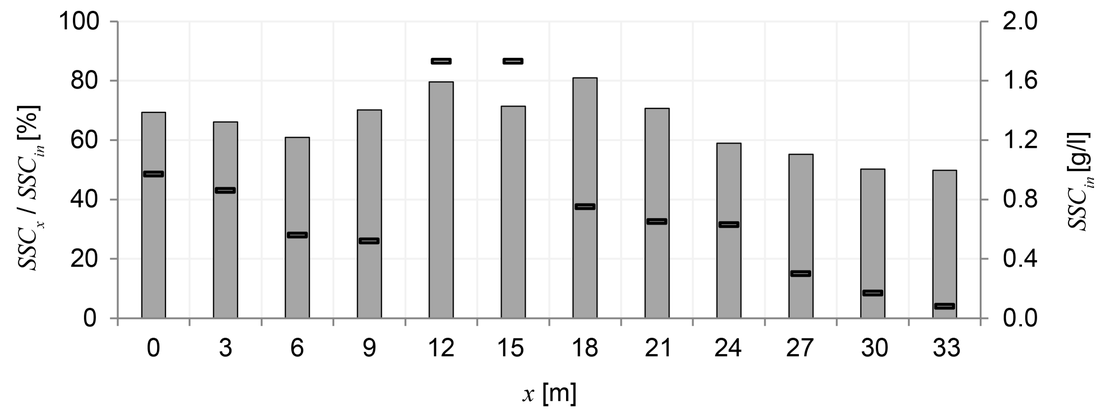

Figure 3 Cross sectional SSC_x normalized (columns) with instantaneous mean SSC_{in} in the inlet channel (horizontal bars) at the *Saas Balen* desanding facility.

Preliminary findings

- The hydraulic design of the investigated desanding facilities is inaccurate to achieve the targeted efficiency → demand for adapted design recommendations exists
- Identified linear correlation of turbidity and SSC could allow for instantaneous monitoring of SSC based on continuous turbidity measurements, provided that temporally varying SSC and particle size distribution are taken into account
- Tranquilizing racks at the basin inlet have a significantly influence on the flow field

Project status

Field experiments
Evaluation and preparation of measurement data
Calibration and validation of numerical model ← Aug. 2016
Systematic parameter studies
Design recommendations based on modelling results

Acknowledgement

This project is financially supported by the Swiss National Science Foundation (NRP70, No. 153861) and technically supported by the Swiss Federal Railways, EnAlpin and Gommerkraftwerke AG.

SCCER SoE
SWISS COMPETENCE CENTER for ENERGY RESEARCH
SUPPLY of ELECTRICITY

SCCER-SoE Annual Conference 2016

In cooperation with the CTI
Energy
Swiss Competence Centers for Energy Research
Schweizerische Eidgenossenschaft
Confédération suisse
Confederazione Svizzera
Confederaziun svizra
Swiss Confederation
Commission for Technology and Innovation CTI

Air-water flows in medium and high-head hydraulic structures

Numa Bertola[1], Hubert Chanson[2], Anton J. Schleiss[1]

[1] Laboratory for Hydraulic Constructions (LCH) – EPFL, [2] The University of Queensland, Australia
Corresponding author:numa.bertola@epfl.ch

Introduction

The present study focused on the aeration of a two-dimensional supported water jets impinging into a relatively large receiving water body at rest. At low approaching velocities, the entrainment of individual air bubbles and packets was documented. The air-water flow properties were measured in the free-falling jet and in the plunge pool.

Experimental apparatus and flow conditions

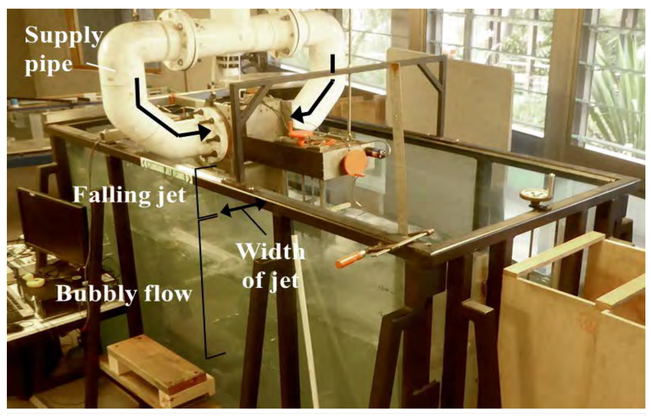

Figure 1. Plunging jet apparatus: jet nozzle and receiving water tank.

Planar jets were produced by a 0.012×0.27 m rectangular nozzle. A 0.35 m long PVC sheet supporting the free-falling jet running into a water tank (2.5 m long, 1 m wide and 1.5 m deep) (Fig. 1). Water was fed from a head tank for discharges smaller than 0.013 m^3/s, or by a high head pump for larger flow rates up to 0.037 m^3/s. The air-water flow impact velocities from 0.9 to 7.4 m/s,

Experiments were conducted with an ultra-high-speed camera (up to 10'000 fps), a dual-tip phase-detection, a Prandtl-Pitot tube, an Acoustic Displacement Meter (ADM) and a total pressure sensor.

Inflow turbulence and pre-entrainment

The free-falling jet was characterised by a rough free-surface through which pre-aeration took place. The free-surface disturbance was linked to the development of air-water shear layer originating at the nozzle edge, and upstream turbulence of the nozzle itself.

Fig. 2 shows the void fraction, bubble count rate, flow velocity, free-surface fluctuations and total pressure fluctuations in the jet. The mean jet thickness was larger than the theoretical value derived from mass and momentum conservation for clear-water because of the pre-aeration (Fig. 2a). The broadening of the free-surface air-water mixing layer was evidenced between the characteristic horizontal positions $y = Y_{10}$ and Y_{90} corresponding to void fractions of 0.1 and 0.9 respectively. The instantaneous pressure fluctuation was a superposition of velocity and void fraction fluctuations (Fig. 2b). The turbulence intensity, Tu was found to be proportional to pressure and jet thickness fluctuation amplitudes. The turbulence intensity was estimated in the order of 10^{-1}.

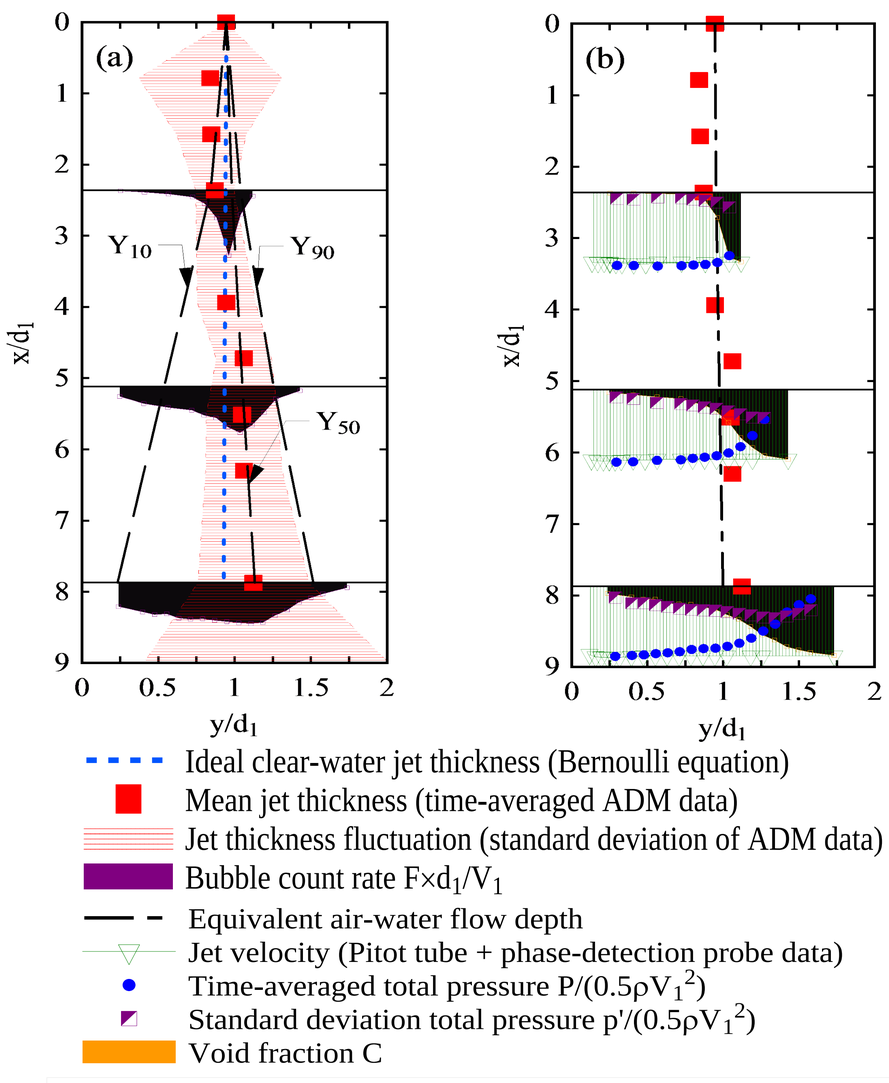

Figure 2. Dynamic characteristics of free-falling jet – two figures for the same jet with V_1 = 7.43 m/s.

Air entrainment mechanisms

The air entrainment mechanism at the impinging point were investigated. The number of entrained bubbles increased with increasing jet impact velocity. The entrainment of both individual bubbles and large air pockets was observed (Fig. 3). While single entrapped bubbles constituted the majority of entrained air entities at onset of air entrainment, the detachment of elongated air cavities became the predominant air entrainment mechanism for larger impact velocities (Fig. 4).

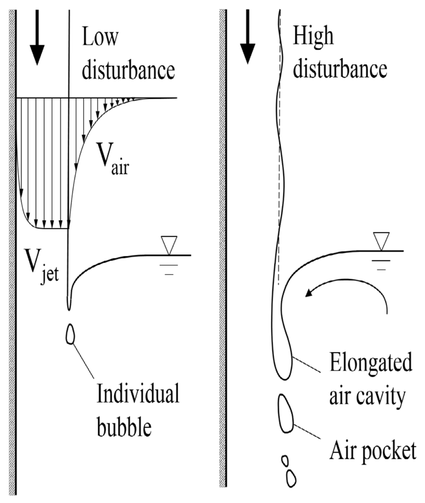

Figure 3. Air entrainment mechanisms for low disturbance jet (left) and high disturbance jet (right).

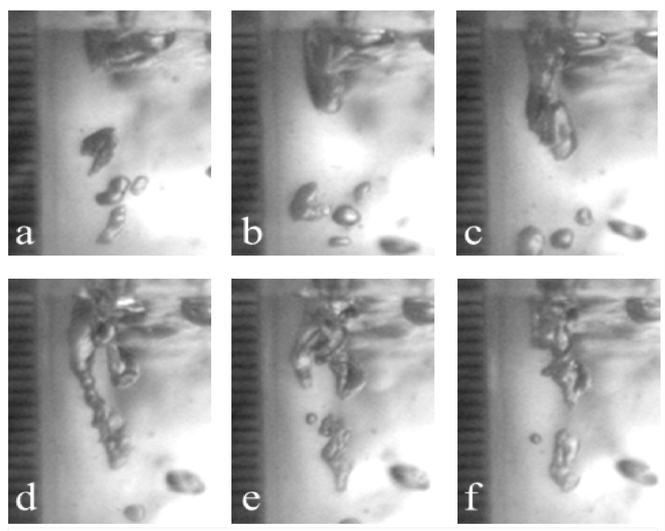

Figure 4. Air finger formation and air pocket pinch-off; flow conditions: V_1 = 1.26 m/s, x_1 = 0.05 m; (a) t = 0s, (b) t = 0.012s, (c) t = 0.023s, (d) t = 0.033s, (e) t = 0.036s, (f) t = 0.040s.

Air-water flow in the plunge pool

The bubble transport in the shear layer was an advective diffusion process, until, further down the pool, stagnation took place and buoyancy became the dominant driving force. Fig. 5a presents typical distributions of time-averaged void fraction C, dimensionless bubble count rate $F \times d_1/V_1$ and time-averaged air-water interfacial velocity V/V_1.

Both void fraction and bubble count rate profiles exhibited a unimodal shape with a marked maximum, although the positions of maximum void fraction and maximum bubble count rate did not coincide because the air diffusion layer and the shear layer did not overlap. The interfacial velocity profiles were quasi-uniform just below the impinging jet: i.e., $(x-x_1)/d_1 < 2$, $y/d_1 < 2.5$. Fig. 5b shows maximum void fraction decrease with increasing depth below the impingement point. The maximum bubble count rate increased further down of the impingement point until reached a maximum highlighting bubble breakup behaviour (Fig. 5c).

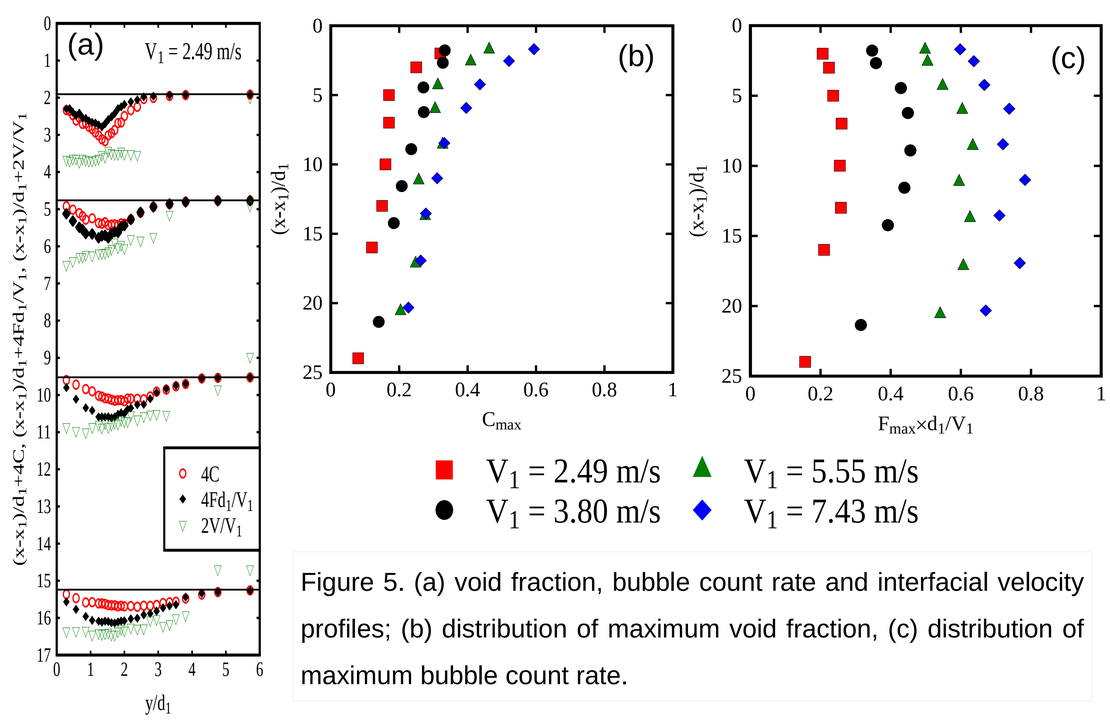

Figure 5. (a) void fraction, bubble count rate and interfacial velocity profiles; (b) distribution of maximum void fraction, (c) distribution of maximum bubble count rate.

Conclusion

New experiments were conducted on aeration in plunging jets. The fluctuations of jet thickness, total pressure and jet velocity in the free-falling jet were coupled with pre-aeration measurements. Several impinging flow patterns were characterised. The streamwise evolution of air-water flow properties were characterised downstream of the impingement point.

Acknowledgements

The author is grateful to Dr. H. Wang (UQ) for his support.

SCCER SoE
SWISS COMPETENCE CENTER for ENERGY RESEARCH
SUPPLY of ELECTRICITY

SCCER-SoE Annual Conference 2016

In cooperation with the CTI
Energy
Swiss Competence Centers for Energy Research
Schweizerische Eidgenossenschaft
Confédération suisse
Confederazione Svizzera
Confederaziun svizra
Swiss Confederation
Commission for Technology and Innovation CTI

Venting turbidity currents to reduce reservoir sedimentation

Sabine Chamoun, Giovanni De Cesare, Anton J. Schleiss

1. Motivation

The sedimentation of reservoirs is a process shortening their lifetime. Sediments transported into reservoirs during floods fill it up and replace volumes dedicated to water storage. Additionally, fine sediment blocks and clogs hydraulic structures such as intakes and outlets. The main means of transportation of fine sediments into reservoirs is through turbidity currents. The latter are triggered during yearly floods and plunge into reservoirs due to their higher density. Turbidity currents can travel long distances without dissipating until reaching the dam structure. Unless an outlet/intake is operating to evacuate the currents, the entrained sediments deposit and fill up the reservoir, blocking and damaging low-level structures.
In order the reduce reservoir sedimentation, the evacuation of turbidity currents can be an economic and environmental solution at the same time. The present research deals with venting of turbidity currents. Like any research, understanding the framework, gaps and needs is fundamental. The conditions to apply venting, its global application, as well as the most influential parameter affecting its efficiency are discussed. Finally, the practical and environmental benefits are exposed.

2. Conditions to vent turbidity currents

Before opting for venting turbidity currents to reduce reservoir sedimentation, dam operators should make sure some conditions are fulfilled:

- Indicators of the presence of turbidity currents: this includes observation of the plunging point where debris can be found floating at the upstream end of the reservoir or measurement of velocity and concentration.
- Maintenance of turbidity currents: some turbidity currents dissipate before reaching the dam. The efficiency of venting is very low in these cases.
- Availability of low-level or bottom outlets/intakes: these structures are ideally included in the dam structure during the design phase.
- Sufficient downstream capacity: venting operations can last for hours or days, therefore, downstream capacity should be available to contain large amounts of water and sediments.

Fig.1: Turbidity current reaching a bottom outlet

3. Venting globally

Despite the complexity of the operation of venting of turbidity currents, many countries in the world opted for this technique given the long-term losses that numerous reservoirs are encountering due to reservoir sedimentation.

Fig.2: Map locating the reservoirs applying turbidity currents venting

As it can be seen in Fig. 2, venting is applied worldwide. However, China is the country with the highest number of reservoirs applying venting. This is mainly due to the presence of the Yellow River, the river with the highest sediment load in the world. The efficiency of venting is highly variable from reservoir to another and from country to another depending on the regulations, the watershed morphology, as well as the financial means that offer the chance to use developed instrumentation for the detection of turbidity currents in reservoirs.

4. Outflow discharges

The efficiency of venting is analysed based on the ratio between the mass of sediments evacuated and the mass of sediments entrained by the turbidity current to the reservoir. Several parameters affect the efficiency of such operations. One of the main parameters that was highlighted in literature is the outflow discharge. The mass of sediments evacuated most probably increases with increasing discharges. However, the loss of clear water also increases. Thus, water losses should be a key criteria to optimize outflow discharges. The latter parameter is crucial in the investigation of turbidity currents venting. However, in order to identify the range of outflow discharges used during potential venting in Switzerland, an estimation of discharges corresponding to 2 and 10 year return period floods were estimated for 22 Swiss dams and compared to the capacity of their existing outlets. Results (Table 1) show that for the cases of Schiffenen, Moiry, and Rossens dams, venting is performed under restrained discharges. However, the maximum capacity of the outlet is rarely used, and the flood discharges usually underestimate the real discharge of turbidity currents due to the high clear water entrainment of the latter before reaching the dam. As a result, a reservoir such as Luzzone for instance would have Q_{outmax}/Q_2 = 110% instead of 193%. Hence, a focus on the investigation of venting under restrained outflow discharges would be more useful for field applications.

Table 1: Common outflow to inflow discharges of potential venting operations in Swiss Dams

Dam	Q_{outmax} [m³/s]	Q_2 [m³/s]	Q_{10} [m³/s]	Q_{outmax}/Q_2 [%]	Q_{outmax}/Q_{10} [%]
Schiffenen (3x outlets)	133	358	500	37	27
Moiry	55	104	153	53	36
Rossens (2x outlets)	150	263	373	57	40
Grande Dixence	35	32	49	110	71
Emosson	95	84	125	112	75
Mattmark	57	50	76	114	75
Rossinière (2x outlets)	193	146	213	131	90
Oberaar	26	18	29	143	90
Nalps	91	56	84	163	108
Mauvoisin	100	60	91	166	110
Zervreila	150	90	133	167	112
Punt dal Gall	200	118	174	169	115
Valle di Lei	123	69	103	179	119
Luzzone (direct)	52	27	42	193	123
Palagnedra	140	69	103	203	135
Santa Maria	124	56	84	223	147
Sambuco (direct)	53	23	36	228	145
Mapragg	214	76	114	280	188
Contra	340	100	148	339	230
Gebidem	250	73	110	342	228
Gigerwald	129	34	53	373	242
Rempen	192	48	73	400	263

5. Conclusions

Venting of turbidity currents to reduce reservoir sedimentation is an economical and environmental technique. However, it shall be used under certain conditions. Venting is applied worldwide and the efficiency of this operation depends on numerous parameters. One of the most important parameters is the outlet discharge. It was shown that for Swiss Dams, venting operations are potentially performed under restrained outflow discharges.

Acknowledgments: This research is funded by Swisselectric Research and the Swiss Committee on Dams.

SCCER SoE
SWISS COMPETENCE CENTER for ENERGY RESEARCH
SUPPLY of ELECTRICITY

SCCER-SoE Annual Conference 2016

In cooperation with the CTI
Energy
Swiss Competence Centers for Energy Research
Schweizerische Eidgenossenschaft
Confédération suisse
Confederazione Svizzera
Confederaziun svizra
Swiss Confederation
Commission for Technology and Innovation CTI

Optimisation des microcentrales de Riddes, avec étude de rehaussement du Lac des Vaux

Valentin Gaillard[1,2], Irene Samora[1], Azin Amini[1], Anton J. Schleiss[1]
[1]Laboratoire de Construction Hydraulique (LCH)- EPFL,[2]VAW-ETHZ
corresponding author: valentin.gaillard@epfl.ch

But du travail

Ce travail a pour principal objectif d'analyser les différentes possibilités d'optimisation de turbinage des eaux de la Commune de Riddes, comprenant :

- o l'eau potable;
- o les eaux usées;
- o l'eau pour l'enneigement mécaniques des pistes de ski.

Lac des Vaux [*Valentin, sept. 2013*]

Motivation

- o Utilisation du lac des vaux comme rétention
- o Optimisation du système existant de turbinage
- o Turbinage des eaux usées.

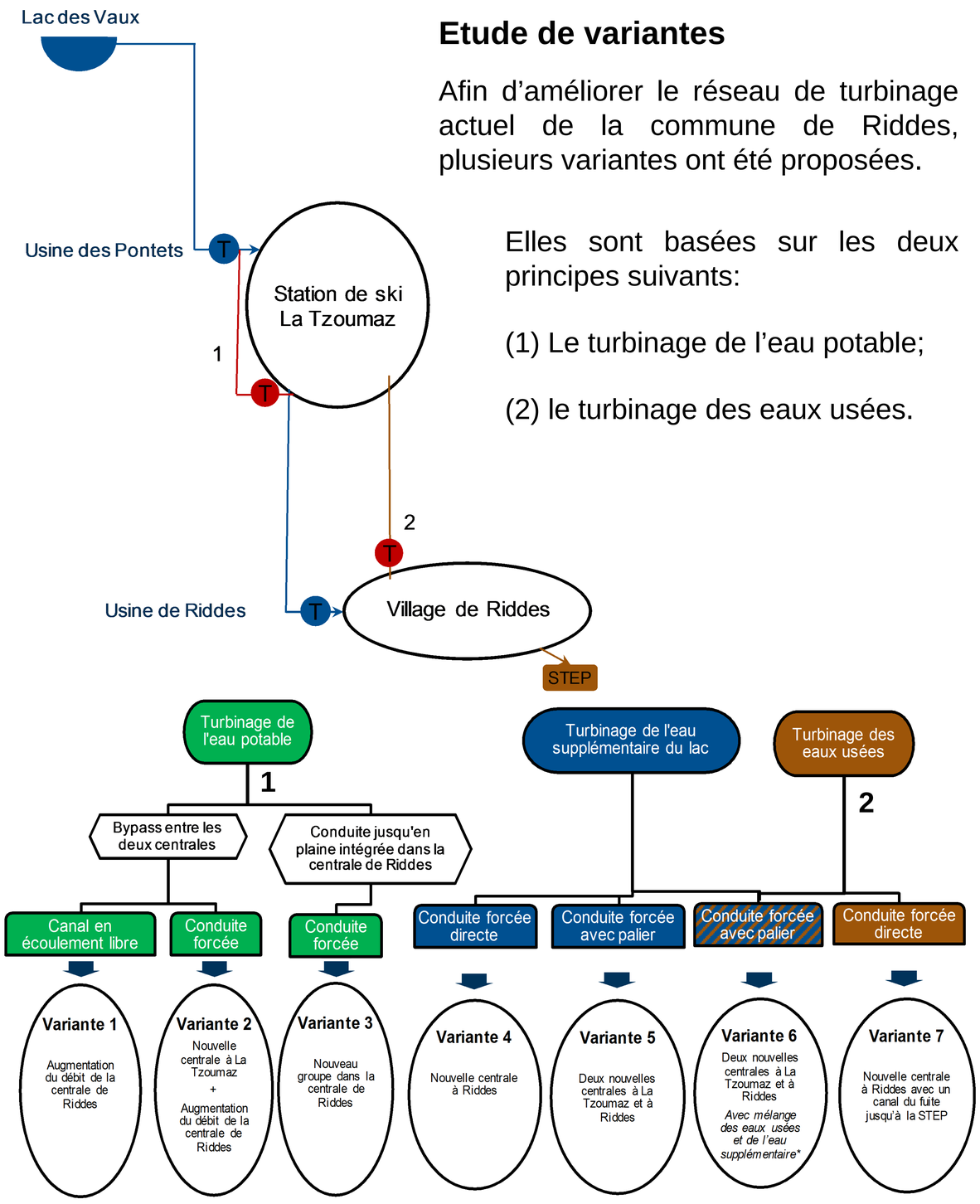

Etude de variantes

Afin d'améliorer le réseau de turbinage actuel de la commune de Riddes, plusieurs variantes ont été proposées.

Elles sont basées sur les deux principes suivants:

(1) Le turbinage de l'eau potable;

(2) le turbinage des eaux usées.

❖ Critère économique :

Coûts de production par kWh < Prix de vente RPC par kWh

❖ Etude comparative des variantes rentables

Aspects sociaux, environnementaux, fonctionnels, économiques et politiques.

➢ **Conclusion :** Le concept retenu propose deux projets

Le projet « Eau potable » pour turbiner l'eau potable du village entre le haut et le bas de La Tzoumaz.

Le projet « Eaux usées » pour turbiner les eaux usées de la station, amenées jusqu'à la STEP.

Projet « Eau Potable »

Le projet « Eau potable » a été dimensionné *selon [1]*.

- Débit équipé de **35 l/s**
- Turbine Pelton à deux jets
- Puissance de **119 kW**
- Production annuelle **env. 676 MWh/an**.
- Augmentation de la production de la centrale de Riddes d'env. **327 MWh/an**

Coûts de construction :

Génie civil:	1'540'000 CHF
Electromécanique:	240'000 CHF
Imprévus & Frais généraux:	840'000 CHF
Total:	**2.62 Mio CHF**

Durée estimée de la construction: **env. 12 mois**

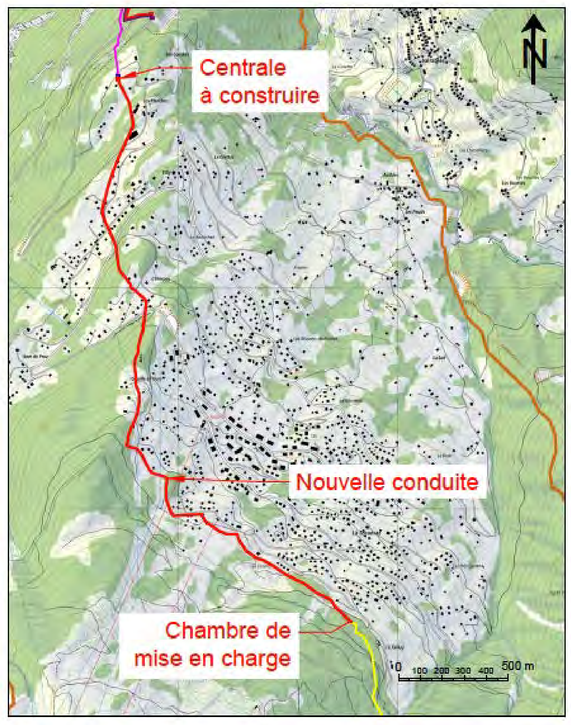

Projet « **Eaux Potable** », *modifié de [2]*

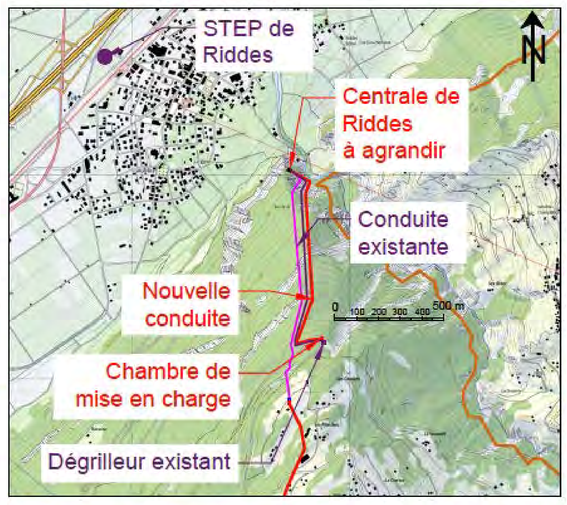

Projet « **Eaux Usées** », *modifié de [2]*

Projet « Eaux Usées »

Le projet « Eaux Usées » a été dimensionné *selon [1].*

- Débit équipé de **40 l/s**
- Turbine Pelton avec deux jets
- Puissance de **181 kW**
- Production annuelle d'env. **303 MWh/an**.

Variante avec utilisation de la conduite existante (*selon [3]*)

- en fonction depuis les années **1990**,
- en **fonte ductile** de **300 mm** de diamètre et
- d'une pression nominale de **64 bar**

Il en ressort que l'**utilisation des installations existantes** permet au projet d'être autofinancé.

Coûts de construction :

Génie civil :	110'000 CHF
Electromécanique:	252'000 CHF
Imprévus & Frais généraux:	136'000 CHF
Total:	**498'000 CHF**

Durée estimée de la construction: **env. 2 mois**
plus **4 mois** pour la construction d'une nouvelle conduite

Références

[1] A. J. Schleiss, « *Aménagements hydrauliques* », 2015.

[2] Swisstopo, « *map.geo.admin.ch* », 2016.

[3] Commune de Riddes, « www.riddes.ch », 2015.

SCCER SoE
SWISS COMPETENCE CENTER for ENERGY RESEARCH
SUPPLY of ELECTRICITY

SCCER-SoE Annual Conference 2016

In cooperation with the CTI
Energy
Swiss Competence Centers for Energy Research
Schweizerische Eidgenossenschaft
Confédération suisse
Confederazione Svizzera
Confederaziun svizra
Swiss Confederation
Commission for Technology and Innovation CTI

Aeration and two-phase flow characteristics of bottom outlets

Benjamin Hohermuth, Lukas Schmocker, Robert Boes

Motivation and Objective

Bottom outlets are a key safety feature of large dams. Future demands on bottom outlets will likely increase due to (i) dam heightening as promoted by the Swiss energy strategy 2050 and (ii) more frequent sediment flushing following increasing reservoir sedimentation rates. The high-speed free surface flow downstream of a bottom outlet gate leads to problems with cavitation and gate vibration (Fig. 3). These problems can be mitigated by sufficient aeration. However, current knowledge does not allow for a coherent design of the air vent. This PhD project aims to enhance design guidelines to ensure the safe operation of bottom outlets.

Hydraulic model tests

The Froude scale hydraulic model features a rectangular tunnel cross-section 0.2 m wide and 0.3 m high, with a maximum length of 20.7 m (Fig. 1). Two high-head pumps deliver a discharge Q_w up to 600 l/s at an energy head H_E of 30 m w.c. The investigated parameters are shown in Fig. 2.

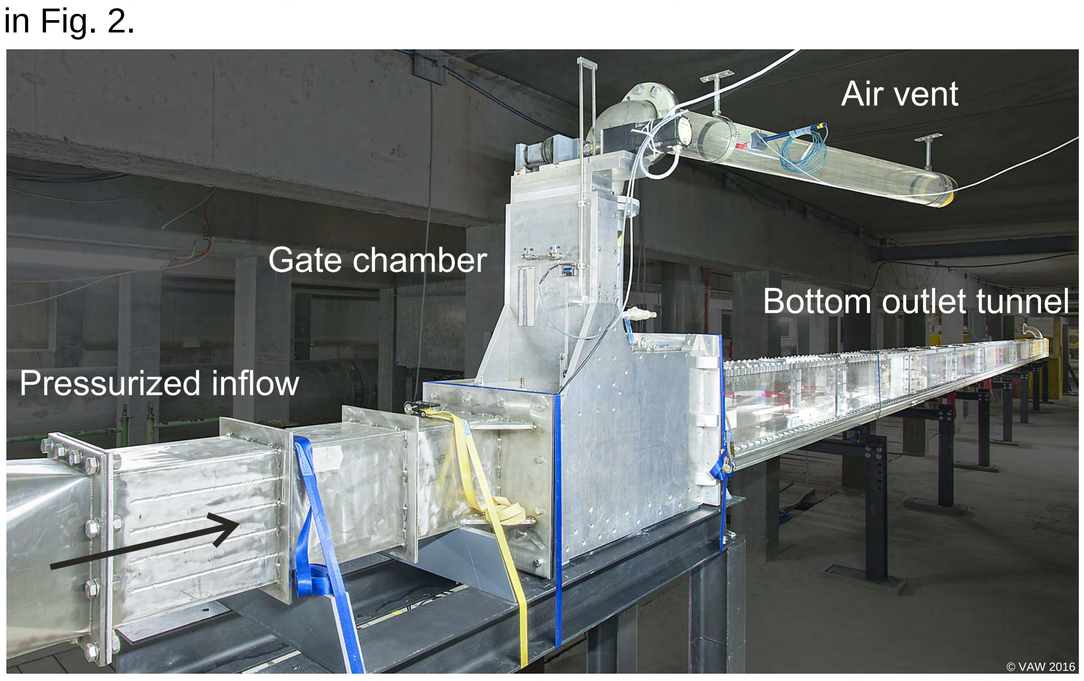

Fig. 1: Hydraulic scale model at Laboratory of Hydraulics, Hydrology and Glaciology (VAW)

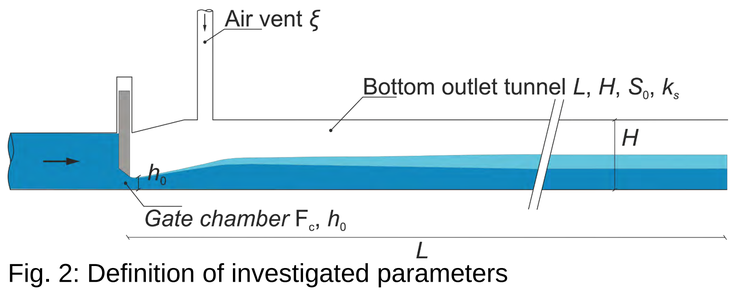

Fig. 2: Definition of investigated parameters

Parameters:
F_c – Froude number at vena contracta
H – Tunnel height
h_0 – Gate opening
k_s – Tunnel roughness
L – Tunnel length
S_0 – Tunnel slope
ξ – Air vent loss coefficient

Field measurements

Air flow in the air vent and from the tunnel outlet as well as air pressures along the tunnel are measured at Luzzone and Malvaglia arch dams (Fig. 4). With a dam height of 225 m for Luzzone and 90 m for Malvaglia the data add to the scarce prototype data for high-head dams.

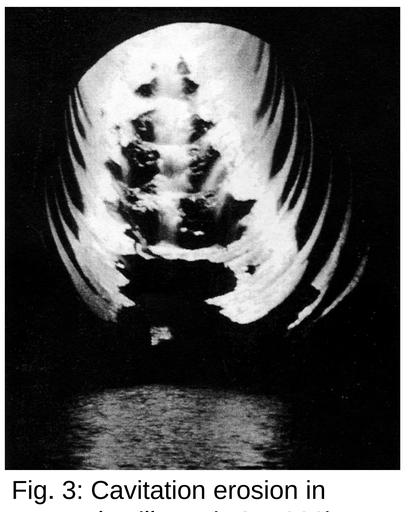

Fig. 3: Cavitation erosion in a tunnel spillway (ACI 1998)

Fig. 4: Malvaglia arch dam

Acknowledgement

Project is funded by the Swiss National Science Foundation (No. 163415). Field measurements are supported by Lombardi Engineering Foundation.

Preliminary results – Air demand

The comparison of model data, available prototype data and existing design equations reveals a large scatter (Fig. 5). In the free flow region (F_c < 30) the model data compare well with the prototype values. For F_c > 30 the model underestimates the air demand, thus spray flow can not be modelled.

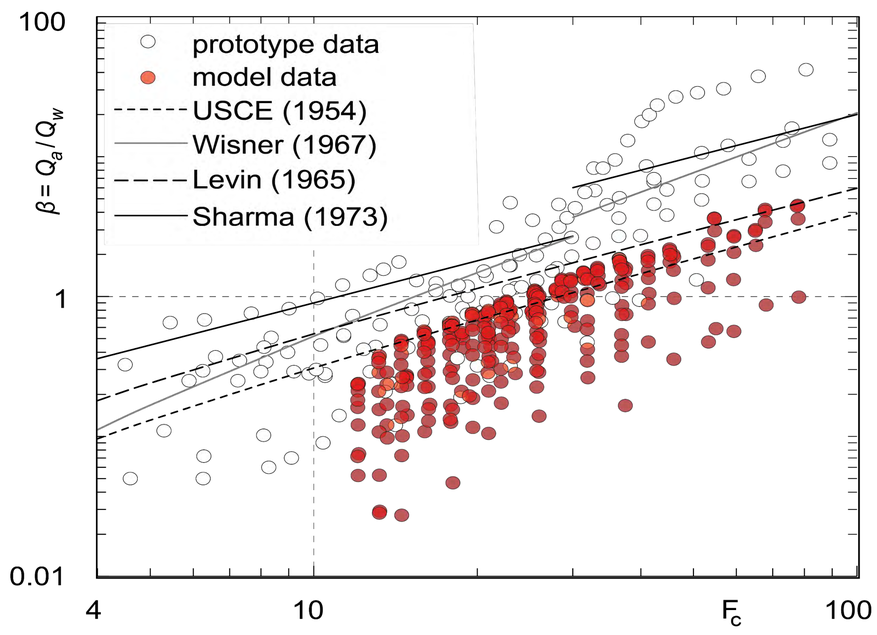

Fig. 5: Comparison of prototype and model data with existing design equations

The dimensional analysis indicates that the air demand $\beta = Q_a/Q_w$ depends on the Froude number F_c, relative opening h_0/H, ξ, relative tunnel length L/H and tunnel slope S_0. For a given geometric configuration the air demand is mainly a function of F_c (Fig. 6). High loss coefficients ξ lead to a smaller air vent flow and consequently to larger negative pressures in the gate chamber. The relative tunnel length has a comparably small effect on the air demand for the investigated range. However, the air flow from the tunnel outlet increases strongly with decreasing L/H.

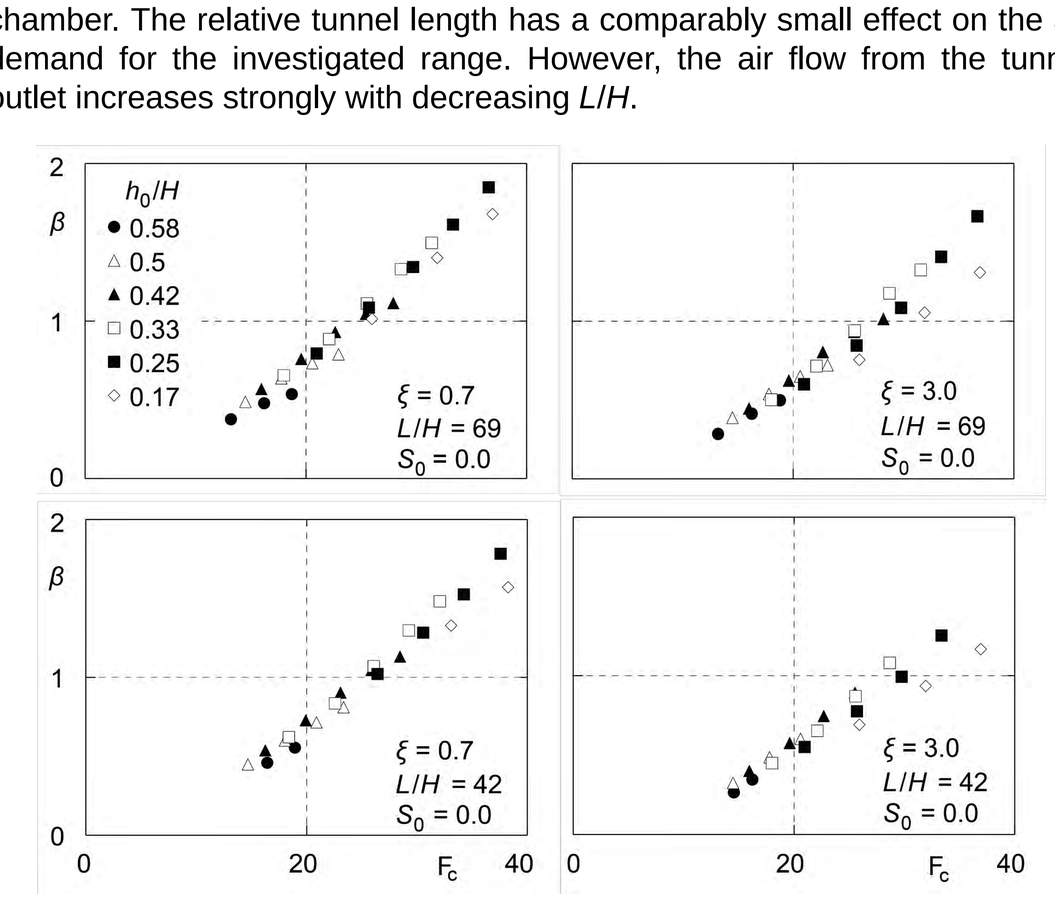

Fig. 6: Air demand for various geometric boundary conditions (model data)

Further analysis of the air demand includes the variation of S_0. Future investigations will also focus on the air concentration distribution to establish criteria regarding cavitation protection.
Field measurements will be conducted yearly over the whole project duration.

References

American Concrete Institute (ACI) (1998). Erosion of Concrete in Hydraulic Structures. *ACI Commitee Report 210*.

Levin, L. (1965). Calcul hydraulique des conduits d'aération des vidanges de fond et dispositifs déversants. *La Houille Blanche*, No. 2, 121-127 (in French).

Sharma, H.R. (1973). Air demand for high head gated conduits. *PhD thesis*. The Norwegian Institute of Technology, Trondheim.

US Corps of Engineers (USCE). (1964). Air demand – regulated outlet works. *Hydraulic design criteria*, sheet 050-1/2/3, 211-1/2, 212-1/2, 225-1.

Wisner, P. (1967). Air entrainment in high speed flows. *Proc. 9th ICOLD Congress*, Istanbul, 495-507.

SCCER SoE

SWISS COMPETENCE CENTER for ENERGY RESEARCH
SUPPLY of ELECTRICITY

SCCER-SoE Annual Conference 2016

In cooperation with the CTI

Energy
Swiss Competence Centers for Energy Research

Schweizerische Eidgenossenschaft
Confédération suisse
Confederazione Svizzera
Confederaziun svizra

Swiss Confederation

Commission for Technology and Innovation CTI

Real-time monitoring of suspended sediments for turbine wear mitigation in hydropower plants

J. Fernandes, D. Felix, I. Albayrak, R. Boes – VAW, ETH Zurich

1. Introduction

Hard minerals of the suspended sediments present in water may cause hydro-abrasive erosion in the turbine components of medium- and high-head hydropower plants (HPP) (Fig. 1).

The changes in the geometry of turbines due to erosion reduce turbine efficiency and hence power generation at HPP. Together with substantial maintenance costs, revenue and sustainable use of HPP are negatively impacted.

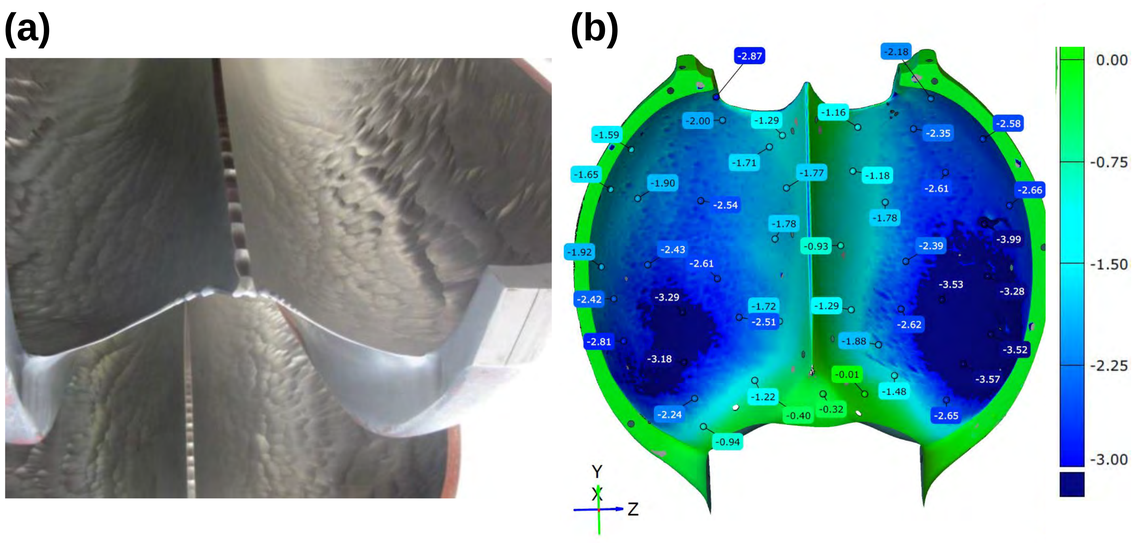

Fig. 1. (a) Photographic image and (b) 3d erosion of one bucket of Pelton turbine (courtesy of TIWAG).

To mitigate turbine erosion and to optimize design and operation of hydraulic structures,

Suspended sediment monitoring in HPPs is of paramount importance

2. Sediment characteristics to be monitored

The erosion potential depends on the following parameters [1] :

- suspended sediment concentration (SSC);
- particle size distribution (PSD);
- particle shape;
- particle density;
- particle hardness and mineralogical composition.

The **particle shape** and **hardness** are quantified from microscope images and mineralogical analysis, respectively. The solid **density** is determined in the laboratory with a pycnometer. These characteristics are assumed to remain constant as they mainly depend on the properties of the catchment area.

However, **SSC** and **PSD** are subjected to strong and quick temporal variations depending on the site conditions and hence needs to be continuously monitored.

3. Monitoring sites

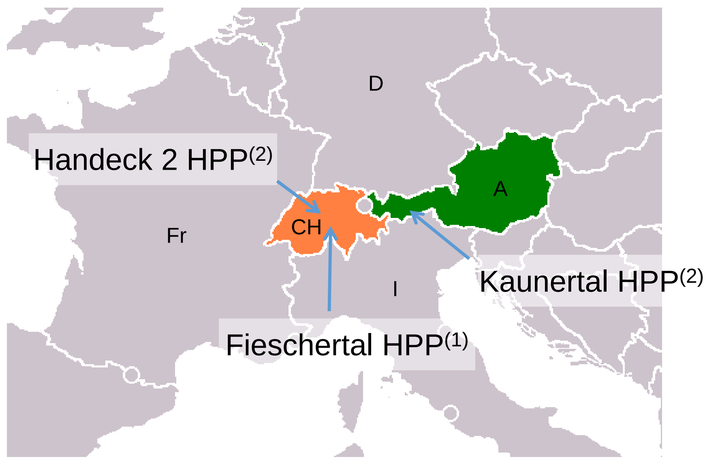

Fig. 2. Location of the monitoring sites.

(1) Continuous monitoring since 2012

(2) Temporary monitoring (≈ 1 month during drawdown of the reservoir)

4. Setup and methods

The water was collected from the valve chamber at Fieschertal HPP (Fig. 3), in the penstock at Kaunertal HPP and from the tailwater in Handeck 2 HPP. This poster focuses on the first HPP. The monitoring comprised the following methods, of which (1) to (3) are in real-time:

(1) Turbidimeter – turbidity → SSC
(2) Laser diffraction (LISST) – volume concentrations → SSC and PSD
(3) Coriolis flow and density meter (CFDM) – density → SSC
(4) Gravimetric method – SSC and PDS from water samples

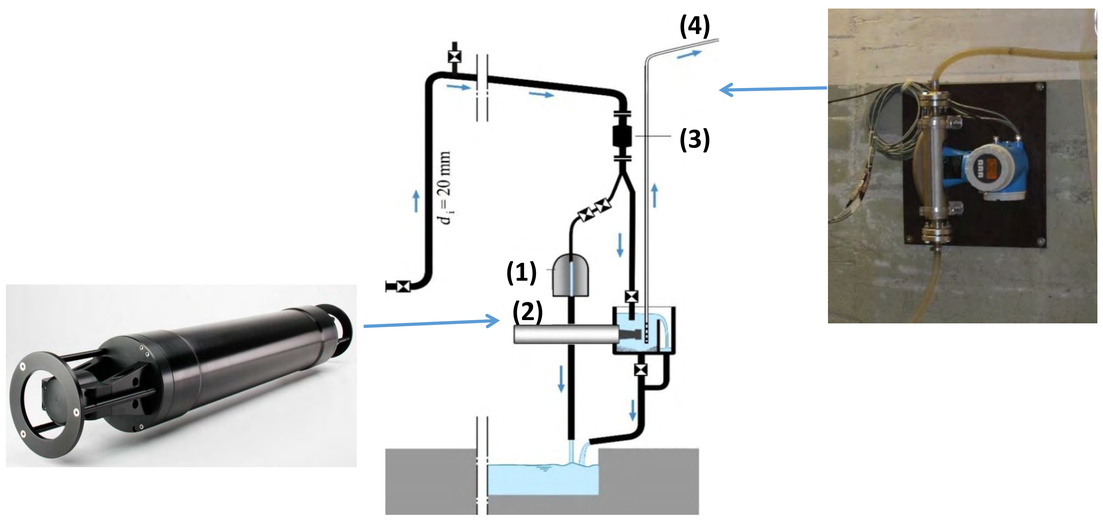

Fig. 3. Schematic setup [2].

5. Results and discussion

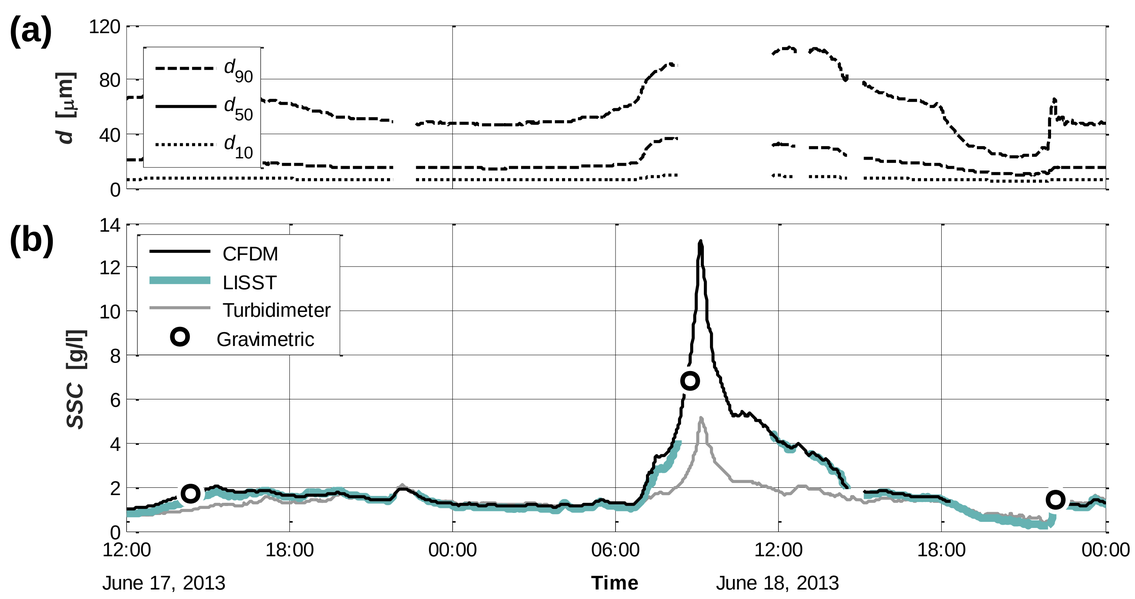

Fig. 4. (a) PSD from LISST and (b) SSC in the valve chamber of Fieschertal HPP .

- High SSC was captured by CFDM (in this case up to ≈ 13 g/l)
- Low values of SSC from LISST and CFDM are well correlated
- High SSC could not be measured by LISST but this equipment offers the advantage of providing PDSs
- The higher values of SSC measured by the turbidimeters are below the CFDM values which may be attributed to their calibration based on low SSC and fine particles
- Water sampling is highly recommended for calibration and validation
- Moreover, the redundancy of instruments or measurement techniques will improve the quality and reliability

6. Operation optimization

- The combination of LISST and CFDM is an economic option for the measurement of SSC in a wide range and PSD at HPPs
- The possibility of conveying sediment-laden water via turbines can be an option to cope with reservoir sedimentation regarding that the concentrations are kept low
- Temporary switch-offs during periods of high SSCs mitigate the turbine erosion

References

[1] Karelin V., Denisov A., Wu Y. (2002). Fundamentals of hydroabrasive erosion theory. In Abrasive Erosion & Corrosion of Hydraulic Machinery, Duan C. G. and Karelin V. Y (eds.)., Imperial College Press, London: 1-51.

[2] Felix D., Albayrak I., Abgottspon A. and Boes R. (2016) Real-time measurements of suspended sediment concentration and particle size using five techniques. Proc. 28th IAHR Symp. on Hydraulic Machinery and Systems, Grenoble: 1057-1066, IOP Conf. Series.

SCCER SoE
SWISS COMPETENCE CENTER for ENERGY RESEARCH
SUPPLY of ELECTRICITY

SCCER-SoE Annual Conference 2016

In cooperation with the CTI
Energy
Swiss Competence Centers for Energy Research
Schweizerische Eidgenossenschaft
Confédération suisse
Confederazione Svizzera
Confederaziun svizra
Swiss Confederation
Commission for Technology and Innovation CTI

Landslide generated impulse waves in reservoirs

Frederic Evers, Lukas Schmocker, Robert Boes

Objective

Landslide generated impulse waves are caused by mass wasting events such as rapid subaerial landslides, avalanches or glacier collapses. These impulse waves represent a particularly relevant natural hazard for reservoirs in the Alpine environment. Fig. 1 shows the three stages of an impulse wave event in a reservoir.

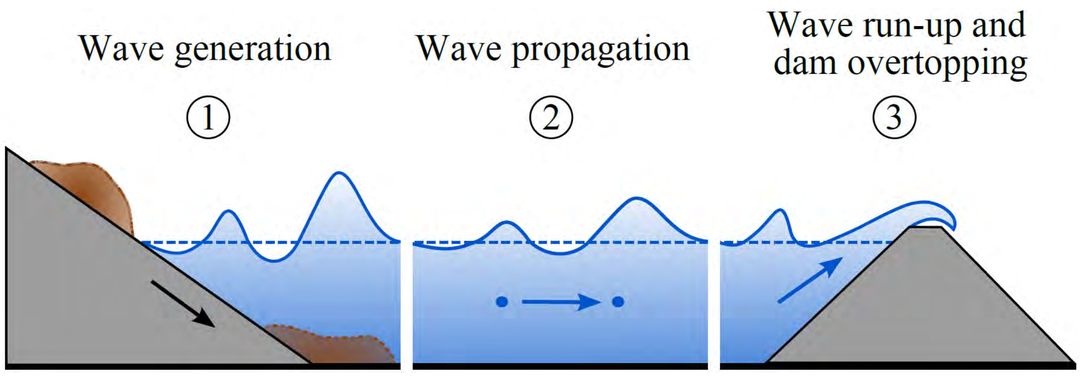

Fig. 1: Three impulse wave stages

Due to glacial retreat, new regions in the Alpine environment become available to hydropower, which may provide an important contribution to the Energy Strategy 2050. However, these regions feature steep and instable slopes, so that mass wasting is a concern. Official regulations require dam operators to take impulse wave hazards into account. Therefore, research at the Laboratory of Hydraulics, Hydrology and Glaciology (VAW) at ETH Zurich aims at providing generally applicable methods for hazard assessments, besides gaining insight into the physical processes related to impulse waves.

Spatial wave propagation

General reservoir geometries feature a spatial 3D layout. Starting from a limited impact zone, the generated wave train propagates radially in all directions (Fig. 3a). To assess whether the impulse wave represents a threat to the shore or the dam, it is of crucial importance to understand the process of impulse wave height decay along its propagation route. Experiments were conducted (Fig. 3b), in which the free water surface was tracked with a videometric measurement system, yielding an unprecedented density of spatial data of the entire water surface elevation and the impulse wave propagation process (Evers & Hager 2016).

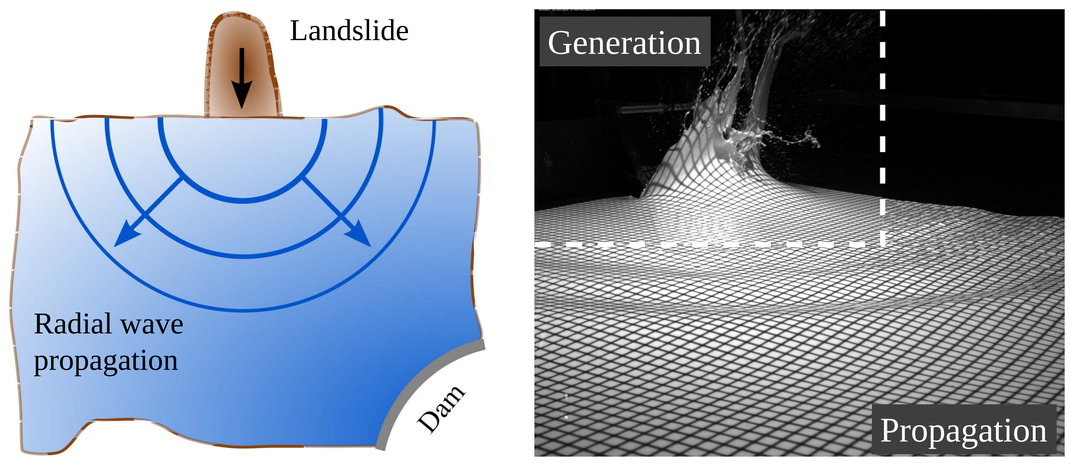

Fig. 3: (a) Spatial wave propagation pattern in a reservoir, (b) impulse wave generation and propagation in the VAW wave basin

Case study and field tests

Within the CTI project FLEXSTOR an assessment of the impulse wave hazards at the future Trift Reservoir currently planned by KWO AG was conducted based on Heller *et al.* (2009) (Fig. 2). In order to validate numerical schemes and empirical equations derived from laboratory experiments for the prediction of impulse wave features, additional large scale field experiments are in the planning stage.

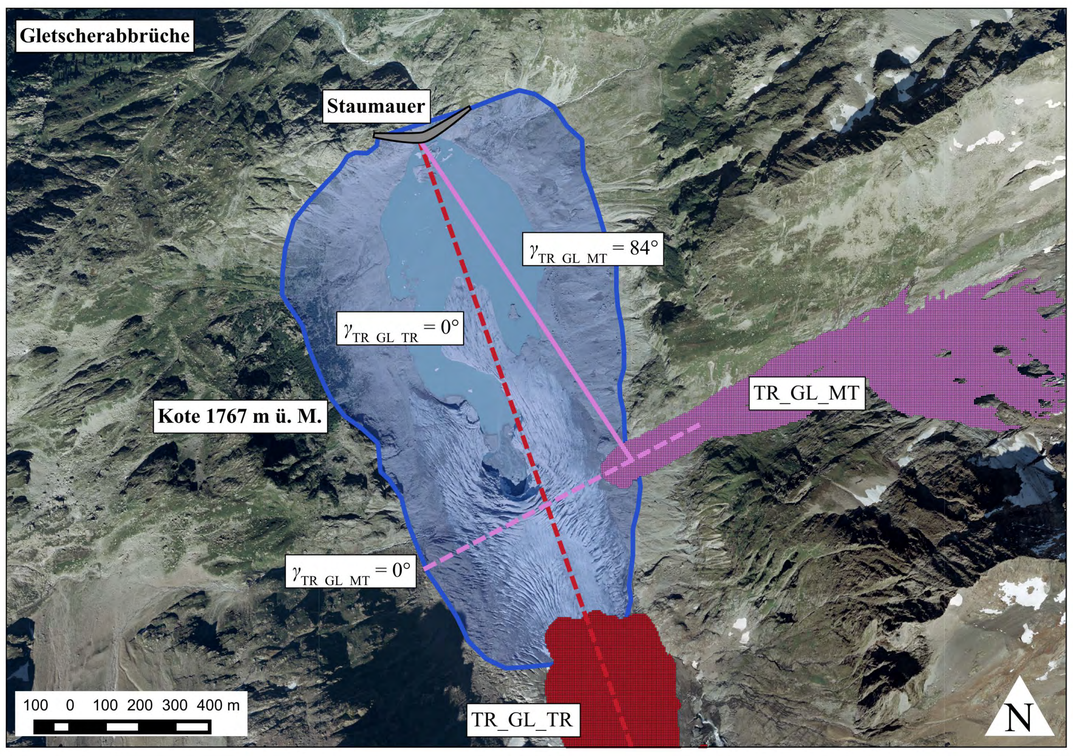

Fig. 2: Ice avalanche scenarios and propagation angles of impulse waves for future Trift Reservoir (KWO AG / in planning stage)

Dam structure overtopping

Dam structures typically represent the lowest section of a reservoir's shoreline and are therefore particularly prone to wave overtopping, which may cause damage at the dam structure as well as downstream flooding. Kobel *et al.* (2016) conducted overtopping experiments in a 2D wave channel for various dam geometries, wave parameters and freeboards (Fig. 4). Equations were derived for the overtopping volume, flow depth, and duration.

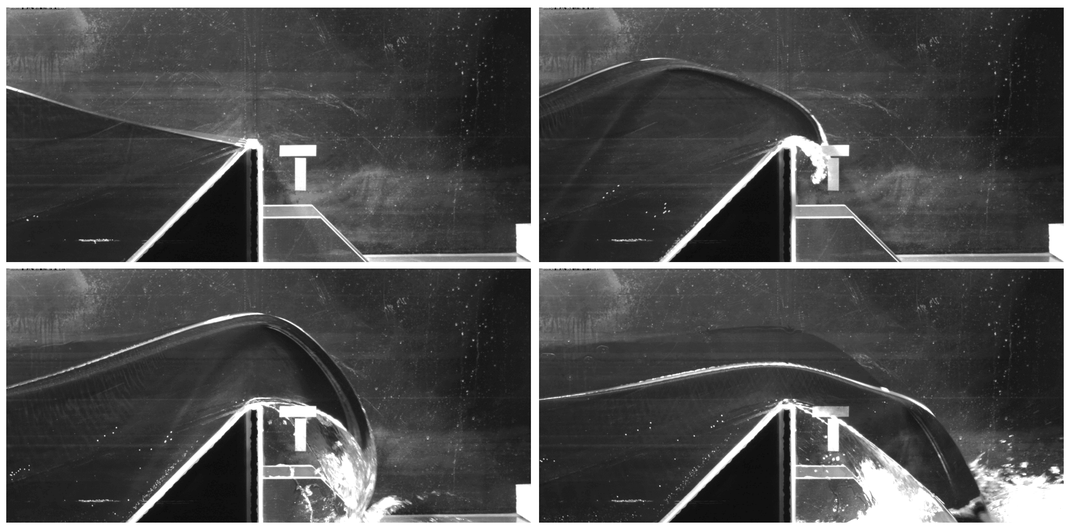

Fig. 4: Wave overtopping experiment in the VAW wave channel

ETH zürich
VAW
Laboratory of Hydraulics, Hydrology and Glaciology

Contact

evers@vaw.baug.ethz.ch
schmocker@vaw.baug.ethz.ch
boes@vaw.baug.ethz.ch

F. M. Evers is funded by the Swiss National Science Foundation (Project No. 200021-143657/1)

References

Evers, F.M.; Hager, W.H. (2016). Spatial impulse waves: wave height decay experiments at laboratory scale. *Landslides.* (advance online publication) doi:10.1007/s10346-016-0719-1

Heller, V.; Hager, W.H.; Minor, H.-E. (2009). Landslide generated impulse waves in reservoirs: Basics and computation. *VAW-Mitteilungen* 211, R.M. Boes, ed., ETH Zurich.

Kobel, J.; Evers, F.M.; Hager, W.H. (2016). Impulse wave overtopping at rigid dam structures. *Journal of Hydraulic Engineering.* (submitted)

SCCER SoE

SWISS COMPETENCE CENTER for ENERGY RESEARCH
SUPPLY of ELECTRICITY

SCCER-SoE Annual Conference 2016

In cooperation with the CTI

Energy
Swiss Competence Centers for Energy Research

Schweizerische Eidgenossenschaft
Confédération suisse
Confederazione Svizzera
Confederaziun svizra

Swiss Confederation

Commission for Technology and Innovation CTI

Potential for future hydropower plants: A systematic analysis of the periglacial environment

D. Ehrbar, I. Delaney, L. Schmocker, A. Bauder, M. Funk, D. F. Vetsch, R. M. Boes – VAW, ETH Zurich

1. Sediment and the Swiss Alps

Climate change and glacier retreat are thought to have caused increased sedimentation in glacierized catchments:
– glacier retreat results in exposure of easily erodible sediments.
– increased glacial runoff could be eroding greater amounts of subglacial sediment.

This has implications for downstream hydropower operators such as:
– deposition of sediments in reservoirs reduces capacity, which require expensive maintenance, such as sediment flushings.
– increased abrasion of turbines and other infrastructure, reducing durability.

Although increased water discharges in the future could favor hydropower operations, larger sediment discharges pose challenges in terms of construction, operation and maintenance. This project aims to assess and model process controlling the erosion of sediment from glacial and periglacial areas and its subsequent deposition in reservoirs.

Figure 1: Griesgletscher in 1986 and 2007. Photos from M. Funk.

2. Reservoir Sedimentation

2.1 Methods

Field measurements:
– Lac de Mauvoisin
– Griessee
– Gebidem

Measuring units:
– suspended sediment concentration (SSC)
– particle size distribution (PSD)
– flow velocities (FV)

Measuring techniques:
– water sample analysis (WSA) with weighing and laser diffraction
– acoustic Doppler current profiler (ADCP) RiverSurveyor M9
– Laser in-situ scattering and transmissometry (LISST) LISST-100X

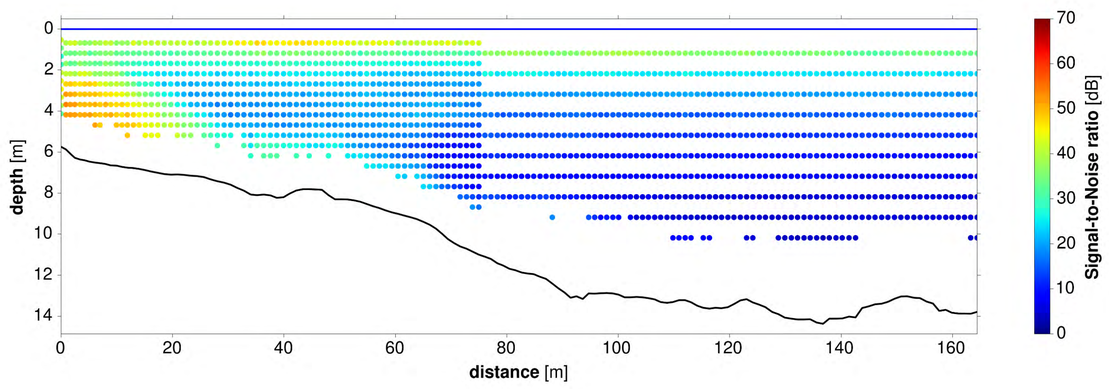

Figure 2: SNR values (proxy for sediment concentration) of an ADCP transsect in Griessee on 8 August 2016 (flow direction: from left to right)

2.2 Results and Discussion

Sediment fluxes in reservoirs:
– median diameters of suspended sediments 2-20 µm (fine-coarse silt)
– average concentrations of 60-100 mg/l in most parts of the reservoir

Application ranges of measuring techniques:
– WSA: depths < 20 m, provides both SSC and PSD
– ADCP: depths < 30 m, provides FV and qualitative[1] SSC profiles over the whole depth range at the same time
– LISST: no depth limitations, provides both SSC and PSD at the same time in certain depth

[1] due to low SSC, no quantitative evaluation is possible

3. Sediment dynamics in the glacial environment

To assess supply sediment from glacierized catchments two processes must be investigated:
1) erosion of unconsolidated sediment in the glacier proglaical area.
2) glaciological processes that effect transport of subglacial sediment.

Periglacial erosion: the Griesgletscher was used to examine periglacial erosion. Annual DSMs were made from aerial photographs from 1986 to 2014 and subtracted.

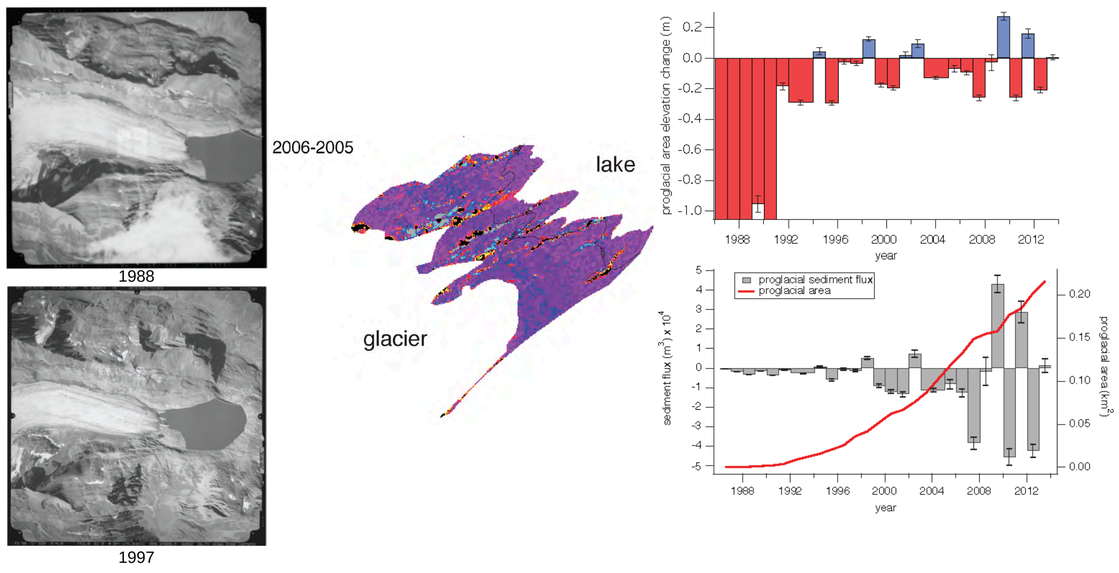

Figure 3: Aerial photographs, DSM subtraction and height volume change.

Hydrology Comparison:
– extreme erosion: higher late-season runoff and maximum runoff over long time periods.
– extreme deposition: runoff variability and maximum runoff on short time periods suggesting higher subglacial water pressures and erosion.

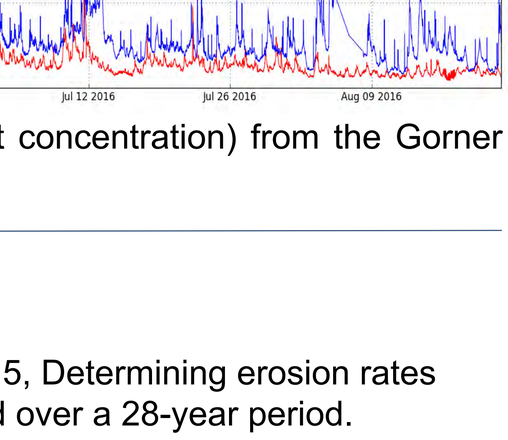

Figure 4: Gries catchment runoff

Subglacial erosion: turbidity meters installed near the outlets of the Gornergletscher and the Aletschgletscher show trends in suspended sediment concentrations originating from subglacial sources. This data will be used to verify subglacial hydraulic models which incorporate sediment dynamics.

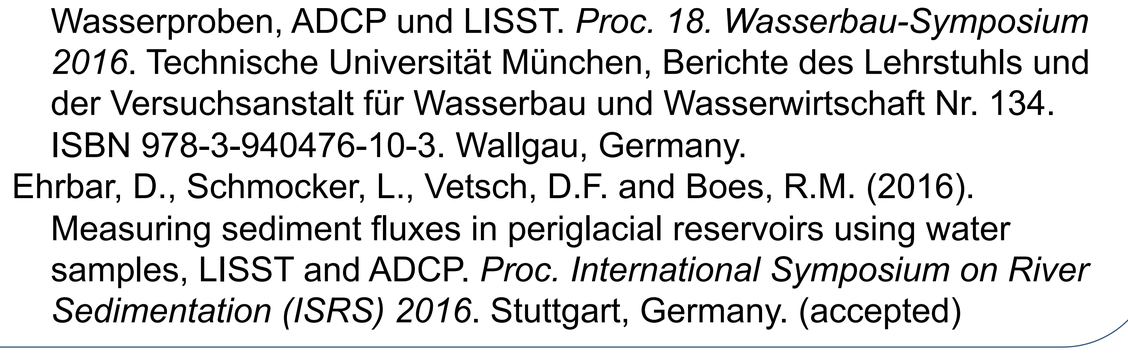

Figure 5: turbidity (proxy for sediment concentration) from the Gorner and Aletsch glaciers.

Publications and presentations

Delaney, I., M. Huss, Y. Weidmann, 2015, Determining erosion rates and processes in a glacier's fore-field over a 28-year period. *American Geophysical Union.*

Ehrbar, D., Schmocker, L., Vetsch, D.F. and Boes, R.M. (2016). Messung von Sedimentflüssen in periglazialen Stauseen mit Wasserproben, ADCP und LISST. *Proc. 18. Wasserbau-Symposium 2016*. Technische Universität München, Berichte des Lehrstuhls und der Versuchsanstalt für Wasserbau und Wasserwirtschaft Nr. 134. ISBN 978-3-940476-10-3. Wallgau, Germany.

Ehrbar, D., Schmocker, L., Vetsch, D.F. and Boes, R.M. (2016). Measuring sediment fluxes in periglacial reservoirs using water samples, LISST and ADCP. *Proc. International Symposium on River Sedimentation (ISRS) 2016*. Stuttgart, Germany. (accepted)

SCCER SoE

SWISS COMPETENCE CENTER for ENERGY RESEARCH
SUPPLY of ELECTRICITY

SCCER-SoE Annual Conference 2016

In cooperation with the CTI

Energy
Swiss Competence Centers for Energy Research

Schweizerische Eidgenossenschaft
Confédération suisse
Confederazione Svizzera
Confederaziun svizra

Swiss Confederation

Commission for Technology and Innovation CTI

Development of a methodology for extreme flood estimation

Fränz Zeimetz[1], J. Garcìa Hernàndez[2], F. Jordan[3], G. Artigue[3], J.-A. Hertig† [4],J.-M. Fallot[4], R. Receanu[1], A. J. Schleiss[1]

[1]Laboratoire de Contructions Hydrauliques (LCH), [2]Centre de recherche sur l'environnement alpin (CREALP), [3]e-dric.ch, [4]Hertig & Lador SA
Corresponding author: franz.zeimetz@epfl.ch

LABORATOIRE DE CONSTRUCTIONS HYDRAULIQUES

ÉCOLE POLYTECHNIQUE FÉDÉRALE DE LAUSANNE

1. Introduction

The development of a methodology for **extreme flood** estimation is the aim of the project CRUEX++. This project follows the CRUEX project which aimed at the development of a PMP-PMF methodology (PMP=Probable Maximum precipitation, PMF=Probable Maximum Flood). Numerous tools, models and methods have been developed during the last years. The goal of the CRUEX++ project is to combine and enrich these elements leading to a methodology for extreme flood estimations in order to verify dam safety. A PhD thesis has been initiated in 2012 to lead this project and to conclude on a final methodology.

2. Approaches

The 2 main families of approaches taken into account are the statistically based methods and the simulation based methods.

In the context of the **statistically based methods**, the theory of extremes, englobing the General Extreme Value Distribution (GEV) and the Peak Over Threshold Method (POT), as well upper bounded statistical distributions are included.

In the domain of the **simulation based methods**, the semi-distributed conceptual hydrological model GSM-Socont is used. This model allows Precipitation-Discharge simulations, respecting the contributions of snow fall, surface runoff, infiltration as well as snow and glacier melt.

The **PMP-PMF approach** based on the Swiss PMP maps, elaborated during the CRUEX project is also considered and allows the estimation of the upper bound for the upper bounded statistical distributions.

3. Case study of Limmernboden

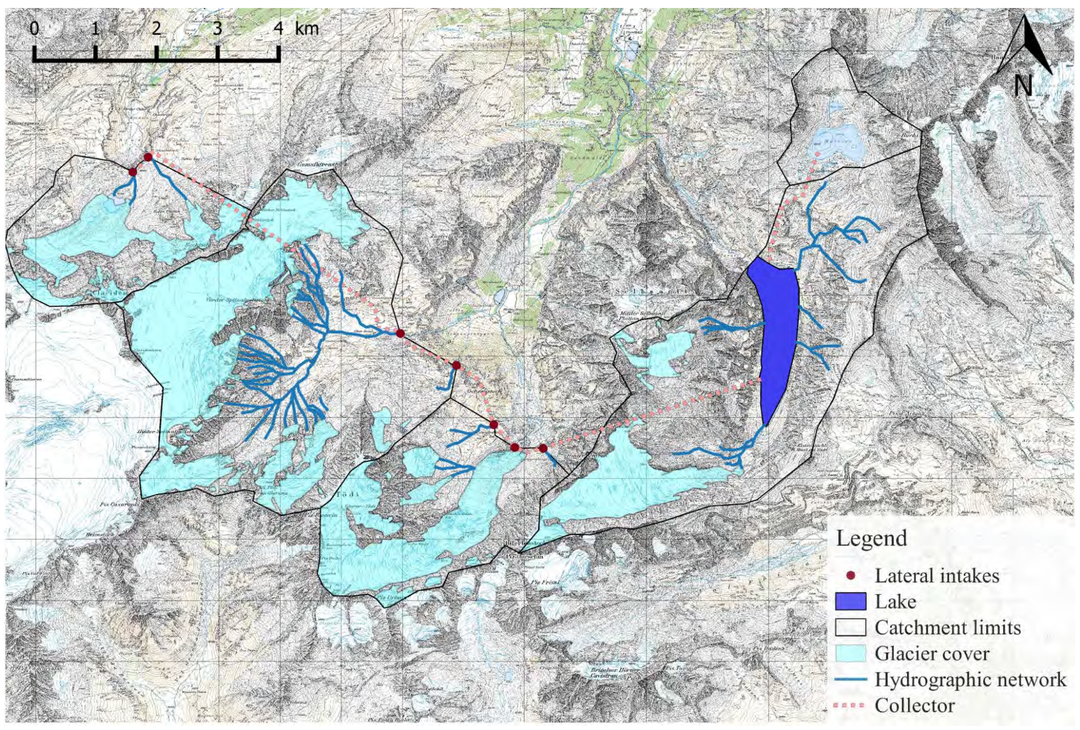

- Northern Swiss Alps
- Area: 17.8 km^2
- 7 lateral intakes
- Additional catchment: 31.8 km^2
- Total glacier cover: 17.5 km^2
- Altitude range: 1870-3614 m a.s.l.
- Karstic behaviour

- A detailed description of the case study has been presented at IUGG 2015 and can be consulted by scanning the following QR code.

- 2 approaches are applied
  1. Statistically based methods;
  2. Simulation based PMP-PMF method.
- The results are combined through the upper bounded distribution LN4.

4. PMP-PMF simulation approach

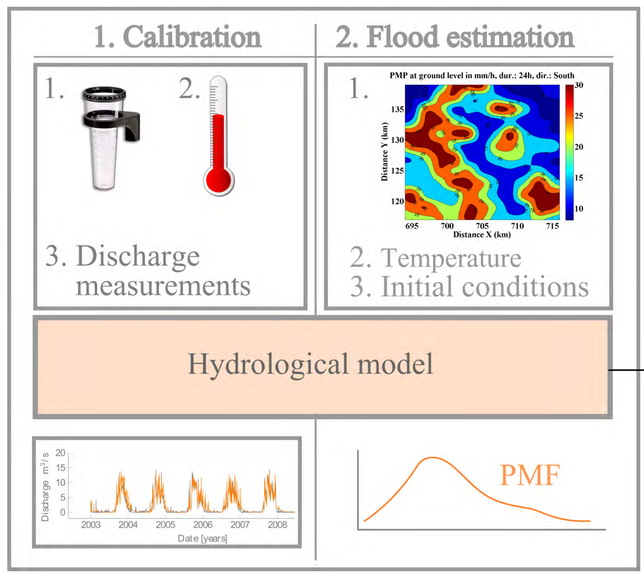

5. Results and discussion

- The critical water level in the lake was reached for a 23h-PMP

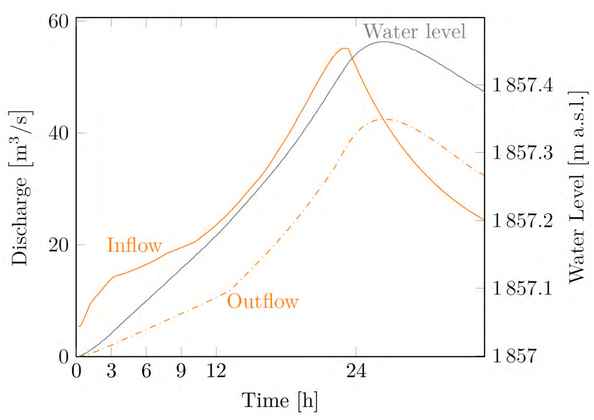

- Statistical extrapolations using GEV, POT and Gradex

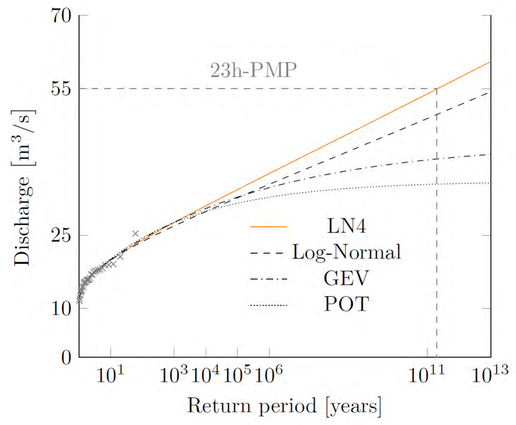

- Comparison between the PMF and the statistical estimation of the safety flood by 1.5Q$_{1000}$ by ratio R defined by $R = \frac{Q_{PMF}}{1.5Q_{1000}}$
- 1.5Q$_{1000}$ is admitted in the Swiss dam safety guidelines as safety flood In this case, there is generally a good agreement among the statistical extrapolations for the estimation of Q$_{1000}$.
- The estimation retained for the comparison is Q$_{1000}$=27 m^3/s.
- The value of R=1.36 indicates that the critical safety flood estimated with the PMP-PMF approach is 36% higher than the statistical approach proposed by OFEN (2008).
- The PMF estimation can be considered reasonable.

6. Conclusions

- The case study of the Limmernboden dam has been used to illustrate the application of the PMP-PMF approach for a Swiss alpine catchment.
- The extrapolations show that the LN4 distribution estimates tend to be larger than conventional statistical distributions.
- This is due to the consideration of the PMF for the extrapolation.
- The extrapolations using conventional statistical distributions only consider what has been measured. If large floods have not been observed, the estimations would probably be underestimated.

Acknowledgements
The CRUEX++ project is funded by the Swiss Federal Office of Energy (SFOE)

SCCER SoE
SWISS COMPETENCE CENTER for ENERGY RESEARCH
SUPPLY of ELECTRICITY

SCCER-SoE Annual Conference 2016

In cooperation with the CTI
Energy
Swiss Competence Centers for Energy Research
Schweizerische Eidgenossenschaft
Confédération suisse
Confederazione Svizzera
Confederaziun svizra
Swiss Confederation
Commission for Technology and Innovation CTI

Design of steel-lined pressure tunnels and shafts

Alexandre J. ***Pachoud****, Anton J.* ***Schleiss*** *& Pedro A.* ***Manso***
Laboratory of Hydraulic Constructions (LCH), Ecole Polytechnique Fédérale de Lausanne (EPFL)
Corresponding author: alexandre.pachoud@epfl.ch

LABORATOIRE DE CONSTRUCTIONS HYDRAULIQUES
ÉCOLE POLYTECHNIQUE FÉDÉRALE DE LAUSANNE

1. Introduction

Due to increasing integration of volatile new renewable energy in the European electric grid, storage hydroelectric power plants have to operate under harsh conditions in order to stabilize the electricity grid. As a result, pressure tunnels and shafts are subject to more frequent pressure. High-strength steels (HSS) are being used to reduce costs of high-head hydropower schemes. The use of HSS limits the thickness of the steel liners but raises new challenges regarding the welding procedure and long-term resistance that are not yet satisfactorily solved. When the rock conditions are adequate, the design can consider load-sharing between the steel liner and the concrete-rock system. In Europe, the C.E.C.T. (1980) recommendations are commonly used for the design, but may no longer be adequate when using HSS. There is still a lack of updated recommendations when using HSS in the specific case of steel-lined pressure shafts. This research project aims at addressing these issues by means of systematic numerical studies, with the finite element method. Several aspects are investigated, namely (1) the influence of anisotropic rock behavior; (2) the influence of geometrical imperfections of the longitudinal welded joints on local stresses; and (3) the probable presence of flaws in the seam welded longitudinal joints (Fatigue crack growth via the Fracture Mechanics approach). This would provide new insights to prototype physical behavior as well as new recommendations for an integrated and probabilistic design approach for steel-lined pressure tunnels and shafts.

2. Steel-lined pressure tunnels and shafts

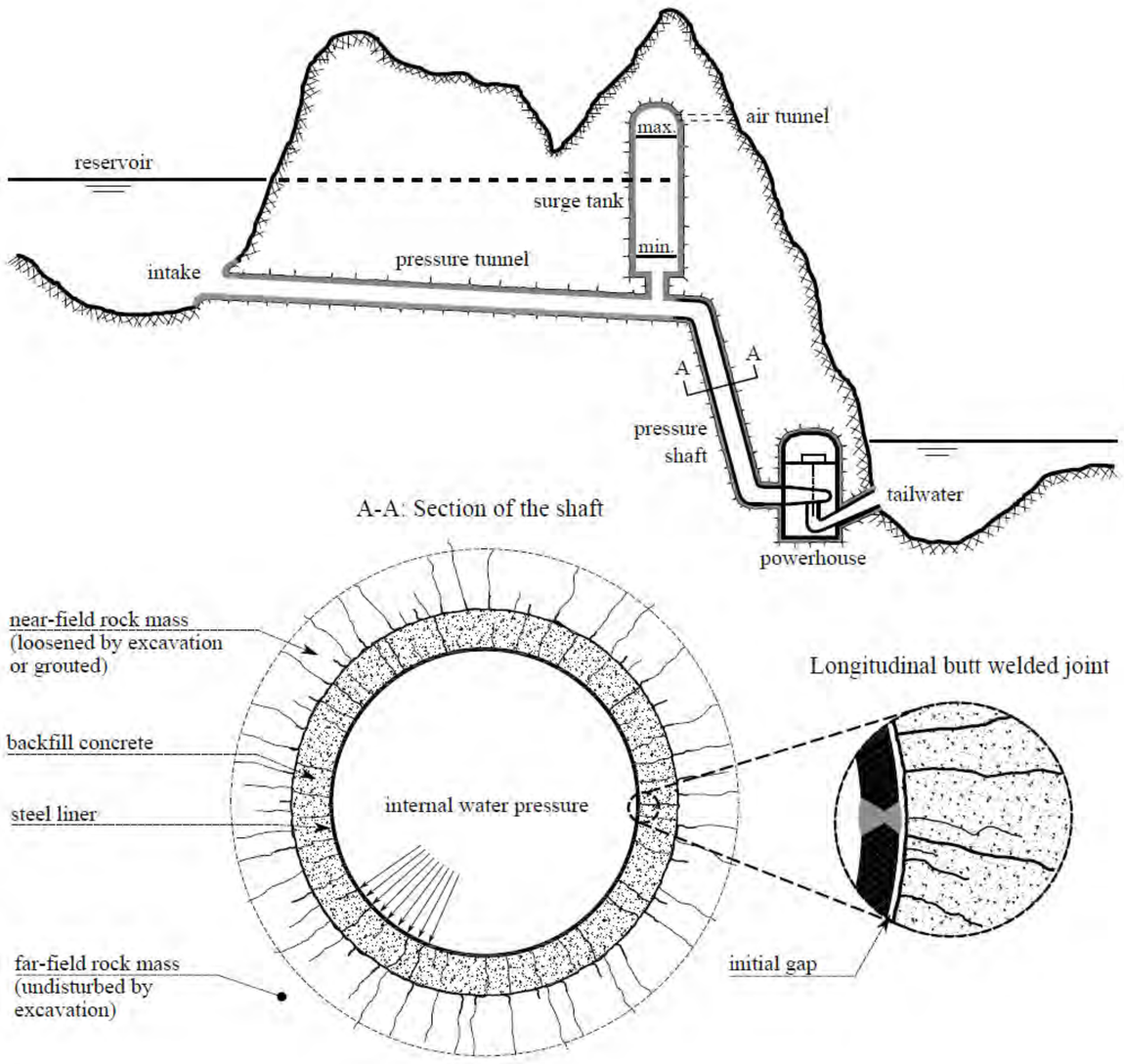

3. Stress concentrations at longitudinal butt welds

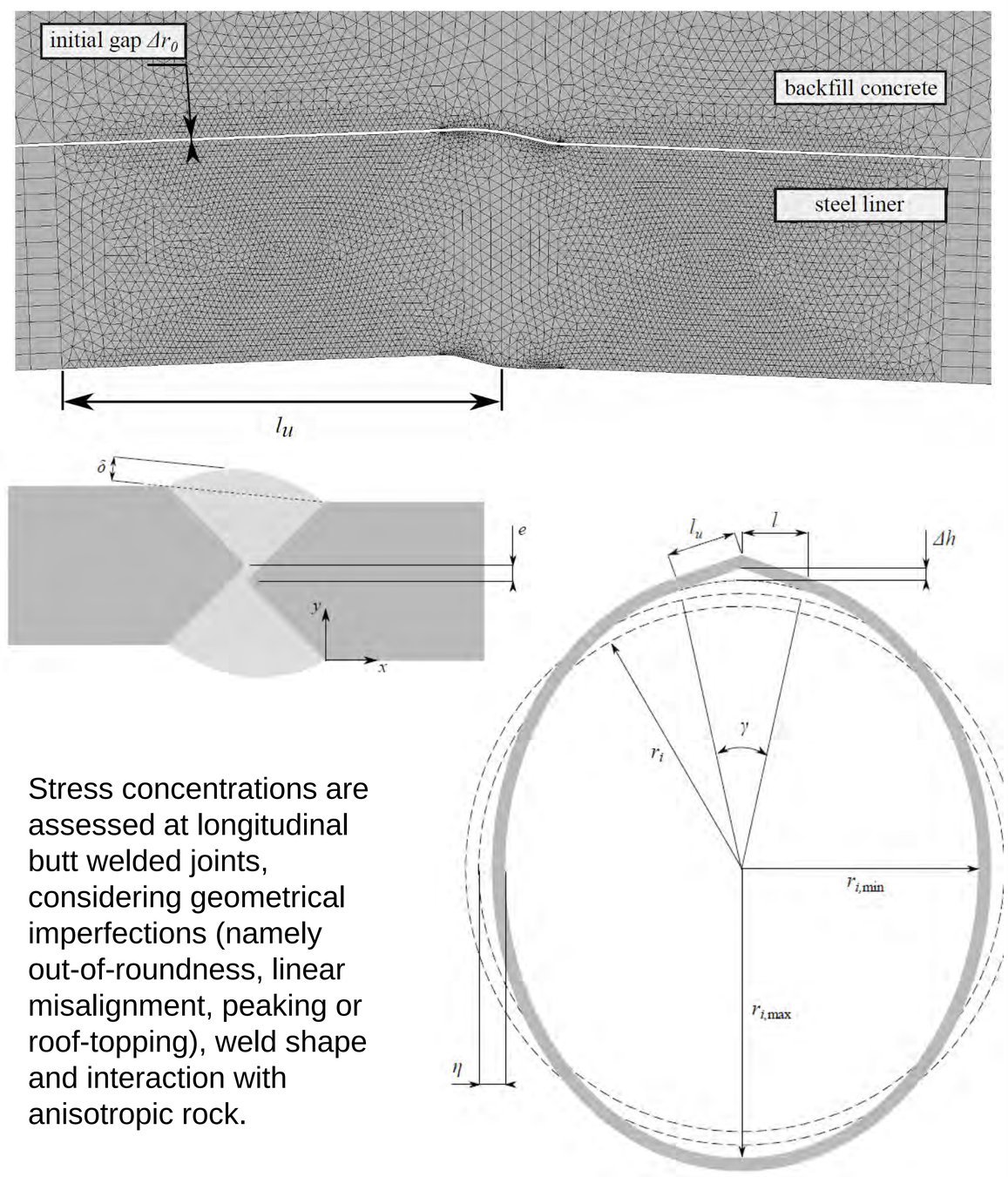

Stress concentrations are assessed at longitudinal butt welded joints, considering geometrical imperfections (namely out-of-roundness, linear misalignment, peaking or roof-topping), weld shape and interaction with anisotropic rock.

4. Stress intensity factors for cracks at longitudinal butt welds

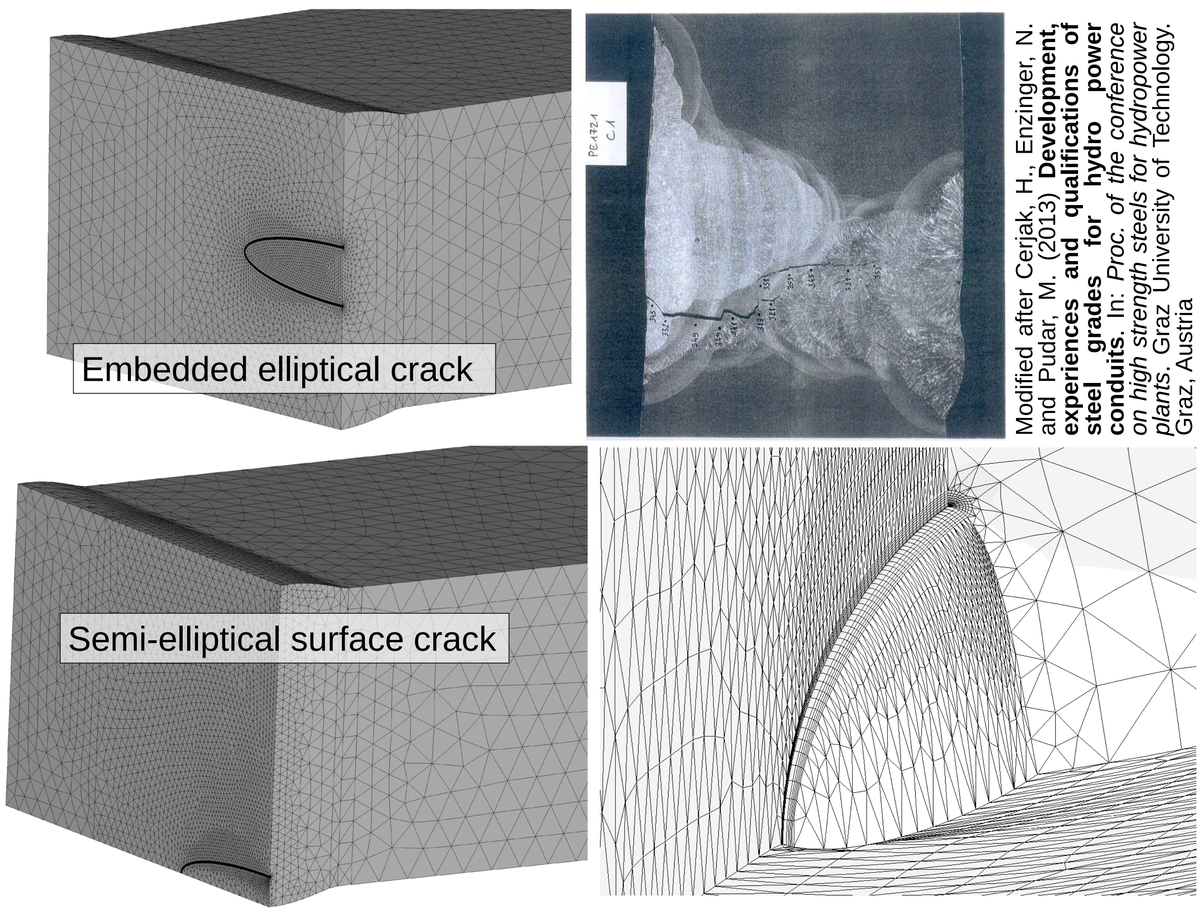

Modified after Cerjak, H., Enzinger, N. and Pudar, M. (2013) **Development, experiences and qualifications of steel grades for hydro power conduits**. In: *Proc. of the conference on high strength steels for hydropower plants*. Graz University of Technology. Graz, Austria

4. Probabilistic model for fatigue crack growth

New and innovative probabilistic model for fatigue crack growth at the longitudinal butt welded joints using the Paris law and linear elastic fracture mechanics. The security factor used for the design of steel liners embedded in rock is assessed against fatigue behaviour, particularly with the use of high-strength steels (e.g., S690 QL, S700 ML, S890 QL, S960 QL)

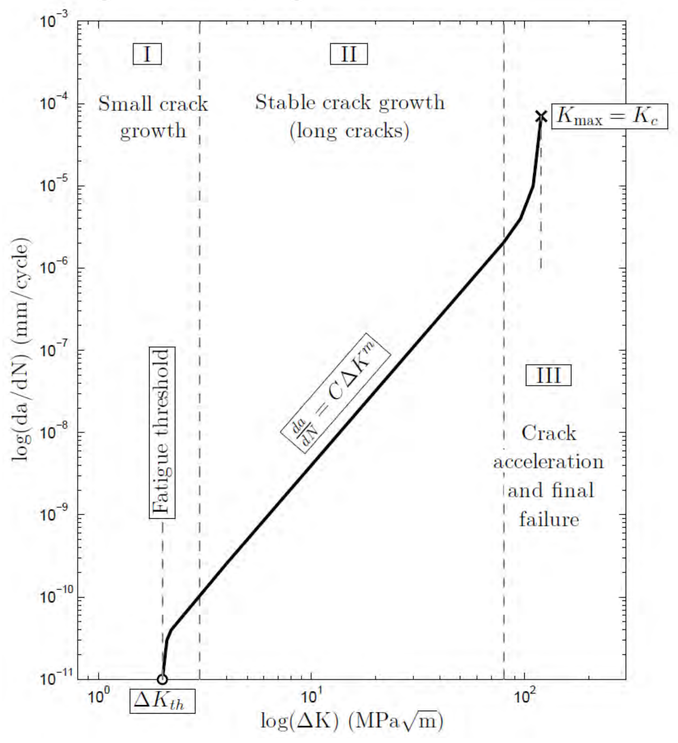

Acknowledgements

This study is part of the consortium *HydroNet 2: Modern methodologies for design, manufacturing and operation of hydropower plants*, a research project funded by the Swiss Competence Energy and Mobility (CCEM-CH). The authors also acknowledge the contributions from Swiss Committee On Dams (SwissCOD) and the Swiss Competence Center for Energy Research -- Supply of Electricity (SCCER-SoE).

List of publications

[1] Pachoud, A. J., Schleiss, A. J. (2016) **Stresses and displacements in steel-lined pressure tunnels and shafts in anisotropic rock under quasi-static internal water pressure**. *Rock Mechanics and Rock Engineering 49:1263-1287*

SCCER SoE
SWISS COMPETENCE CENTER for ENERGY RESEARCH
SUPPLY of ELECTRICITY

SCCER-SoE Annual Conference 2016

In cooperation with the CTI
Energy
Swiss Competence Centers for Energy Research
Schweizerische Eidgenossenschaft
Confédération suisse
Confederazione Svizzera
Confederaziun svizra
Swiss Confederation
Commission for Technology and Innovation CTI

Physical modelling optimization of a filter check dam

LABORATOIRE DE CONSTRUCTIONS HYDRAULIQUES

Sebastian SCHWINDT, Giovanni DE CESARE & Anton J. SCHLEISS

ÉCOLE POLYTECHNIQUE FÉDÉRALE DE LAUSANNE

Introduction

The upper branch of the Drance river is flowing from south-east to north-west as indicated in Figure 1. Downstream of the village of Les Valettes, a canyon stretch with steep hill slopes receives several lateral torrents just upstream of the urbanized area of Martigny-Croix and Martigny. The trapping of sediment is foreseen at the downstream end of the canyon stretch by means of a filter check dam. The project site is confined laterally by steep hill slopes which impede the excavation of a retention basin. Therefore, the height of the filter check dam is designed to retain the sediments in the canyon for a 100-year flood. A design project was reproduced by means of a physical model for its optimization.

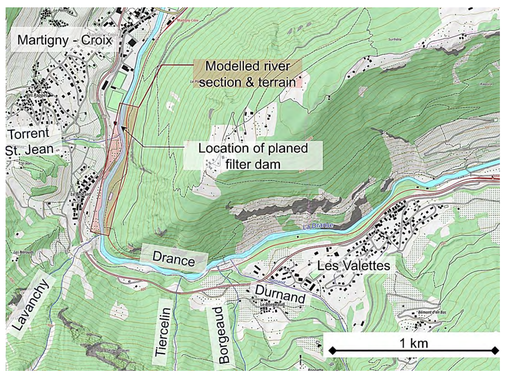

*Figure 1: **Project location** (with the authorization of Swisstopo JA100120)*

Physical Model

Design parameters:

- reproduction of a 850 m long reach, starting 600 m upstream of the filter check dam;
- bed slope varying between 2.4% and 2.1% (river width: 12-18 m);
- geometric scale 1:42, respecting Froude - and sediment transport similarity;
- grain sizes (channel bed) D_{50} = 92 mm and D_{90} = 435 mm;
- grain sizes (travelling bed load) D_{50} = 43 mm and D_{90} = 156 mm.

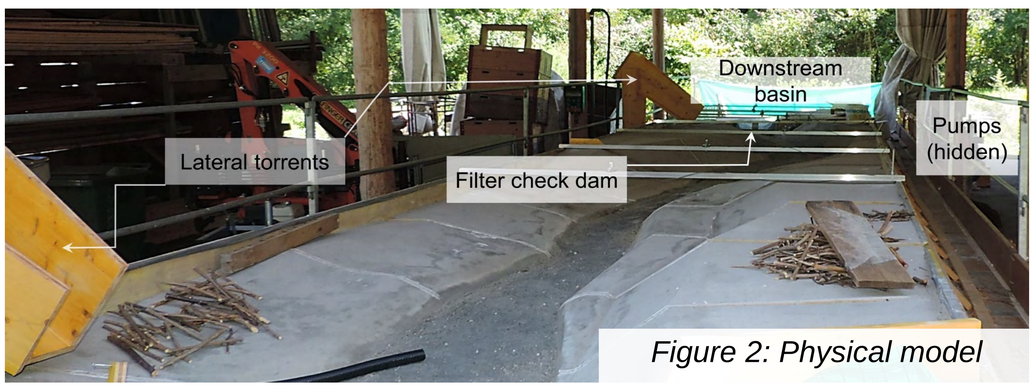

Figure 2: Physical model

Experiment scenarios

The filter check dam was analysed and improved for:

- without bedload for constant discharges in the range of:

Discharge	Prototype *[m³/s]*	Model *[l/s]*
Q mean	10	0.9
Q d	30	2.6
HQ 2.33	86	7.5
HQ 5	105	9.2
HQ 10	119	10.4
HQ 20	130	11.4
HQ 50	175	15.3
HQ 100	230	20.1
HQ 300	280	24.5
HQ 500 (EHQ)	345	30.2

- with bedload: hydrograph and sediment curve of a 100-years flood according;

- driftwood: repeated injection of 15 short logs (5 m), 10 long trunks (10 -15 m) and 2 root stocks as besides shown for 100-year flood (HQ100) and the 500-years flood (EHQ).

Figure 3: Sample of injected driftwood piles

Optimization of energy dissipation in the stilling pool

The flow acceleration over the spillways is broken down in the stilling basin which is covered with blocks (Ø 1.5 m) for increasing roughness.

Observations & improvements:

- the energy dissipation was gradually increased by adapting the basin shape (rectangular to elliptic), increasing the basin depth and length (about 25%);
- further improvement was reached by a supplementary asymmetric basin deepening to counter curve effects as the structure is situated in a right-hand bend of the Drance river.

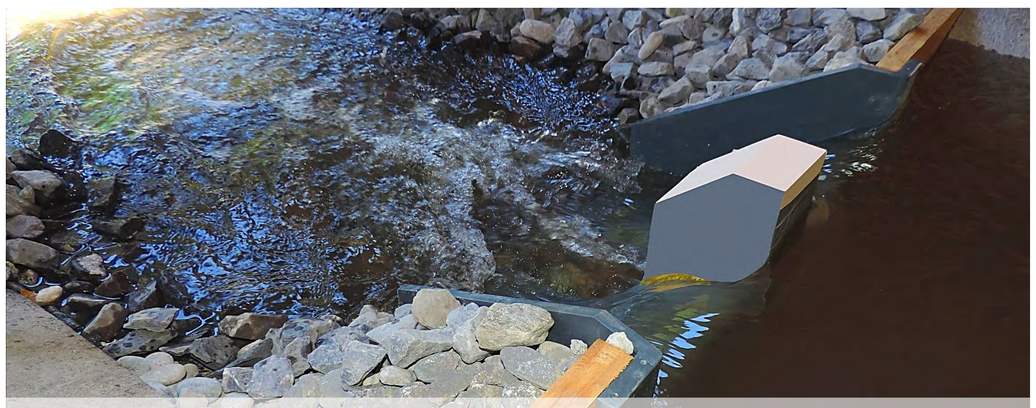

Figure 4: Illustration of the optimized stilling pool for energy dissipation

Optimization of sediment transfer of the filter check dam

According to the initial project, the orifice is 4 m wide, 2.5 m high and has an unsubmerged discharge capacity of 30 m³/s. Once this discharge is exceeded it is intended that the bedload deposits along the induced backwater. The obstruction of the orifice should be forced by a gate when the discharge exceeds 100 m³/s.

Observations & improvements:

- backwater occurs already for smaller discharges and the orifice is submerged for discharges higher than 33 m³/s;
- in case of a technical failure of the sluice gate, 25% of the injected sediment is retained and in case of closed orifice, about 40% of the injected sediment is retained (HQ100);
- an alternative to initiate passive obstruction was tested by installing a screen in front of the orifice;
- driftwood blockage can be annulled by removing the central pile.

Figure 5: Illustration of a) the initial design of the filter check dam and b) the optimized design with screen for passive obstruction

Conclusions

- cost effective experimental optimization of the hydraulic structure
- development of an alternative design for initiating passive obstruction of the orifice by sediment aggradation

SCCER SoE

SWISS COMPETENCE CENTER for ENERGY RESEARCH
SUPPLY of ELECTRICITY

SCCER-SoE Annual Conference 2016

In cooperation with the CTI

Energy
Swiss Competence Centers for Energy Research

Schweizerische Eidgenossenschaft
Confédération suisse
Confederazione Svizzera
Confederaziun svizra

Swiss Confederation

Commission for Technology and Innovation CTI

Blocking probability at spillway inlets under driftwood impact

Paloma Furlan, M. Pfister, J. Matos and A.J. Schleiss*
**corresponding author: paloma.furlan@epfl.ch*

Introduction

In order to maintain a required level of safety under different operational conditions, spillways must be designed taking into account floods as water, sediments and floating material.

If floating material reaches a hydraulic structure located within a stream (Figure 1), it may be caught and accumulate while narrowing the waterway opening. If it continues to accumulate, effects of floods, scouring or sediment deposition will be intensified.

It is already known that some characteristics of large woody debris (LWD) are decisive when encountering a hydraulic structure, but it has not been quantified yet what is the level of influence of each parameter in the blocking probabilities at a spillway inlet.

Figure 1: Picture from downstream of Takato Dam, Japan. Upstream of the gates it can be seen the accumulation of LWD (www. commons.wikimedia.org)

In this project, the innovative approach is to link the LWD characteristics to the hydraulic features and the geometry of an ogee, using systematic laboratory experiments, in order to be independent of study cases.

Methodology and experiments

A physical model was designed and constructed in the facilities of LCH (Figure 2). An ogee crested spillway with round nose piers was chosen as it is a widely used structure and has a great ability to pass floods.

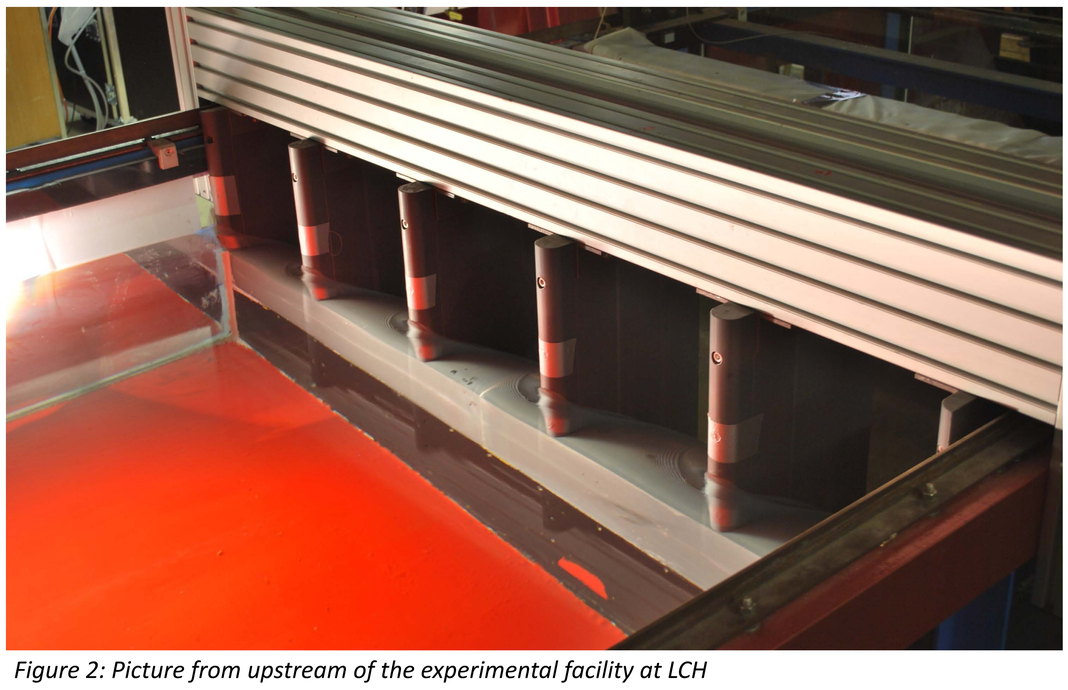

Figure 2: Picture from upstream of the experimental facility at LCH

Different configurations of experiments are being tested, always having a reservoir approach. In Figure 3, one of the many parameters to be changed can be seen.

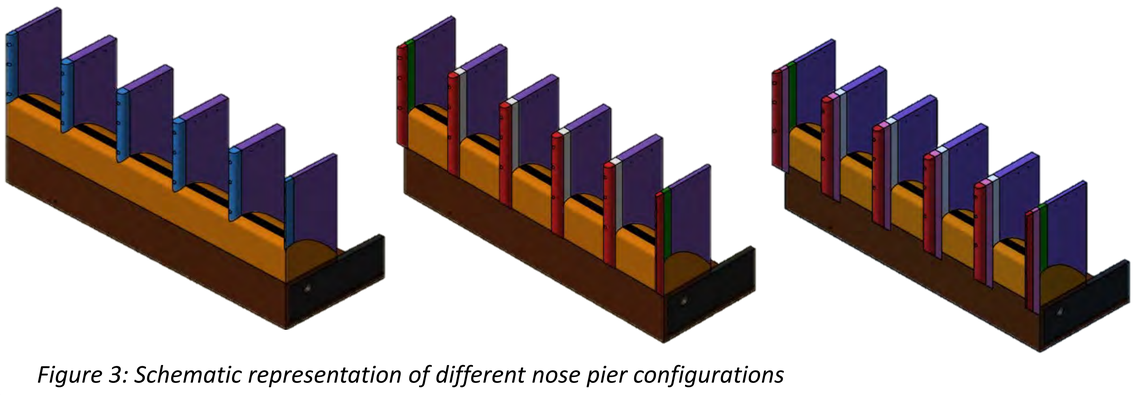

Figure 3: Schematic representation of different nose pier configurations

Parameters

The focus is on estimating blocking probabilities in relation to:

- **Repeatability**;
- **Density** of floating material;
- **Size** of LWD;
- **Group influence** and interactions between LWD;
- Amount of functioning **bays**;
- **Volume** of LWD blocked and head increase;

Preliminary results

BP(i) is defined as blocking probability of the individual *i* and it is computed as follows:

$$BP(i) = \frac{\sum blocked\ logs}{\sum amount\ of\ logs}$$

As it can be seen in Figure 4, the amount of times one experiment is repeated (keeping all the parameters constant), can strongly influence the final blocking probability. In this case, it can be seen that a blocking probability evaluated after 20 repetition for a certain combination of parameters will have a difference of almost 20% with a blocking probability evaluated after 80 repetitions. Otherwise, Figure 5 shows that for a different combination of parameters the result is not so sensitive to the amount of repetitions.

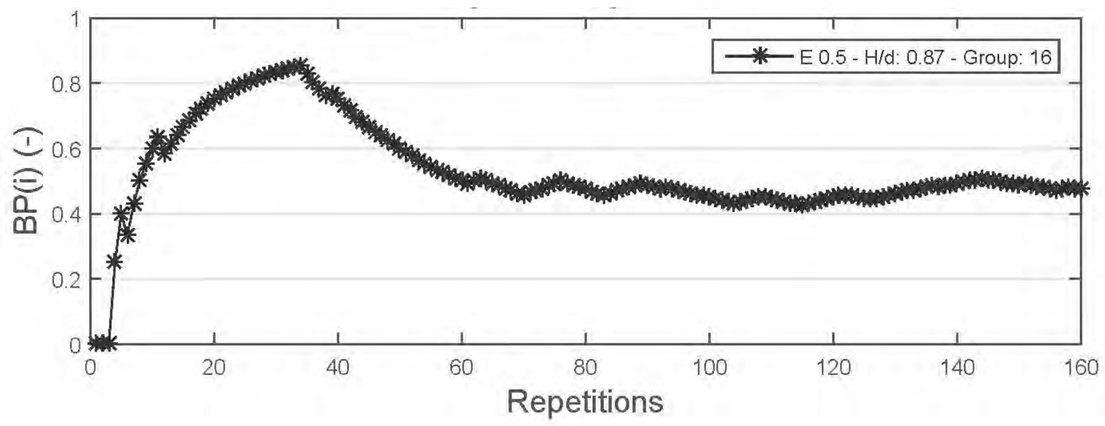

Figure 4: The pointed line shows the modification of the blocking probability along the amount of repetitions for Class E of logs, groups of 16 logs.

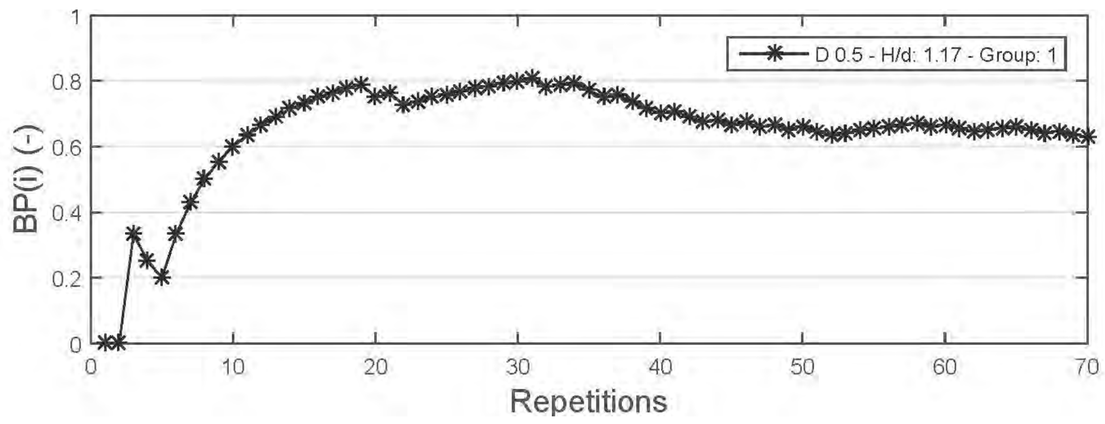

Figure 5: The pointed line shows the modification of the blocking probability along the amount of repetitions for Class D of logs, groups of 1 log.

Conclusions

Interesting results are being obtained. Blocking probabilities of large woody debris continues to be a random process, nevertheless some trend lines of behavior start to appear for some combination of parameters. A wide spectrum of combinations has been made to analyze the **repeatability** and its influence. Also, experiments to quantify the influence of **density** in the blocking probability have been made.

Plenty of work is still to be done. Experiments with different combinations of individuals or groups are being made. In the next phase of work, analysis of **head increments** due to a blocked volume of large woody debris will be made.

Acknowledgments

This research project is developed in the scope of the Ph.D. Thesis by Paloma Furlan under the joint IST-EPFL doctoral program. It is funded by the Portuguese Foundation for Science and Technology , LCH-EPFL and EDF.

SCCER SoE
SWISS COMPETENCE CENTER for ENERGY RESEARCH
SUPPLY of ELECTRICITY

SCCER-SoE Annual Conference 2016

In cooperation with the CTI
Energy
Swiss Competence Centers for Energy Research
Commission for Technology and Innovation CTI

GPU-SPHEROS – A GPU-Accelerated Particle-Based Solver for Hydrodynamic Simulation of Hydraulic Turbines

Siamak Alimirzazadeh, Ebrahim Jahanbakhsh, Audrey Maertens, Sebastian Leguizamon, François Avellan

1. Introduction

The present research is framed within the CTI project No. 17568.1 PFEN-IW to improve the performance of a versatile particle-based arbitrary Lagrangian Eulerian in-house solver, called SPHEROS. SPHEROS is a finite volume particle method (FVPM) parallel solver which inherits desirable features of both Smoothed Particle Hydrodynamics and mesh-based Finite Volume Method and is able to simulate the interaction between fluid, solid and silt. The GPU version of SPHEROS (GPU-SPHEROS) is being developed by the SPHEROS team to speedup the aforementioned software. It features GPU-accelerated libraries such as Thrust to improve the development productivity and handle complicated structures.

2. SPHEROS/GPU-SPHEROS Overall Algorithm

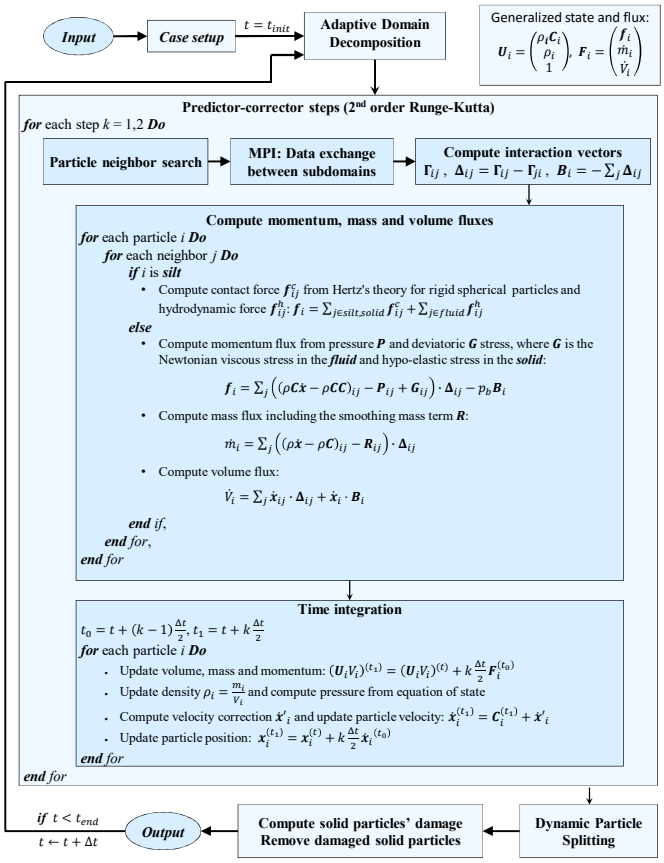

3. Particle neighbor search and reordering data

The key point to achieve high performance in GPU programming is to adapt the data structure to the unique requirements of the GPU architecture. In this regard, the performance can be improved by reordering the particles data using space filling curves (SFCs) leading to more efficient memory access. SFCs can also be utilized for massively parallel octree search algorithm which is an important part of particle-based methods. In GPU-SPHEROS, the octree search and particle ordering has been implemented based on Morton curve which leads to a remarkable speedup

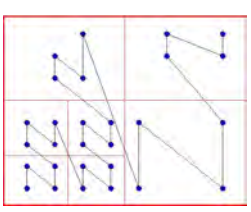

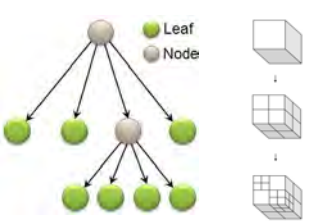

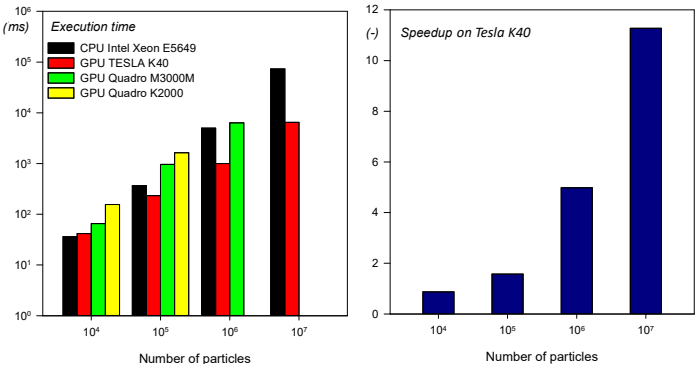

4. CUDA kernels optimization

In GPU-SPHEROS, there are both compute-bound and memory-bound kernels to optimize. For instance, the kernels which compute the volume integral gradients (VIG) and weighted least square (WLS) regression, are good examples of memory-bound and compute-bound algorithms, respectively. The optimization of memory-bound kernels is much more challenging since they require a lot of communication. The procedure for VIG memory bound kernel is illustrated in the following table. After optimization, the execution time of VIG has been decreased by a factor of around 10x compared to the primary version.

Optimization level	Technique	Exe. Time [ms]	Improvement [-]
0	Thrust sequential reduction	≈100	–
1	for loop inside the kernel	23.69	x
2	Unrolling loops	5.27	4.49x
3	Using Structure of Arrays instead of Array of Structures	3.23	7.33x
4	Pointers aliasing	2.89	8.19x
5	Manipulating No. of used registers	2.51	9.43x
6	Optimized number of threads per block	2.36	10.03x

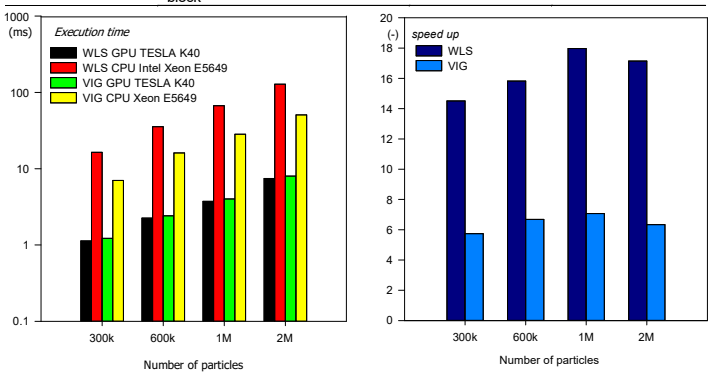

5. Validation and Applications

SPHEROS has been successfully validated against a series of test cases including lid-driven cavity flow, fluid-structure interaction, free surface flow, silt erosion, etc. For instance, the impinging jet and the flow through a rotating Pelton turbine simulations are shown below:

[1]

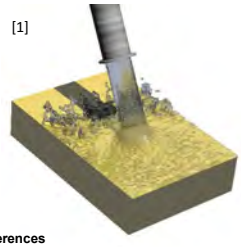

[2]

References
[1] E. Jahanbakhsh, "Simulation of Silt Erosion Using Particle-Based Methods", EPFL PhD Thesis N° 6284 (2014)
[2] C. Vessaz, "Finite Particle Flow Simulation of Free Jet Deviation by Rotating Pelton Buckets", EPFL PhD Thesis N° 6470 (2015)

SCCER-SoE Annual Conference 2016

SWISS COMPETENCE CENTER for ENERGY RESEARCH
SUPPLY of ELECTRICITY

In cooperation with the CTI
Energy
Swiss Competence Centers for Energy Research
Schweizerische Eidgenossenschaft
Confédération suisse
Confederazione Svizzera
Confederaziun svizra
Swiss Confederation
Commission for Technology and Innovation CTI

Characterisation of hydraulic behavior of surge tanks orifices

N.J. ADAM[(1)], G. DE CESARE[(1)] , A. J. SCHLEISS[(1)]& C. MUENCH-ALLIGNÉ[(2)]
[(1)]Laboratory of Hydraulic Constructions (LCH), Ecole Polytechnique Fédérale de Lausanne (EPFL) [(2)] Institut Systèmes Industriels, HES-SO Valais-Wallis
Corresponding author: nicolasjean.adam@epfl.ch

1. Introduction

Hydroelectric plants have produced almost 60% of the total electricity production since 2000 in Switzerland. They take part in the Energy Strategy 2050 due to their key role in the Swiss electricity market. According to this strategy, the mean annual hydropower production has to be increased by 1.5 TWh/year (under present framework) and by 3.2 TWh/year (under optimized conditions)
The Swiss storage power plants produced almost one third of the total production [SFOE, 2015].Furthermore, this type of plants, and specifically high head power plants (Figure 1), are useful to follow cyclic peak demands (daily, weekly and seasonal) as they can provide large amount of electricity in a short lapse of time. Owners and producers may consider an increase of the peak generation of these plants to reach the Energy Strategy 2050 and in order to adapt to the new renewable energy.

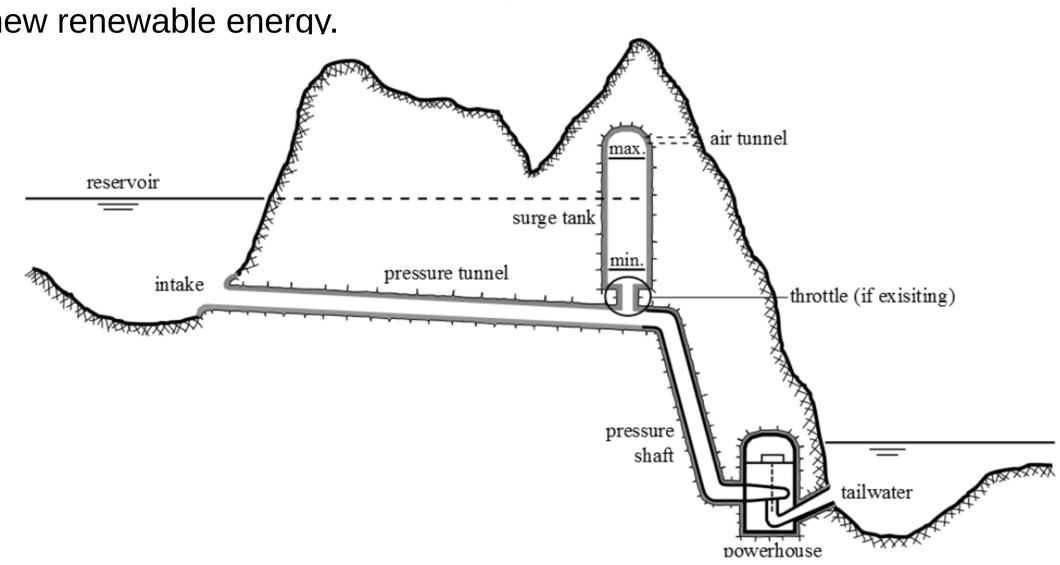

Figure 1 : Schematic view of a typical alpin high head power plant (H>200m) [Courtesy of A.J. Pachoud]

2. Throttled surge tanks

A surge tank is usually an excavated volume, which is connected to the waterway system and generally open to the atmosphere. The introduction of surge tanks allows reducing the construction cost of the pressure tunnel by minimising and reflecting the water hammer in/from pressure shaft. Mass oscillations appear between the upstream reservoir and the surge tank and could increase the time between two discharge variations.

Throttles are hydraulic devices accelerating the water flowing through and producing a given amount of head losses. The goal of a throttle placement is to keep extreme mass oscillations within the surge tank geometry (Figure 2).

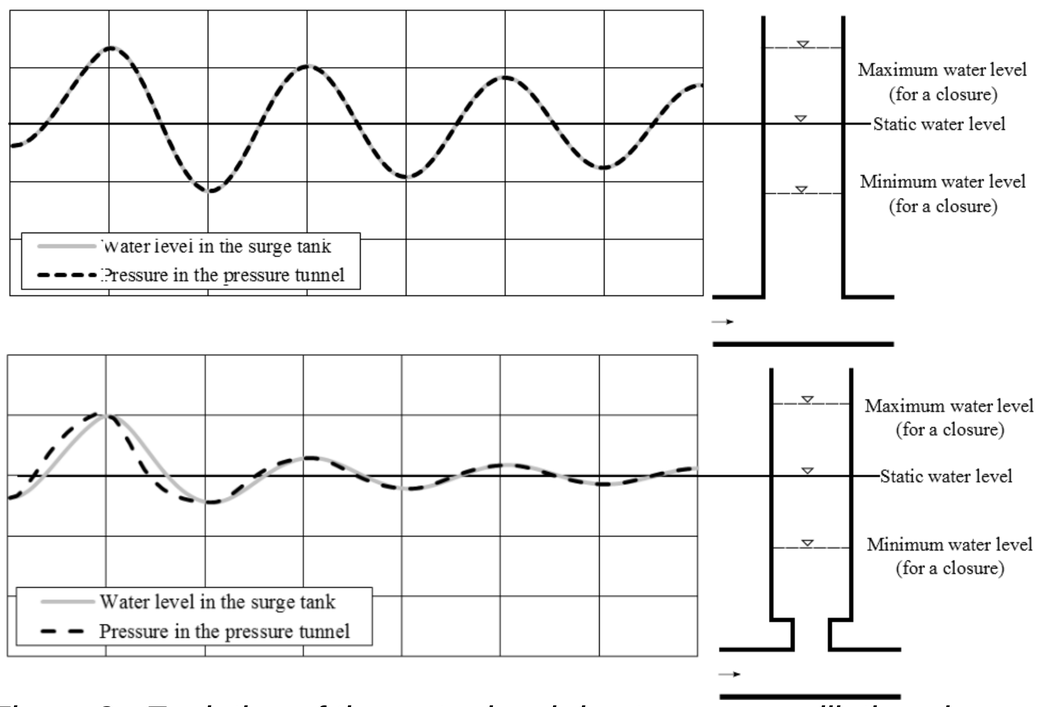

Figure 2 : Evolution of the water level due to mass oscillations in a simple surge tank (up) and a throttled surge tank (down)

The main disadvantage of the placement of a throttle is that the dynamic pressure produced by the water hammer increases in the pressure tunnel.

3. Different types of throttle

Throttles can be divided in, at least, three main categories: orifices, racks or vortex throttles. Orifices and racks can be either symmetric or asymmetric while vortex throttles are only asymmetric.

- Orifice: An orifice is a local geometry restrictions which may have different opening shape (circular, rectangular, etc.). The streamline expansion at the downstream is the same in all direction. Asymmetrical orifice shape allows introducing asymmetrical head losses up to 1:3 – 1:4.
- Rack throttle: A rack throttle is composed with a framework of parallel spaced bars or beams. The downstream streamlines expansion are forced in one direction. The different expansions should influence each others.
- Vortex throttle: This type of throttle is mainly present in Austrian surge tanks. It allows producing a higher asymmetry ratio up to 1:20 – 1:50 due to the complex swirling flow in the vortex throttle.

An orifice or a rack throttle could be placed during a refurbishment while vortex throttle must be placed during the construction due to its complexity

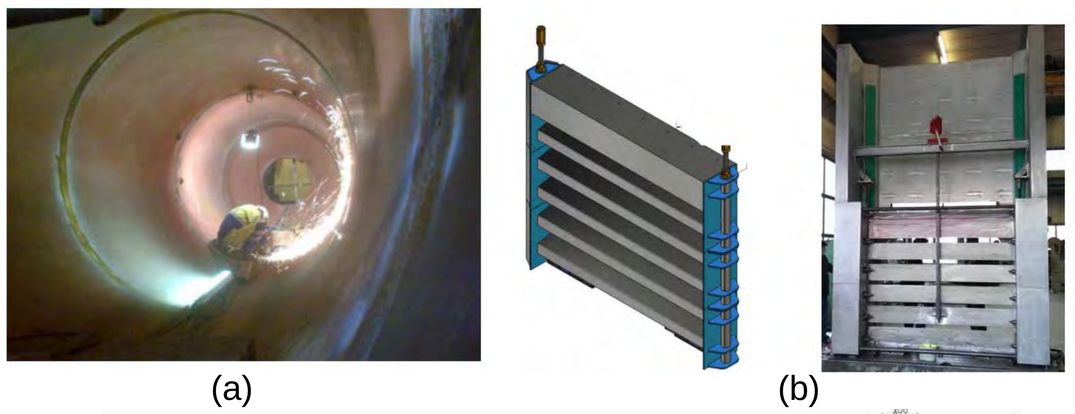

Figure 3 : Different existing throttles: (a) orifice in FMHL+; (b) Rack throttle in Gondo; and (c)Vortex throttle in Austria;

4. Conclusions and outlooks

The placement of a throttle is useful to manage the extreme water levels occurring during mass oscillations between the surge tank and the upstream reservoir. It allows reducing the construction cost and adapting an existing surge tank submitted to an increase of discharge in the waterway (during a refurbishment).

A research is performed at the LCH to build a catalogue of orifice geometries with physical and numerical experiments. The main goal is to improve the design of surge tank orifices by practical engineers.

Partners

The numerical orifice model was built and performed in collaboration with the “Institut Systèmes Industriels (Hydroélectricité)” of the HES-SO Valais/Wallis. The first part of the research was financed by “The Ark: promoting innovation in Valais”. The second part is financed by “BFE section Wasserkraft”.

Publications

[1] Adam, N.J., De Cesare G. & Schleiss A.J., (2016). **Head loss coefficients trough sharp-edged orifices.** *In 28th IAHR Symposium on Hydraulic Machinery and Systems, Grenoble, France, July 4-8.*
[2] Adam, N.J., De Cesare G. & Schleiss A.J., (2016). **Experimental assessment of head losses trough elliptical and sharp-edged orifices.** *In 4th IAHR Europe Congress, Liège, Belgium, July 27-29.*
[3] Adam, N.J., De Cesare G. & Schleiss A.J. (2016). **Surge tank throttles for safe and flexible operation of storage plants***. In Hydro Conference 2016.*

SCCER SoE

SWISS COMPETENCE CENTER for ENERGY RESEARCH
SUPPLY of ELECTRICITY

SCCER-SoE Annual Conference 2016

In cooperation with the CTI

Energy
Swiss Competence Centers for Energy Research

Schweizerische Eidgenossenschaft
Confédération suisse
Confederazione Svizzera
Confederaziun svizra

Swiss Confederation

Commission for Technology and Innovation CTI

Artificial sediment replenishment to restore the natural morphological conditions downstream of dams

Elena Battisacco, Mário J. Franca, Anton J. Schleiss*
Ecole Polytechnique Fédérale de Lausanne - Laboratory of Hydraulic Constructions (Switzerland)

LABORATOIRE DE CONSTRUCTIONS HYDRAULIQUES

ÉCOLE POLYTECHNIQUE FÉDÉRALE DE LAUSANNE

1. Introduction

Dams interrupt the longitudinal continuity of river reaches since they store water and trap sediment in the upstream reservoir (Fig. 1a, 1b). Sediment replenishment is used for restoring the continuity in rivers and for reestablishing the sediment regime. Artificial deposit of finer sediments are placed along these disturbed reaches (Fig.1c).

A new approach with multiple sediment replenishment is herein performed. The effect of different geometrical configurations of sediment replenishment on the evolution of the bed morphology by systematic laboratory experiments is evaluated.

Figure 1: (a, b) river condition upstream and downstream the Echo Dam, Utah (USA); (c) sediment replenishment below Keswick Dam along the Sacramento river (USA) [photo by Kondolf G.M.]

2. Laboratory facility

The experimental channel at a scale of about 1:10 represents a straight alpine gravel channel with a slope of 1.5%, a length of 15 m, a width of 0.4 m and a trapezoidal cross section with a bank slope of 2:3 (V:H) (Figure 3 (right), Figure 2(1)). Two morphologically identical channels are created (Figure 2 (2)).

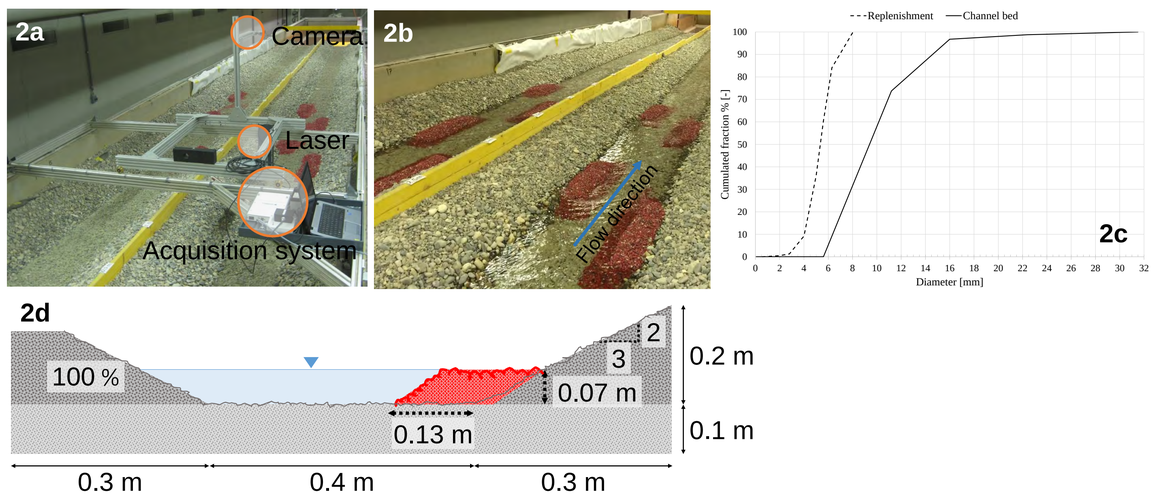

Figure 2: (a) channel instrumentation, (b) replenishment of volume on channels, (c) grain size distribution for bed and replenishment, (d) cross-section and flow condition

2. Parameters

Alternating (B, C and E) and parallel (A, D and F) replenishment configurations (Fig. 3). Following the tested parameters:

- Covered surface $CS\ [\%] = \frac{\sum(A_{or})}{\sum\ (A_{oi})}$
- Compactness $NDC\ [\%] = \frac{C_b - C_{b,min}}{C_{b,max} - C_{b,min}}$
- Occupation ratio $OCR_x\ [\%] = \frac{\sum(Red\ grains\ along\ \mathrm{x}) * pixel\ area}{w}$

The area of interest Aoi corresponds to the channel bed (0.4m x 10m) and Aor corresponds to the area covered by red grains. Cb, Cb,min and Cb,max refer to the bed form connecting bounderies as proposed by Bribiesca (1997).
The channel width, w, is equal to 0.4m. The observational length is indicated as x, and corresponds to 10m.

4. Results

- The CS values varies between 20% and 40%. The highest value are obtained for configuration B (Fig. 4a). The NDC of bed forms is higher for configurations B and C (Fig. 4b)
- The OCR distributions show peaks of denser replenishment areas for alternated configuration
- Smoother distributions result for parallel replenishment geometries (Fig. 5b)
- The Welch's function, applied to the OCR-signal, shows a more pronounced periodicity for alternated configurations (Fig. 4c). The wavelength of these bed forms is equal to the replenishment length

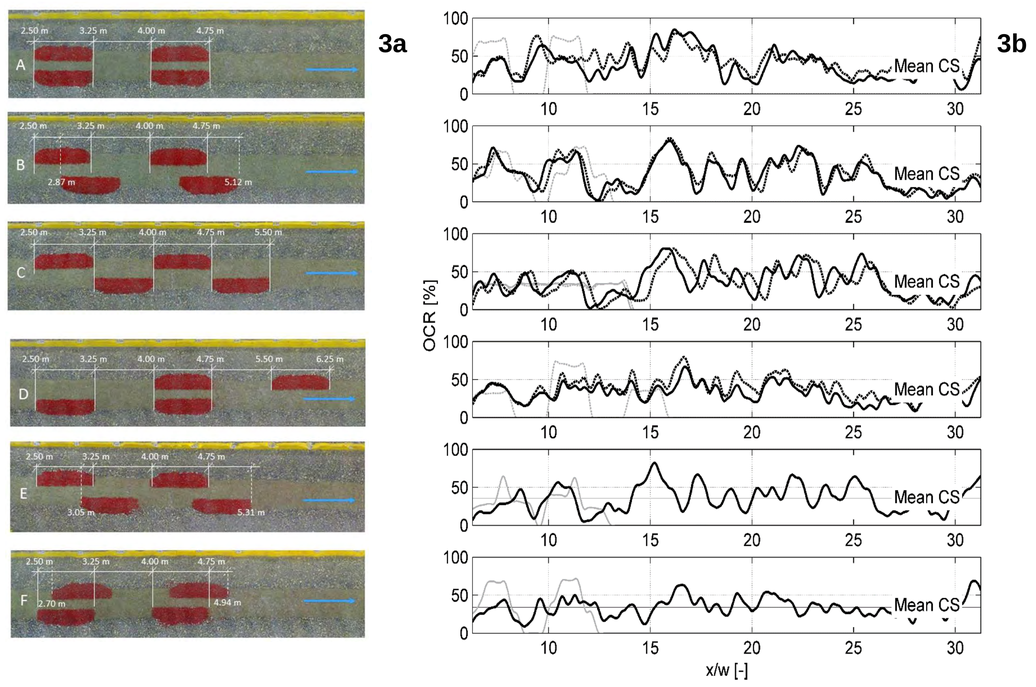

Figure 3: (a) (from the top) performed configurations at EPFL. Replenishment length of 0.75m, height of 0.07m and width of 0.13m per each volume. Distance along the channel length. Flow direction from left to right, (b) occupation ratio per each tested configuration, initial state (grey line) and final state (black line) after 3 hours testing. Channel length normalized by channel width (w=0.4 m)

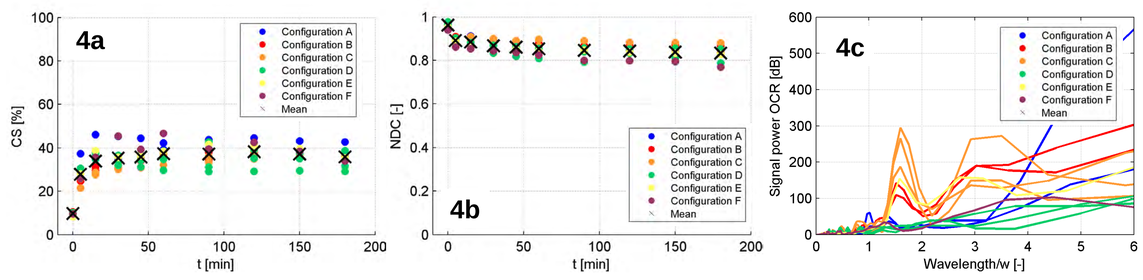

Figure 4: (a) covered surface CS, (b) compactness NDC, (c) power spectrum density of OCR-signal; for all the configurations and ratio of 100% submergence

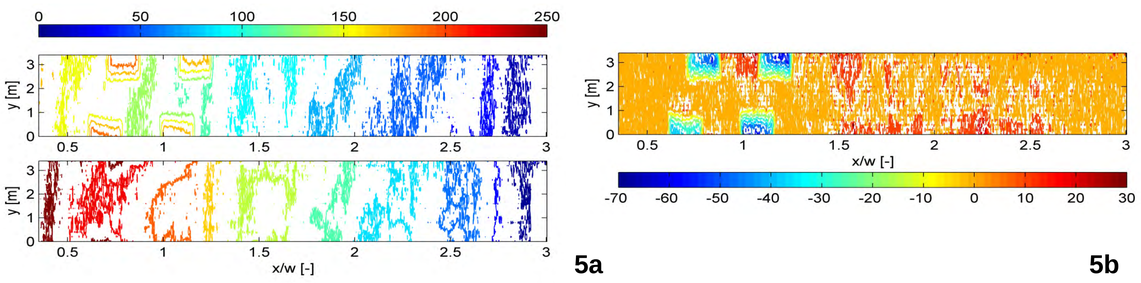

Figure 5: (a) laser measurements for configuration B and ratio of 100% submergence: (top) initial state, (middle) final state after 3 hours, (b) bed elevation changes for the tested configuration

5. Conclusions

- The erosion of the replenishment is mainly occurring during the first 45 minutes, for then decreasing and attending an equilibrium state
- A ratio of 100% submergence of replenishment volume is necessary to obtain a complete volume erosion and transportation of eroded grains (Fig. 5b)
- The replenishment material is spread on the entire channel bed applying parallel configurations of volumes (Fig. 3b)
- Parallel configurations (A, D and F) can be useful for obtaining a diffuse bed fining. More compacted cluster and bigger portion of the channel bed are affected when placing alternating configurations (B, C and E)
- Alternating replenishment configuration may be preferred in order to re-establish bed form morphology downstream of dams since they enhance the creation of bed pattern (Fig. 4c)
- These bed forms can be used as new spawning grounds by fishes

Acknowledgements
This research is founded by the Federal Office for the Environment, Switzerland.

*Corrisponding author:*elena.battisacco@epfl.ch*

SCCER SoE

SWISS COMPETENCE CENTER for ENERGY RESEARCH
SUPPLY of ELECTRICITY

SCCER-SoE Annual Conference 2016

In cooperation with the CTI

Energy
Swiss Competence Centers for Energy Research

Schweizerische Eidgenossenschaft
Confédération suisse
Confederazione Svizzera
Confederaziun svizra

Swiss Confederation

Commission for Technology and Innovation CTI

The influence of Fluid-Structure Interaction (FSI) during hydraulic transients in pressurized pipes

Ferras D., Manso P., Covas D. I.C., Schleiss A.J.

(1) Laboratoire de Constructions Hydrauliques, Ecole Polytechnique Fédérale de Lausanne, (2) CEris Instituto Superior Técnico, University of Lisbon
Corresponding author: david.ferras@epfl.ch

LABORATOIRE DE CONSTRUCTIONS HYDRAULIQUES

TÉCNICO LISBOA

ÉCOLE POLYTECHNIQUE FÉDÉRALE DE LAUSANNE

1. Introduction

Classical waterhammer theory is based on the simplification of pressure waves in pipes as a periodic flow dominated by fluid compressibility and pipe-wall distensibility and damped by steady friction. However, in real systems friction losses are not described by steady state formulae, the flow may cavitate, the pipe-wall may show hysteresis, the conduit may contain air, move, leak, or have blockages, *et cetera*; and classical theory is not accurate enough to describe such phenomena.

Literature in the field of waterhammer offers means to solve the aforementioned, though, the inclusion of these add-ons into classical theory is challenging, requiring the development of advanced mathematical models.

The aim of the present research is to give experimental and numerical insight on the **distinction, identification** and **description** of two strongly related phenomena that frequently affect in a similar manner the transient pressure wave: **fluid-structure interaction** and **pipe-wall non-elastic rheological behavior**.

2. Methodology

Experimental data collection:
- Copper straight pipe facility
- Copper coil pipe
- Polyethylene coil pipe

Numerical analysis:
- Fluid-structure interaction solver
- Viscoelastic model
- Unsteady friction model
- Integration of the three models

3. Experimental analysis

Copper straight pipe:

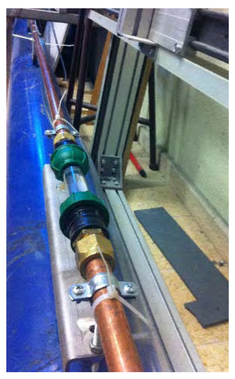

L = 15.49 m
D = 0.020 m
e = 0.001 m
E = 105 GPa
ν = 0.33
a = 1239 m/s

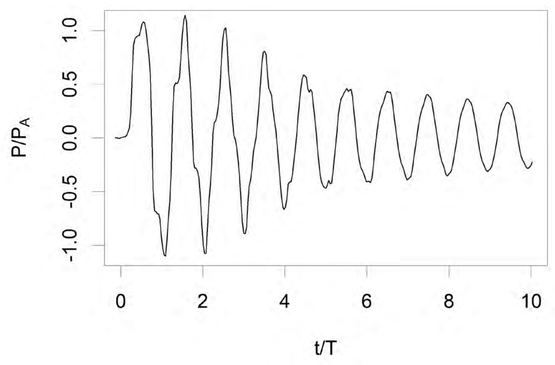

Copper coil pipe:

L = 105 m
D = 0.020 m
e = 0.001 m
E = 105 GPa
ν = 0.33
a = 1193 m/s

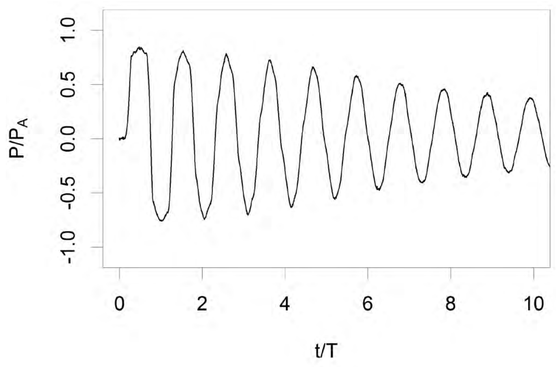

HDPE coil pipe:

L = 203 m
D = 0.043 m
e = 0.003 m
E = 1.42 GPa
ν = 0.43
a = 315 m/s

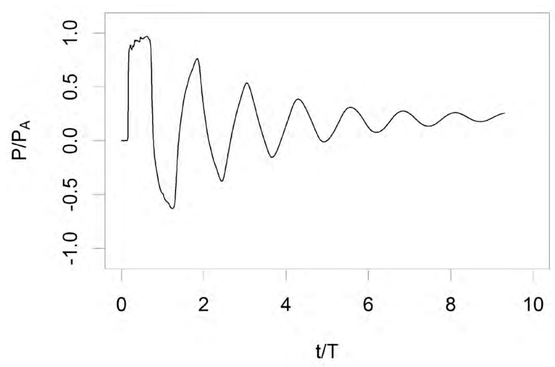

4. Numerical analysis

Model implementation, internal conditions:

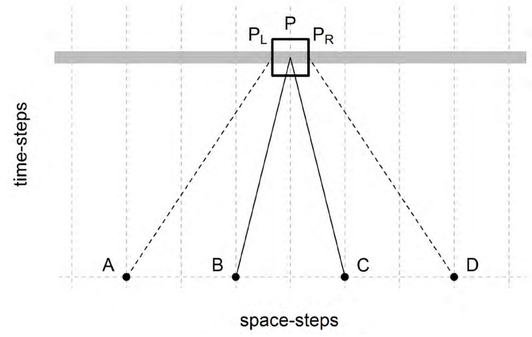

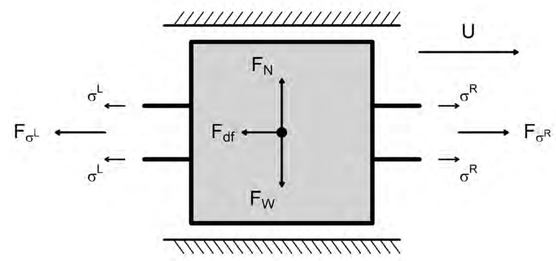

Output for copper straight pipe:

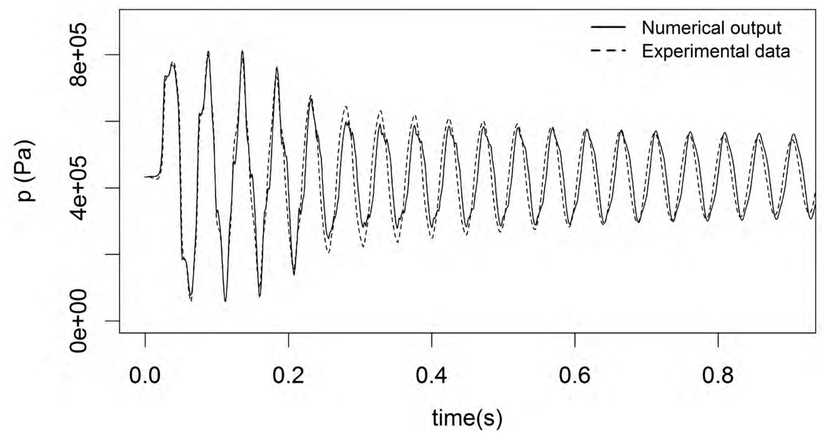

Output for copper coil pipe:

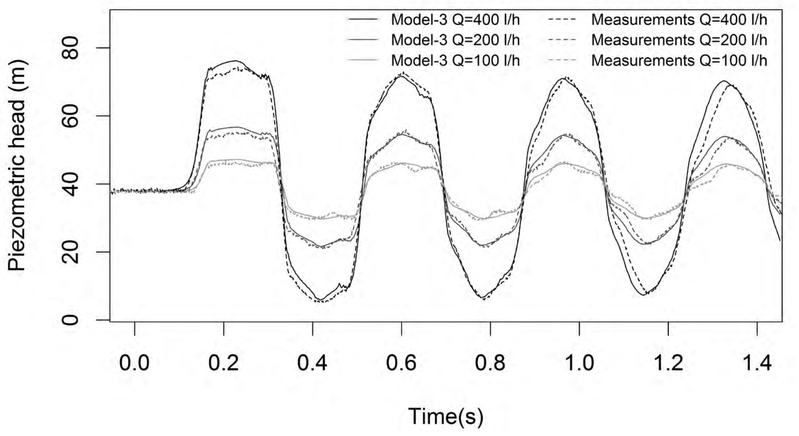

5. Conclusions

- The system response of a straight pipe is strongly influenced by the downstream anchoring conditions. **FSI through junction coupling** changes maximum pressure, wave shape and overall damping.
- A systematic pressure wave amplitude reduction is observed in coil pipes due to a "**breathing effect**" originated from the radial deformation of the coil rings.
- The viscoelasticity of the HDPE pipe-wall significantly affects the dissipation, shape and phase of the transient pressure wave due to the **retarded response** of the polyethylene material (hysteresis).
- Adequate modelling assumptions are crucial in the distinction of fluid-structure interaction and **wave dissipation mechanisms** for an accurate description of pipe systems behavior during hydraulic transients.

6. PhD outputs

- Enhanced knowledge on hydraulic transients.
- Robust transient solvers for engineers and consultants.
- Designing and diagnosis guidelines for pressurised systems.
- Safer pressurised water systems

Reference papers

Ferras D., Covas D., Schleiss A.J. Stress-strain analysis of a coiled copper pipe for inner pressure loads. *Journal of Fluids and Structures,* 2014.

Ferras D., Manso P., Covas D., Schleiss A. J.. Comparison of conceptual models for fluid-structure interaction in pipe coils during hydraulic transients. *IAHR Journal of Hydraulic Research* (accepted for publication), 2016.

Ferras D., Manso P., Covas D., Schleiss A. J.. Experimental distinction of damping mechanisms during hydraulic transients in pipe flow. *Journal of Fluids and Structures* (accepted for publication), 2016.

Ferras D., Manso P., Covas D., Schleiss A. J.. Fluid-structure interaction in straight pipelines: friction coupling mechanisms. *Computers and Structures* 175 (2016) 74–90 (http://dx.doi.org/10.1016/j.compstruc.2016.06.006)

Ferras D., Manso P., Covas D., Schleiss A. J.. Fluid-structure interaction in straight pipelines anchored against longitudinal movement. *Journal of Sound and Vibration* (submitted for publication), 2016.

SCCER SoE

SWISS COMPETENCE CENTER for ENERGY RESEARCH
SUPPLY of ELECTRICITY

SCCER-SoE Annual Conference 2016

In cooperation with the CTI

Energy
Swiss Competence Centers for Energy Research

Schweizerische Eidgenossenschaft
Confédération suisse
Confederazione Svizzera
Confederaziun svizra

Swiss Confederation

Commission for Technology and Innovation CTI

Design of steel-lined pressure tunnels and shafts: new and innovative probabilistic approaches for reliability assessment

Gabrielle Muller(1), A. Pachoud(1), P. Manso(1), A. Schleiss(1), A. Nussbaumer(2)

(1) Laboratoire de Constructions Hydrauliques, École polytechnique fédérale de Lausanne (EPFL); (2) Resilient Steel Structures Laboratory, EPFL
corresponding author: gabrielle.muller@alumni.epfl.ch

LABORATOIRE DE CONSTRUCTIONS HYDRAULIQUES

ÉCOLE POLYTECHNIQUE FÉDÉRALE DE LAUSANNE

Context

Hydroelectric power plants work under tough conditions to satisfy demand from electricity grid, thus subjecting the steel liners to more frequent pressure surges than in the past. High strength steel (HSS) is used to reduce liner's thickness and project costs. The brittle behavior of the welded HSS raises new challenges regarding welding procedures and resistance to fatigue.

The liner thickness is determined according to the design procedures and is a function of the maximum allowable internal pressure, the liner radius and the yield strength. The global safety factor for the design thickness of a liner subjected to internal pressure is 1.1.

Challenge

The classical design approach of keeping stresses below yielding strength of the steel is no longer satisfactory since cyclic loads can cause cracks to initiate and existing cracks to propagate, thereby endangering the safety of the power plant. Fracture mechanics is used to study the phenomenon of crack propagation under cyclic loading.

Objectives

To *conceive* a transparent and adaptable method for assessing failure probability of steel liners, to *provide* a basis of simulation results and to *outline* further research ideas to enhance the accuracy of the method.

Studied case

The case of internal surface cracks in longitudinal butt welded joints is analyzed. The initial cracks are due to the welding process and are assumed to be above the crack initiation size.

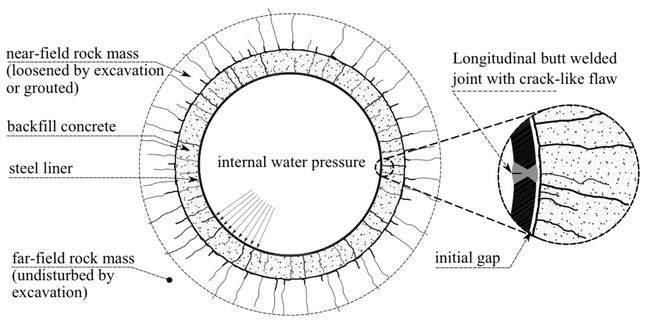

Fig. 1 – Steel-lined tunnel cross-section

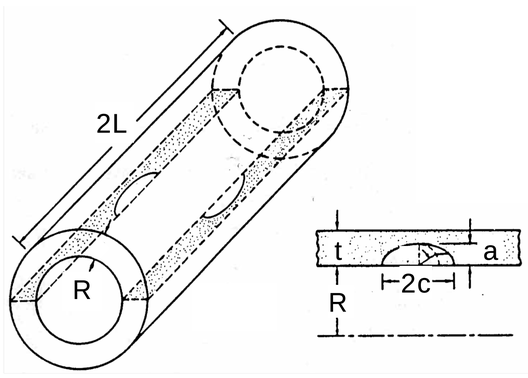

Fig. 2 – Sketch of crack in steel liner, [Murakami, 1986]

Methodology

For *N* Monte Carlo runs

INPUT

Target lifespan

Geometry & material parameters

Initial crack size a_i, liner radius R, steel type, m & C (Paris law), threshold value ΔK_{th}, toughness K_{Ic}, crack shape ratio a/c

Internal loading conditions

pressure fluctuations

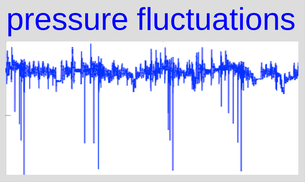

MODEL

failure criterion attained in *target lifespan* ?

NO → no failure in *target lifespan*

YES → failure in *target lifespan*
update number of failures n_f

OUTPUT

Compute failure probability
$p_f = n_f / N$

- user-defined parameters
- model characteristics

Simulation results

User-defined input parameters:

Pressure head p_{mean} = 5 MPa, R = 3 m, a_i = 2 mm, steel type S690, target lifespan = 100 years

Illustration of scatter of stress intensity factor K_{max} at the end of target lifespan, final crack size a_f and number of years for 10^5 Monte Carlo runs

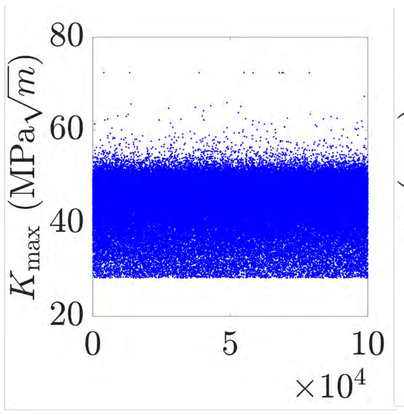

Fig.3 – Scatter of K_{max}

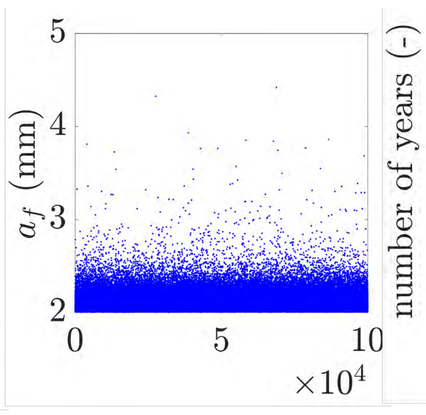

Fig. 4 – Scatter of a_f

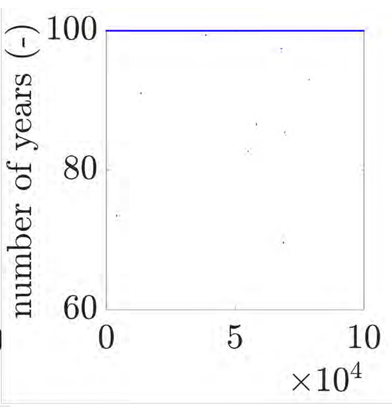

Fig. 5 – Scatter of number of years

Evolution of failure probability with time

Set Number	p_{mean} (MPa)	R (m)	a_i (mm)	Steel type
1	5	2	2	S690
2	5	2	3	S500
3	5	2	3	S690
4	7.5	2	3	S690
5	15	2	5	S690
6	15	2	10	S500
7	15	2	10	S690

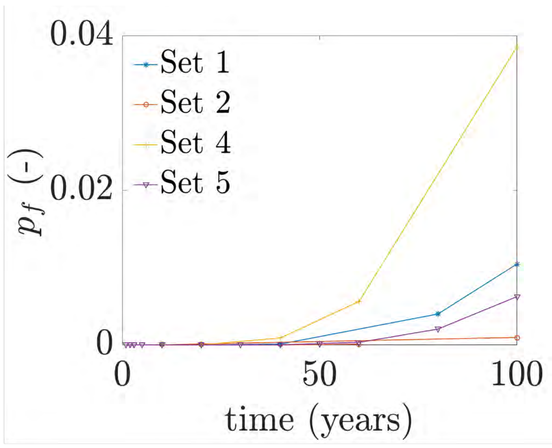

Fig. 6 – Evolution of p_f with time, sets with low p_f

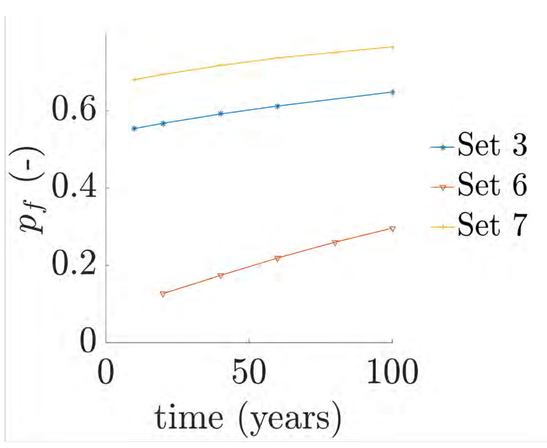

Fig. 7 – Evolution of p_f with time, sets with high p_f

Conclusions

Failure probability is highly dependent on liner thickness. Parameters influencing thickness need to be determined with care. For future work, corrosion and rock mass participation shall be included in the model.

Monte Carlo simulations are time-consuming. Efforts are required to minimize the computation time of each run to ensure the feasibilty of the study.

References

– Bannister AC. Structural Integrity Assessment Procedures for European Industry, Detemination of fracture toughness from Charpy impact energy: procedure and validation, 1998.
– Baptista C. Multiaxial and variable amplitude fatigue in steel bridges. Ph.D. thesis; EPFL & Tecnico Lisboa, 2016.
– Hachem F.E., Giovanola F. Fatigue Cracks Propagation in steel-lined Pressure Shaft of pumped-storage Power Plants under normal Operation Conditions, 2013.
– Pachoud A.J, Schleiss A.J. Stresses and displacements in steel-lined pressure tunnels and shafts in anisotropic rock under quasi-static internal water pressure. Rock Mechanics and Rock Engineering, 2016.

SCCER SoE
SWISS COMPETENCE CENTER for ENERGY RESEARCH
SUPPLY of ELECTRICITY
NSERC CRSNG NATURAL SCIENCE AND ENGINEERING RESEARCH COUNCIL OF CANADA

SCCER-SoE Annual Conference 2016

In cooperation with the CTI
Energy
Swiss Competence Centers for Energy Research
Schweizerische Eidgenossenschaft
Confédération suisse
Confederazione Svizzera
Confederaziun svizra
Swiss Confederation
Commission for Technology and Innovation CTI

Hydrograph variability applied to the gravel bed rivers

Ben Plumb[2], C. Juez[1], M. J. Franca[1], A. J. Schleiss[1] & W. K. Annable[2]

[1]Laboratory of Hydraulic Constructions, EPFL, Lausanne, Switzerland, [2]Department of Civil & Environmental Engineering, University of Waterloo, Waterloo, Canada
Corresponding author: bdplumb@uwaterloo.ca

LABORATOIRE DE CONSTRUCTIONS HYDRAULIQUES
ÉCOLE POLYTECHNIQUE FÉDÉRALE DE LAUSANNE

INTRODUCTION

Hydromodification is the alteration of natural watershed hydrologic processes, which changes the magnitude and frequency of hydrographs entering a given river reach. In the case of urbanization or dam construction, this change has manifested through individual hydrograph characteristics (resulting in a decrease in duration and in the time-to-peak), as well as through the increase of the frequency of morphologically significant flood events. These hydrologic changes have been documented to impact the morphology of gravel-bed rivers, often resulting in channel degradation. However, the actual extent that urbanization, including dams, changes bedload transport characteristics, which is known to be the most important driver of channel morphology, are not yet known.

The objective of this study is to determine the influence of these changes in specific hydrograph parameters (time-to-peak, duration and frequency) on bedload transport and channel morphology in a highly bimodal sand and gravel experimental channel.

EXPERIMENTAL METHODS

Laboratory experiments were carried out using an 8 m long (3.5 m control section) and 0.5 m wide, tilting flume at the Laboratory of Hydraulic Constructions (LCH) of the École Polytechnique Fédérale de Lausanne.

The discharge and sediment feed rates were chosen based on an approximate Froude scaling of 1:24 with the prototype systems used to obtain the hydrologic data (see Hydrologic Scenarios). A slope of 1% was selected based on a pilot test where the slope was allowed to adjust until an equilibrium condition was achieved.

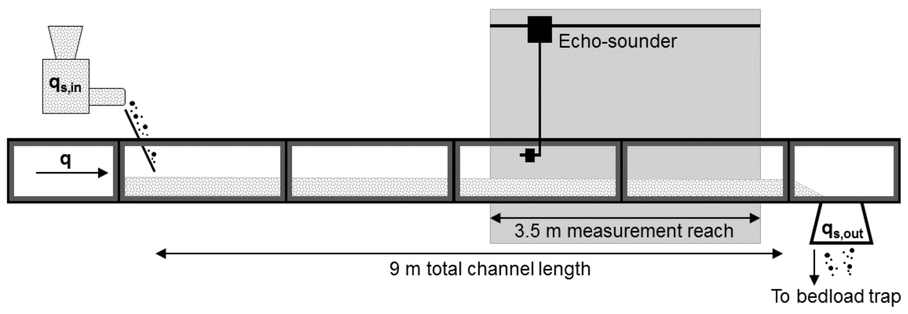

Figure 1: Sketch of the experimental setup

Water discharge for each hydrograph was controlled by a calibrated manual valve, and constantly measured using a v-notch weir at the flume inlet. The sediment mixture was fed into the system by a calibrated sediment feeder situated upstream.

Water height was recorded and bedload samples were taken. Changes in morphology were assessed by a combination of high-resolution topography scans using a mini echo-sounder and aerial bed photographs.

HYDROLOGIC SCENARIOS

The hydrograph parameters and frequencies were derived from long term (>45 years) hydrometric stream-gauge records of two urbanizing watercourses in Southern Ontario, Canada. In LU1 (pre-development), between 0-20% was urban land-use, in LU2 (urbanized) the urban land-use was between 40-60% and in LU3 (highly urbanized) the urban land-use was between 60-80%.

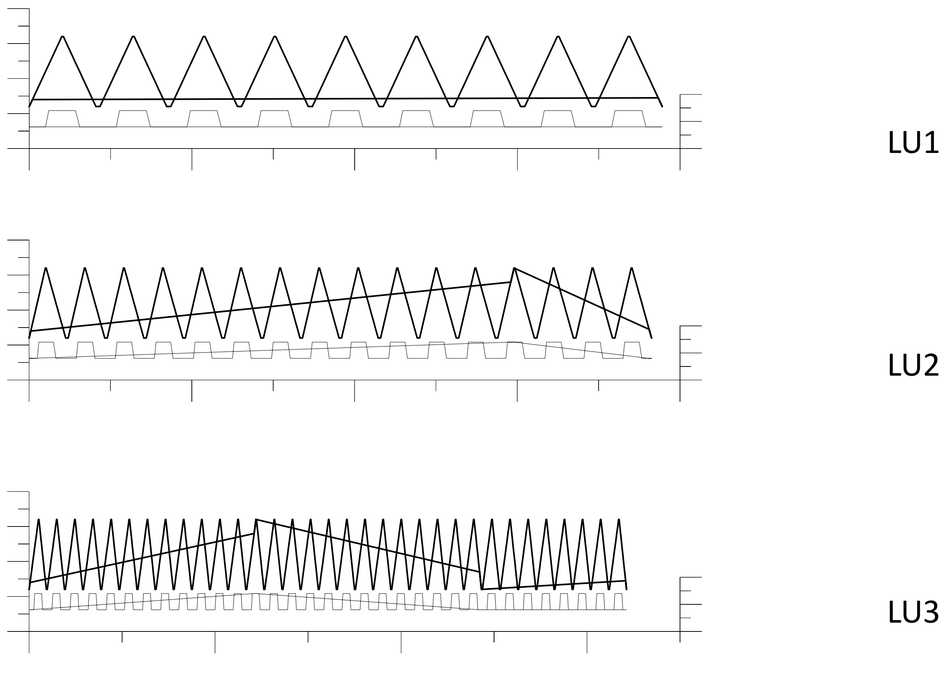

PRELIMINARY RESULTS

Preliminary results from bed scans of the first two hydrologic scenarios (LU1 and LU2) indicate that the channel approaches equilibrium more quickly with the shorter duration hydrographs (higher urbanization scenario). In both experiments, there is significant erosion caused by the first hydrograph due to the initial conditions of the screeted bed. Afterwards, sediment deposition becomes dominant as the eroded material gets replenished by the upstream supply. Although a topographic equilibrium is reached quicker, there is more variability in the net erosion and deposition in LU2. The dominant fraction of the bed oscillates between erosion and deposition. Conversely, the dominant fraction of the bed for LU1 remains in a state of deposition, resulting from the initial flush of sediment after the first hydrograph.

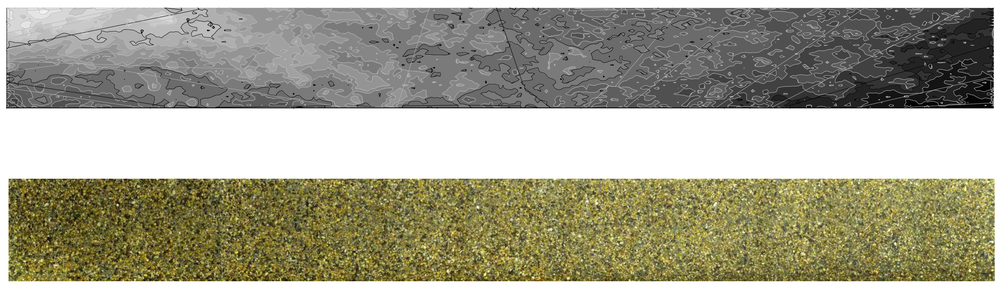

Figure 3: Example bed scan (top) and example stitched aerial bed photograph mosaic (bottom)

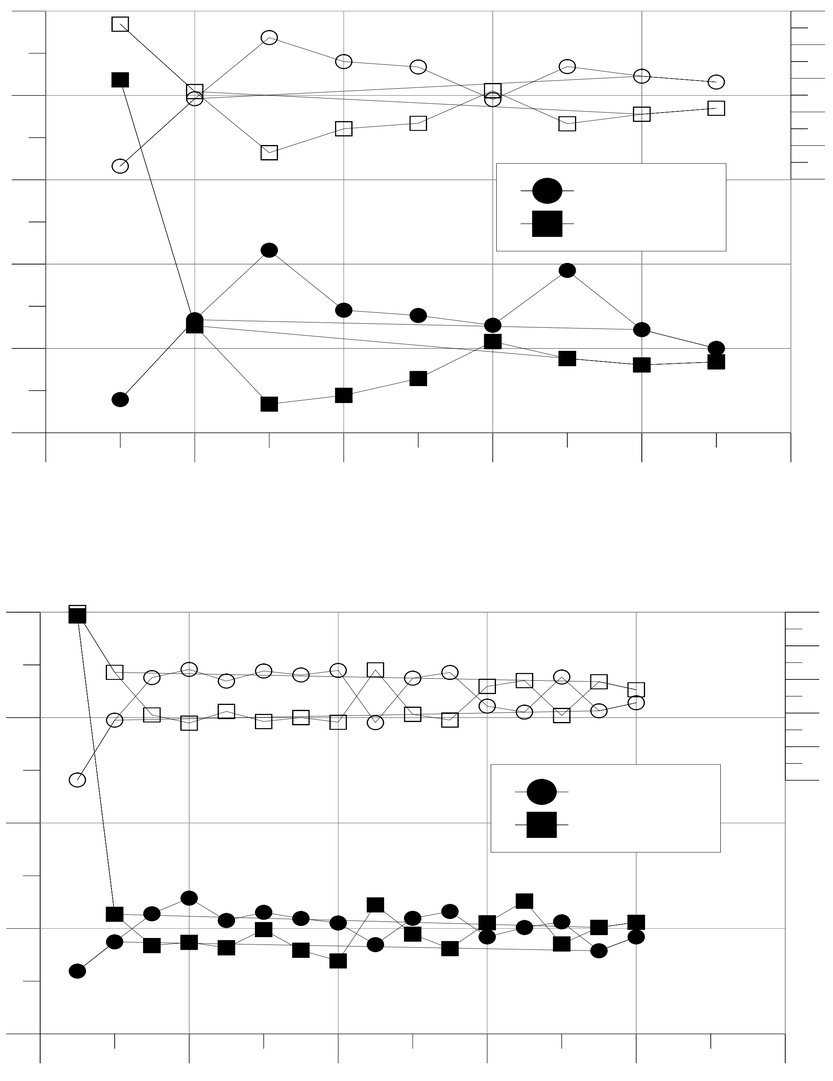

Figure 4: Channel averaged erosion and deposition depths and fraction of the bed with erosion and deposition for LU1 (top) and LU2 (bottom). Equilibrium is considered when the depths are approximately equal and when the bed fractions are both at approximately 50%.

CONCLUSIONS

Preliminary results indicate that the shorter duration hydrographs (consistent with a more urban watershed) reach a topographic equilibrium quicker, but with more oscillation between the dominant process (erosion or deposition) than the longer duration hydrographs.

Future work consists of performing fractional bedload transport analyses on the bedload samples and using additional metrics on the bed scans to further assess the changes in morphology under the different hydrologic regimes. Further, the bed photographs will be processed to investigate the evolution of surface texture.

SCCER SoE
SWISS COMPETENCE CENTER for ENERGY RESEARCH
SUPPLY of ELECTRICITY

SCCER-SoE Annual Conference 2016

In cooperation with the CTI
Energy
Swiss Competence Centers for Energy Research
Schweizerische Eidgenossenschaft
Confédération suisse
Confederazione Svizzera
Confederaziun svizra
Swiss Confederation
Commission for Technology and Innovation CTI

Mitigation des effets négatifs du changement climatique sur l'aménagement de Gebidem grâce à un nouveau volume de stockage à Oberaletsch

Calixte E., Zeimetz F., Manso P., Schleiss A.
(1) Laboratoire de Constructions Hydrauliques, École polytechnique fédérale de Lausanne (EPFL)
Contact: emeline.calixte@gmail.com

LABORATOIRE DE CONSTRUCTIONS HYDRAULIQUES
ÉCOLE POLYTECHNIQUE FÉDÉRALE DE LAUSANNE

Motivations et Objectifs

Le barrage de Gebidem, appartenant à la société anonyme Electra-Massa, capte aujourd'hui les eaux d'un bassin versant recouvert à 63 % de glaciers. Avec un volume utile de 8.7 hm³, la retenue ne représente que **2 %** de l'ensemble des apports de son bassin versant. Le barrage est donc sujet à de nombreux déversements, ainsi qu'une purge annuelle permettant l'évacuation d'un fort apport en sédiments.

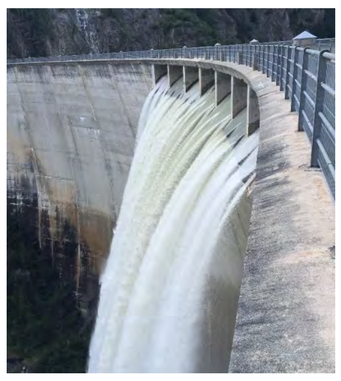

Évolution des apports hydrauliques et sédimentaires

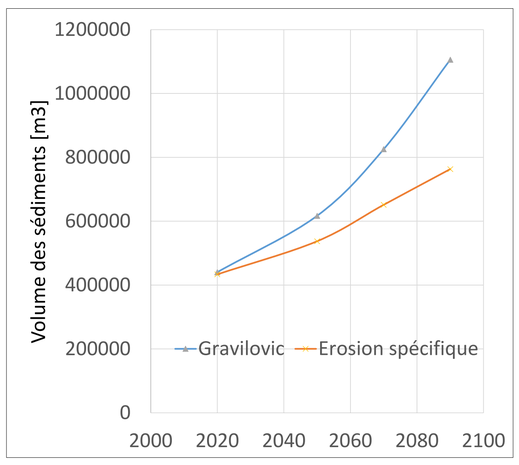

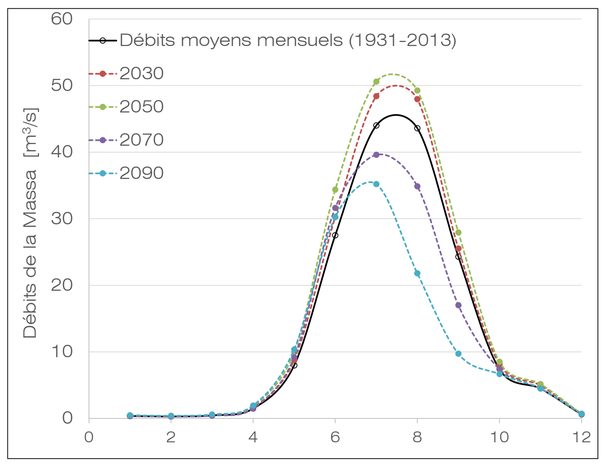

Les prévisions du recul du glacier de Grosser aletsch ont permit d'établir les résultats précédents. Avec l'accélération de la fonte, les apports hydrauliques vont augmenter jusqu'en 2050, puis diminuer avec la disparition des glaciers. Ce phénomène va laisser place à des sols très érodibles, les moraines, ce qui se traduira par une augmentation globale de l'apport en sédiments.

Trois concepts d'aménagement distincts

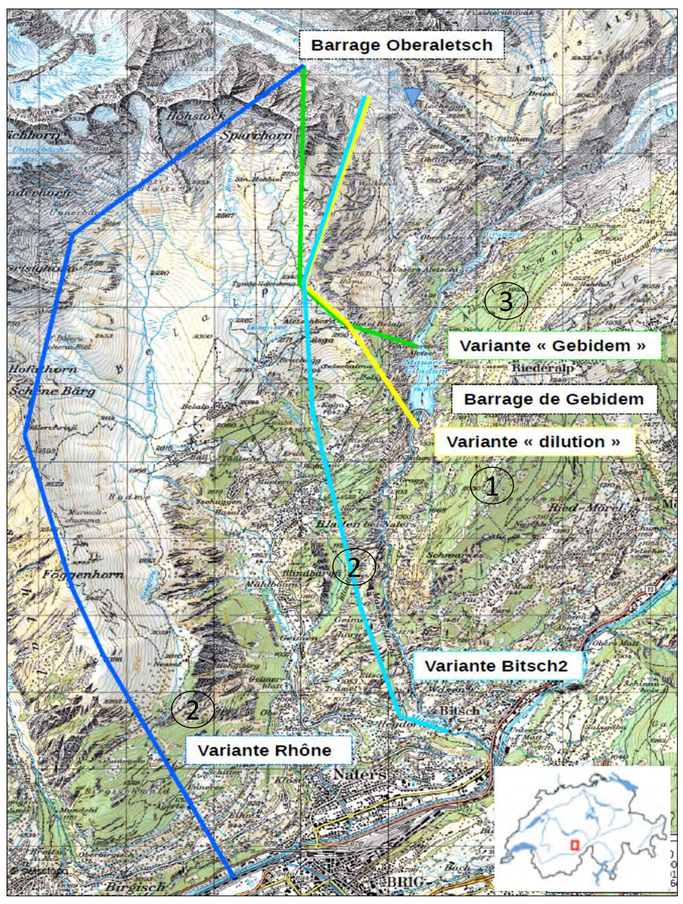

Concernant l'étude de variantes, trois différents emplacements d'une nouvelle centrale, trois adductions, ainsi que diverses hauteurs de barrage sont considérées.

Une combinaison de ces possibilités permet de comparer 21 variantes en considérant les apports hydrauliques estimés pour 2050, 2070 et 2090.

Photo en aval de l'emplacement du futur barrage d'Oberaletsch

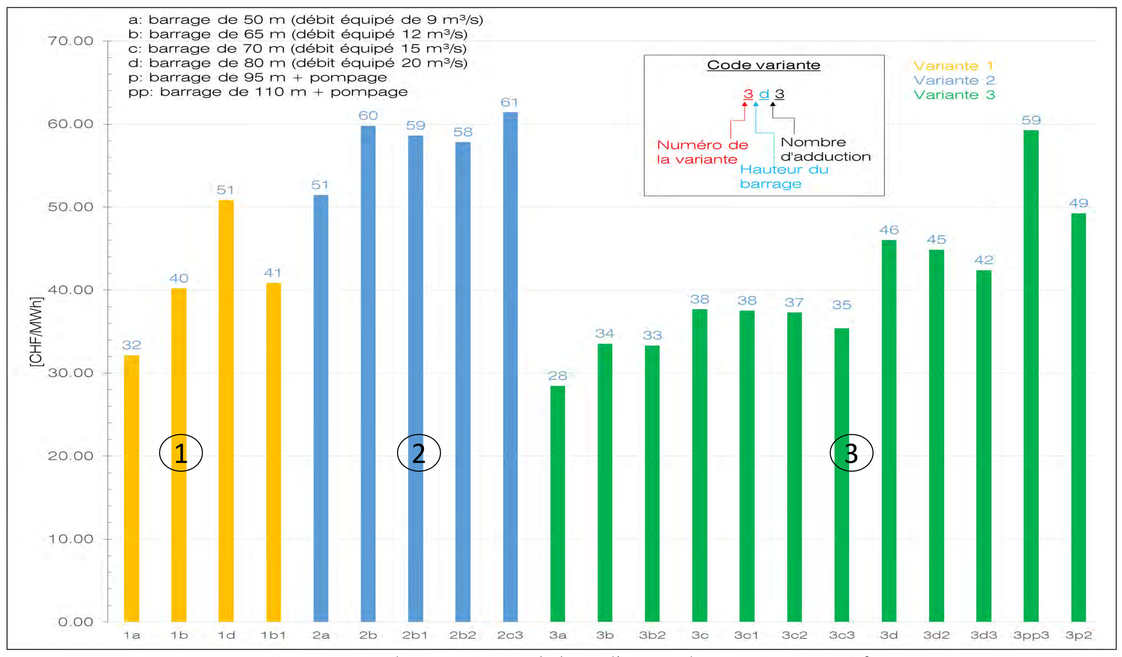

Comparaison des variantes sur la base d'un prix de revient comparatif

Analyse multicritère et choix d'un concept d'aménagement

Critères	Variante 1	Variante 2	Variante 3 (hors pompage)	Variante 3 (pompage)
Quantité d'énergie productible à Oberaletsch [GWh]	≈ 100	≈ 165-320	≈ 80-160	≈ 165-220
		Selon adductions		
Quantité d'énergie productible à Gebidem [GWh]	≈ 440	≈ 380 – 440 (selon adductions)	≈ 530	≈ 530
Part d'énergie hivernale totale	≈ 25 %	≈ 25 – 31 %	≈ 25 – 37 %	≈ 39 – 47 %
Protection contre les crues	Améliorée	Améliorée	Fortement améliorée grâce à une bonne gestion des deux barrages	
Flexibilité de la gestion	Moyenne	Moyenne	Assez forte	Très forte
Augmentation de la dilution	Durant toute l'année	Durant toute l'année dans le canal de chasse	Pendant les purges	

<u>Variante retenue:</u>
Hauteur de barrage : 70 m
Volume utile de la retenue : 52 hm³
Eaux captées :
i. 2050 : 65 hm³ (Oberaletsch)
ii. 2070 : 68 hm³ (ajout de 2 adductions)
iii. 2090 : 82 hm³ (ajout adduction)

Vue aval aérienne du futur barrage d'Oberaletsch

Nouveau aménagement hydroélectrique

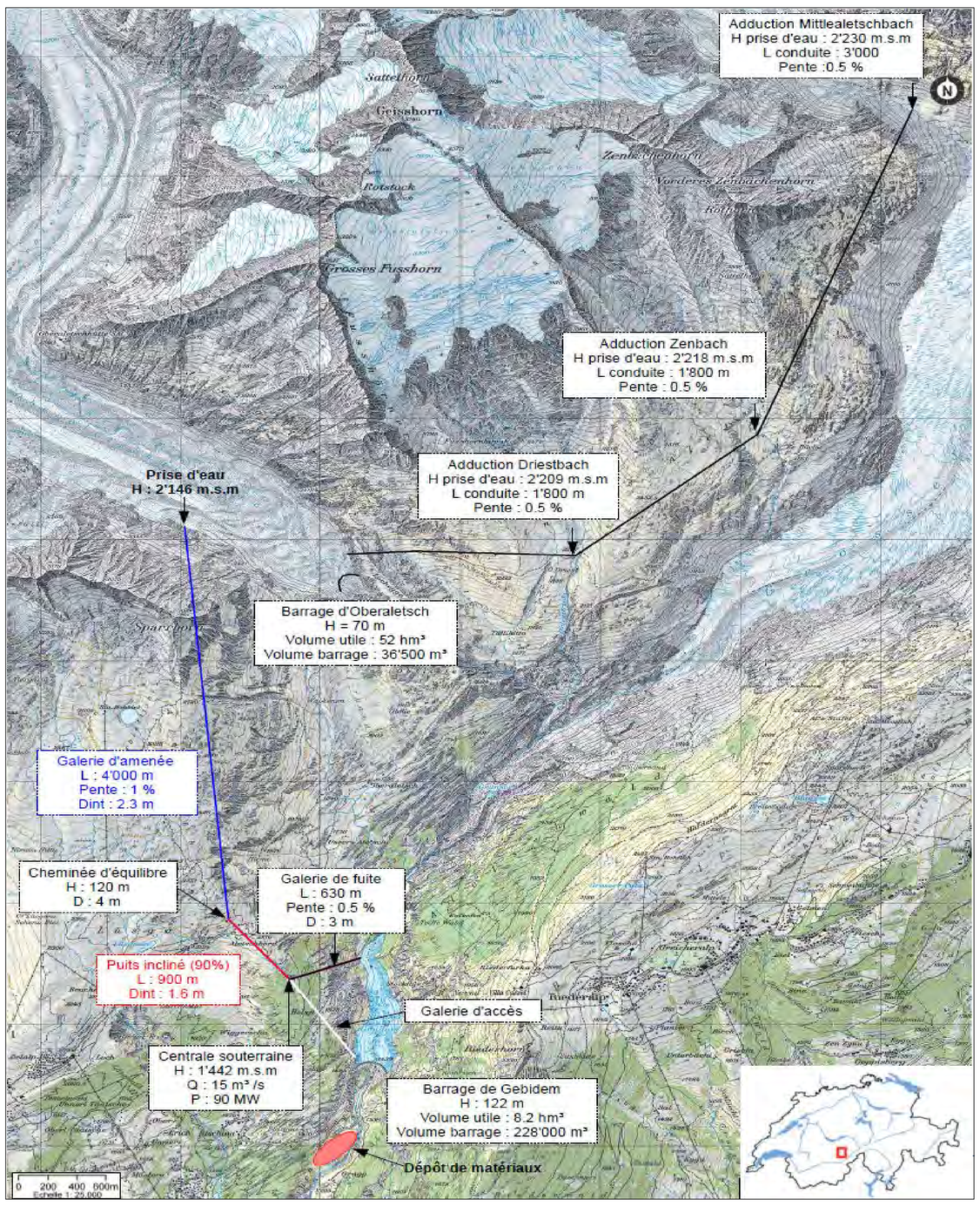

Conclusion

L'étude mets en évidence les risques que le changement climatique présente pour l'aménagement de Gebidem, ainsi que différentes solutions pour mitiger ses effets négatifs tant au niveau de la gestion des sédiments comme de la production d'électricité. La solution retenue contribue aussi aux objectifs de la stratégie énergétique 2050.

SCCER-SoE Annual Conference 2016

SCCER SoE
SWISS COMPETENCE CENTER for ENERGY RESEARCH
SUPPLY of ELECTRICITY

In cooperation with the CTI
Energy
Swiss Competence Centers for Energy Research
Schweizerische Eidgenossenschaft
Confédération suisse
Confederazione Svizzera
Confederaziun svizra
Swiss Confederation
Commission for Technology and Innovation CTI

Potentiel hydroélectrique dans la vallée de Gorner suite au retrait du glacier

George-Molland P. , Stähly S., Manso P., Schleiss A.
Laboratory of Hydraulic Constructions (LCH), Ecole Polytechnique Fédérale de Lausanne (EPFL)
Correspondant: philippe.george-molland@epfl.ch

LABORATOIRE DE CONSTRUCTIONS HYDRAULIQUES
ÉCOLE POLYTECHNIQUE FÉDÉRALE DE LAUSANNE

Contexte

Le réchauffement climatique provoque le recul des glaciers alpins, dont celui du Gorner, situé en Valais à l'amont de Zermatt. Ce recul crée des menaces pour l'exploitation hydroélectrique et la sécurité du territoire, mais aussi de nouvelles opportunités d'exploitation du potentiel hydroélectrique et d'augmentation de la valorisation de l'eau de la rivière de Gornera, dans le cadre de la transition énergétique en Suisse.

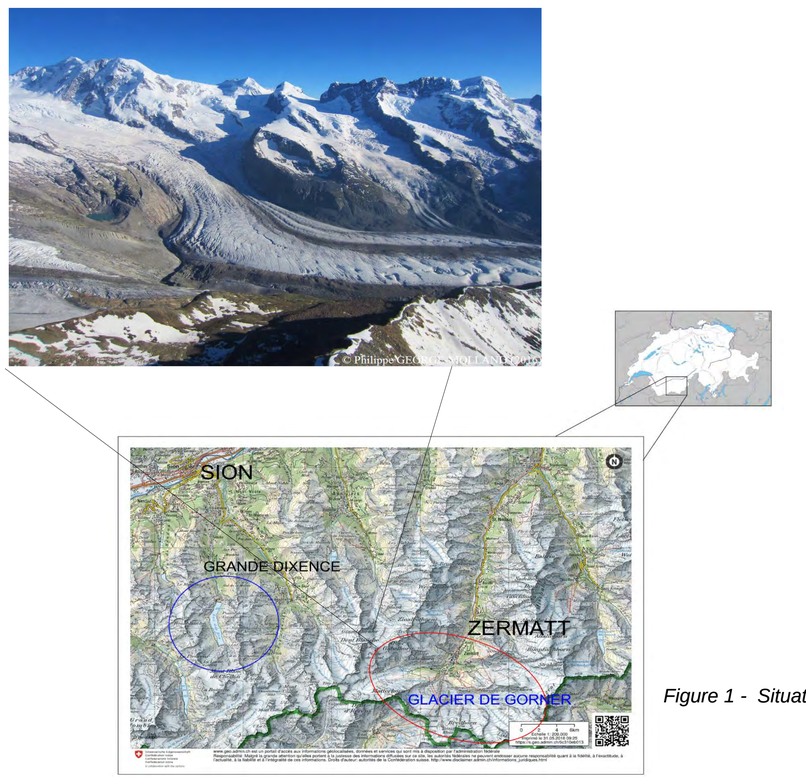

Figure 1 - Situation

Utilisation des eaux de la Gornera par la Grande-Dixence

Actuellement les eaux de la Gornera sont en partie captées et dérivées vers la retenue de Grande Dixence pour ensuite être turbinées dans les centrales de turbinage en vallée du Rhône. Ce travail s'est d'abord attaché à comprendre les mécanismes de la valorisation de cette eau via ce complexe existant, qui a ensuite été modélisé. Cet outil a permis la simulation de variantes de nouveaux aménagements hydroélectriques exploitant l'eau de la Gornera, intégrées au complexe hydroélectrique existant.

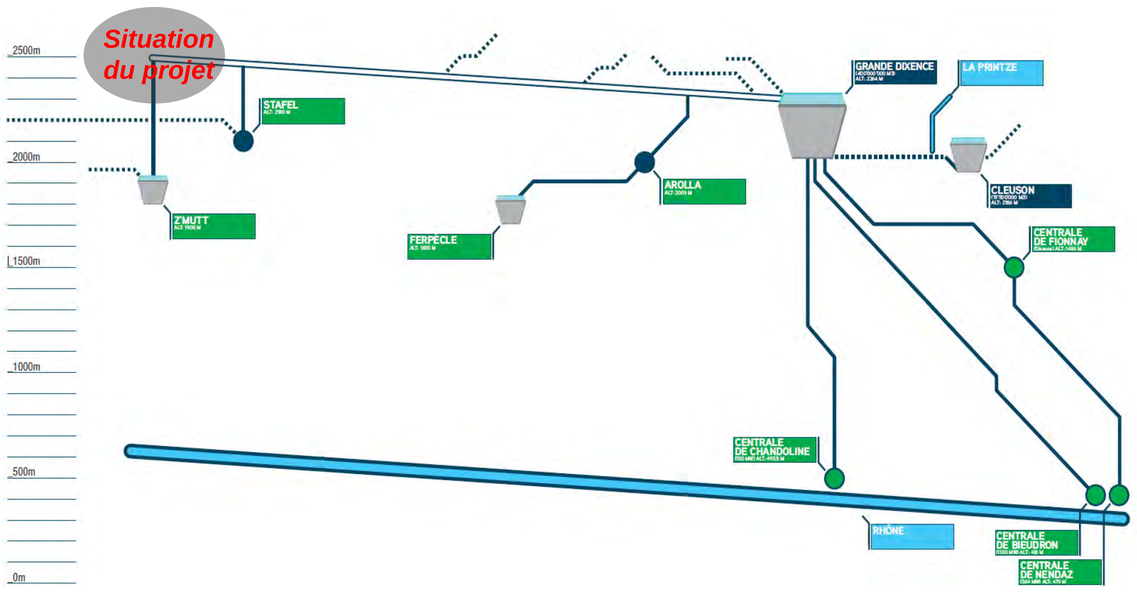

Figure 2 - Profil en long simplifié des installations de la Grande Dixence S.A (Source : Alpiq)

Etude de variantes d'aménagement

5 variantes d'aménagements, répondant à 3 concepts de valorisation de l'eau de la Gornera, ont été élaborées puis analysées et comparées selon 3 critères : économique, énergétique et financier. Les critères énergétique et financier ont été évalués grâce à la modélisation du complexe de Grande Dixence, modifiée en conséquence. L'analyse a pris en compte **la dimension temporelle** en considérant 3 scénarii d'apport en eau : les apports mesurés entre 2006 et 2013 pour le premier scénario, ces mêmes apports augmentés de 20% (prévisions des apports en 2030) et enfin diminués de 15% (prévisions des apports en 2080). Donc un total de 15 sous-variantes a été analysé.

Changement climatique : menaces et opportunités

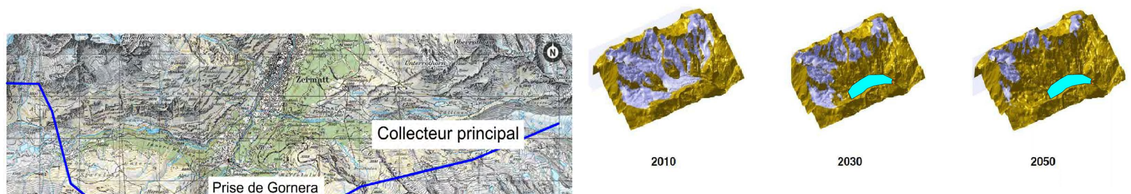

Pellicciotti, F., et al. (2013)

Selon plusieurs études, le glacier de Gorner aura disparu en dessous de 2500 m s.m. d'ici 2030. Le projet considère donc l'absence du glacier dans la nouvelle retenue de Gorner et une modification des apports en eau dans l'horizon de projet jusqu'en 2100.

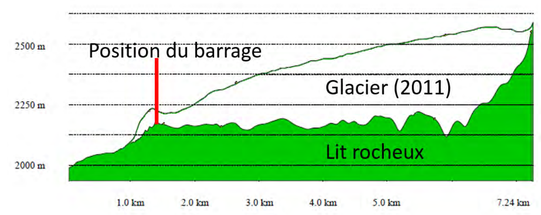

Profil en long du thalweg du bassin de Gorner

Courbe niveau/volume sans glacier

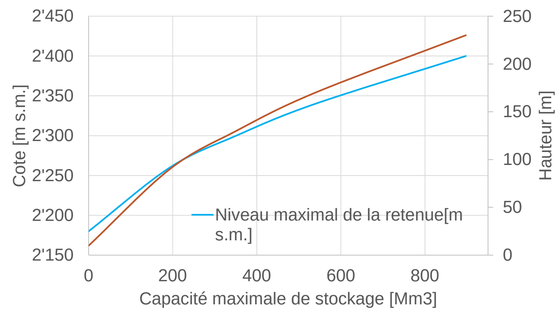

Nouvelle retenue à Gornera

① Retenue de Gorner
② Retenue de Grande Dixence
③ Collecteur principal
④ Amenée en charge depuis 1
⑤ Caverne de pompage
⑥ Jonction puits - collecteur
⑦ Galerie d'accès depuis le pied du barrage
⑧ Galerie d'accès depuis Zermatt
Eau captée en rivière
Eau du barrage de Gorner

Caractéristiques principales

Prix de revient du kWh : 12 cts/kWh

Puissance de pompage : 77 MW

Débit installé : 29 m^3/s

Hauteur de refoulement max : 270 m

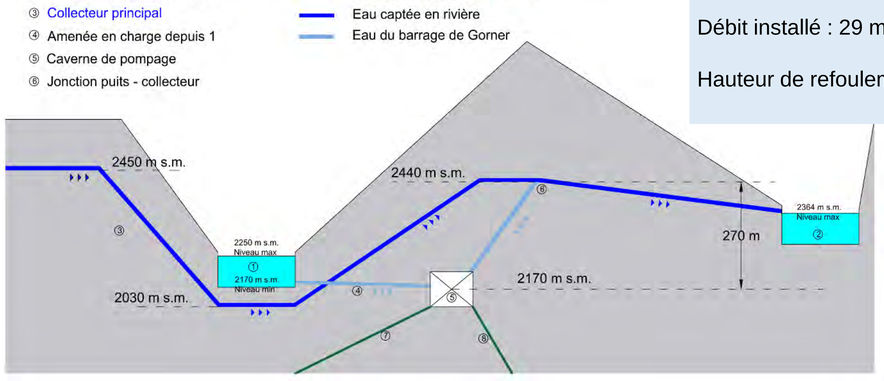

Profil en long schématique de l'avant-projet

Intégration du barrage projeté dans l'environnement

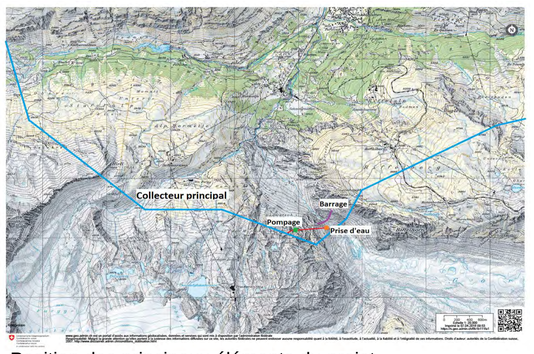

Position des principaux éléments du projet

Suite à l'analyse de variantes, un barrage de 72 m de hauteur à l'amont de Zermatt est projeté (**capacité de retenue : 130 hm^3**), avec un transfert de l'eau de sa retenue vers le barrage et les centrales de turbinage de Grande Dixence par un système de pompage. Les ouvrages impliqués ont été dimensionnés puis évalués économiquement : l'investissement a été estimé à **337 MCHF** pour un gain énergétique net annuel de **149 GWh, c'est-à-dire +7%** de la production actuelle du plus grand complexe hydroélectrique de Suisse.

Remerciements

Les auteurs remercient la collaboration d'Alpiq S.A dans la collecte de données de base.

Références

- Bezinge , A. et R. Aeschlimann. *30 ans d'expériences sur les captages d'eaux glaciaires à Grande Dixence*. Sion: Association valaisanne des producteurs d'énergie électrique, 1988.
- Haeberli, W., et al. *NELAK (2013) : Neue Seen als Folge des Gletscherschwundes im Hochgebirge - Chancen und Risken. Formation des nouveaux lacs suite au recul des glaciers en haute montagne - chances et risques.* Zürich: Forschungsbericht NFP 61, s.d.
- Office fédérale de l'énergie OFEN. *Le potentiel hydroélectrique de la Suisse - Potentiel de développement de la force hydraulique au titre de la stratégie énergétique 2050*. Berne, 2012.
- Pellicciotti, F., et al. «Changes in glaciers in the Swiss Alps and impact on basin hydrology : Current state of the art and future research.» *Science of the Total Environment* 10 May 2014: 1152-1170.
- George-Molland P., Stähly S, Manso P., Schleiss A. *Mitigation des effets négatifs des changements climatiques par aménagement d'une nouvelle retenue dans la vallée de la Gornera en Suisse*. La Houille Blanche (en préparation).